

*Synthesis and Characterisation of
Thermoplastic Ionomers based on
Natural Rubber*

Thesis submitted to the
Cochin University of Science and Technology
in partial fulfillment of the requirements for
the award of the degree of

Doctor of philosophy

Under the
FACULTY OF TECHNOLOGY
By

Mr. Thommachan Xavier

DEPARTMENT OF POLYMER SCIENCE AND RUBBER TECHNOLOGY
COCHIN UNIVERSITY OF SCIENCE AND TECHNOLOGY
KOCHI- 682022

March 2002

Dr. Thomas Kurian
B. Sc., B. Tech., M. Tech., Ph. D., MISTE
Reader

Phone Off. 0484-555723
Phone Res. 0484-425244
Fax: 0484- 542747
Email: tkurian@cusat.ac.in

Department of Polymer Science and Rubber Technology
COCHIN UNIVERSITY OF SCIENCE AND TECHNOLOGY
Kochi - 682 022, India

Date: 22-03-2002

CERTIFICATE

This is to certify that the thesis entitled "***Synthesis and Characterization of Thermoplastic Ionomers based on Natural Rubber***", which is being submitted by **Mr. Thommachan Xavier**, in partial fulfillment of the requirements of the degree of Doctor of Philosophy, to the Cochin University of Science and Technology (CUSAT), Kochi is a record of the bonafied research work carried out by him under my guidance and supervision

Mr. Xavier has worked on this research problem for about three years and six months (1998 - 2002) in the Department of Polymer Science and Rubber Technology of CUSAT. In my opinion the thesis has fulfilled all the requirements according to the regulation and has reached a standard necessary for submission. The results embodied in this thesis have not been submitted for any other degree or diploma.

Thomas Kurian

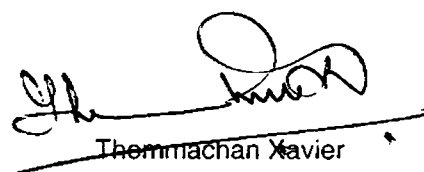
Thomas Kurian
(Supervising Teacher)

Declaration

I here by declare that the thesis entitled 'Synthesis and Characterisation of Thermoplastic Ionomers based on Natural Rubber' is the original work carried out by me under the guidance of **Dr. Thomas Kurian**, Reader, Department of Polymer Science and Rubber Technology, Cochin University of Science and Technology, Cochin, and no part of this thesis has been presented for any other degree from any other institution.

Kochi

25-03-2002



Thommachan Xavier

Contents

Preface

Abstract

- Chapter 1:** General Introduction & Review of literature
- Chapter 2:** Materials and Measurements
- Chapter 3:** Ionomers based on Radiation Induced Styrene Grafted Natural Rubber
- Chapter 4:** Alternative Synthesis of Ionomers
- Chapter 5:** Effect of Fillers on the Properties of Ionomer based on RISGNR
- Chapter 6:** Electrical Behavior of Ionomers at Microwave Frequencies
- Chapter 7:** Ionomer as Compatibilizer in the SBR/NBR blend system
- Chapter 8:** Conclusions

List of abbreviations

List of publications

* Detailed contents are given at the beginning of each chapter

Preface

A novel feature emerges from the study of the history of the wide variety of ionomers. Although the field of ionomers is currently less than half a century old, hosts of new applications ranging from membranes to paints in industry have appeared. The ionomer field underwent a multiplex growth producing surprisingly large number of papers and patents per year. The presence of ions in polymers is an additional structural parameter available for the modification of properties and provides a route for the polymer chemist in tailoring material properties to particular applications. The compositional variety of ionic polymers is matched by the variety of their usages. The reprocessability of the rubber-based ionomers helps them to be used for injection and blow moulding. Synthesis of ionic cross-linked rubbers, therefore, became an area where many research and developments had taken place and the efforts were proved to be fruitful.

The present thesis aims at the synthesis of the ionomers based on natural rubber. Consisting of eight chapters, the thesis portrays an introduction and literature survey in the first chapter, and describes the materials and methods employed for the study in the second chapter. Novel ionomers based on radiation induced styrene grafted natural rubber and alternative methods of synthesis of natural rubber ionomers have been incorporated in to the chapters 3 & 4 respectively. The effect of fillers on the properties of ionomers forms the basis of the fifth chapter. Sixth chapter narrates the electrical behavior in the microwave frequency. Use of the ionomer as a compatibilizer on the SBR/NBR immiscible blend system is the content of the seventh chapter. The major findings in the present study along with further scope for the research have been summarized in the final chapter 8.

A thesis such as this one would have been impossible without the generous, enthusiastic and inspiring guidance of my dear supervising teacher Dr. Thomas Kurian, Reader, Department of Polymer Science and Rubber Technology (PS & RT), Cochin University of Science and Technology (CUSAT), Cochin, INDIA. It is a pleasure to express my deep gratitude to Prof.Dr. K.E.George and Dr. Rani Joseph for their innumerable suggestions involving both scientific and linguistic aspects. The benefit of valuable discussions and suggestions of Professor A.Eisenberg, Dept. of Chemistry, McGill University, CANADA is also gratefully acknowledged. May I express my deep indebtedness to Prof. Joon-Seop Kim and Su-Hwan Kim, Dept. of Polymer Science and Engineering, Chosun

University, Kwangju, SOUTH KOREA for extending their collaboration and work experience in analyzing the samples using DSC and DMTA. Several personalities were most helpful during the course of my studies. In this connection special thanks are due to the distinguished faculties of the PS & RT, CUSAT, Cochin, INDIA, doctors Kuriakose, Eby Thomas Thachil, Philip Kurian, and Sunil. K.N. My sincere thanks are due to Mr. Jacob Samuel, fellow research scholars and supporting staff for all their encouragements. Extensive support of Dr. Schmit Pauline and Mr. Sony Varghese of the Eindhoven University of Technology, The Netherlands in connection with the SEM analysis was very important in making this thesis possible. My acknowledgements are due to Dr. K.T.Mathew, Dr. Joe Jacob and other colleagues in the department of electronics, CUSAT, Cochin, INDIA for accomplishing microwave studies. I want to thank Dr. K.T.Thomas, Deputy Director, Rubber Research Institute of India, Kottayam, INDIA for providing the samples for my research work. I gratefully acknowledge the permission granted by Rev. Fr. Manager, and Principal of Sacred Heart College, Thevara, Cochin, Kerala, INDIA, for completing my study. I am thankful to many colleagues in the post graduate department of chemistry and other friends in the college who have encouraged me and given me advice on many issues. I thank my parents, relatives, in-laws and neighbors for their moral support and unselfish encouragement through out my research work. And, of course, I thank my wife Tessy, and my loving children Tomin and Teslin for the understanding and patience they have shown at all times, but most conspicuously during the writing of this thesis. Finally to the almighty for showering up on me thy choicest blessings for the completion of the research work.

Thommachan Xavier

thommachan@cusat.ac.in

Abstract

Chemically modified novel thermo-reversible zinc sulphonated ionomers based on natural rubber (NR), radiation induced styrene grafted natural rubber (RI-SG NR), and chemically induced styrene grafted natural rubber (CI-SG NR) were synthesized using acetyl sulphate/zinc acetate reagent system. Evidence for the attachment of sulphonate groups has been furnished by FTIR spectra, which was supplanted by FTNMR results. Estimation of the zinc sulphonate group was done using spectroscopic techniques such as XRFs and ICPAES. The TGA results prove improvement in the thermo-oxidative stability of the modified natural rubber. Both DSC and DMTA studies show that the incorporation of the ionic groups affect the thermal transition of the base polymer. Retention of the improved physical properties of the novel ionomers even after three repeated cycles of mastication and molding at 120 °C may be considered as the evidence for the reprocessability of the ionomer. Effect of both particulate (carbon black, silica & zinc stearate) and fibrous fillers (nylon & glass) on the properties of the radiation induced styrene grafted natural rubber ionomer has been evaluated. Incorporation of HAF carbon black results in maximum improvement in physical properties. Silica reinforces the backbone chain and weakens the ionic associations. Zinc stearate plays the dual role of reinforcement and plasticization. The nylon and glass filled ionomer compounds show good improvement in the physical properties in comparison with the neat ionomer. Dispersion and adhesion of the fillers in the ionomer matrix has been amply supported by their SEM micrographs. Microwave probing of the electrical behavior of the 26.5 ZnS-RISG NR ionomer reveals that the maximum relative complex conductivity and the complex permittivity appear at the frequency of 2.6 GHz. The complex conductivity of the base polymer increases from 1.8×10^{-12} S/cm to 3.3×10^{-4} S/cm. Influence of fillers on the dielectric constant and conductivity of the new ionic thermoplastic elastomer has been studied. The ionomer / nylon compound shows the highest microwave conductivity. Use of the 26.5 ZnS-RISG NR ionomer as a compatibilizer for obtaining the technologically compatible blends from the immiscible SBR/NBR system has been verified. The heat fugitive ionic cross-linked natural rubber may be, therefore, useful as an alternative to vulcanized rubber and thermoplastic elastomer.

Chapter 1

General Introduction & Review of literature

Part of the work presented in this chapter has been published in:

1. *Prog. Rub. Plast. Tech.* 16, 1 (2000)
 2. *Chemweb.com/CPS: macrochem/0103001* (2001)
-

- 1.1 *Introduction*
- 1.2 *Historical Aspects*
- 1.3 *Classification of ionomers*
- 1.4 *Synthesis of ionomers*
- 1.5 *Morphology of ionomers*
- 1.6 *Ionomer behaviour- A generic view*
- 1.7 *Investigation of ionomers*
- 1.8 *Properties of ionomer*
- 1.9 *Chemical reactions in ionomers*
- 1.10 *Glass ionomers*
- 1.11 *Ionomers in service of mankind*
- 1.12 *Recent studies on ionomers*
- 1.13 *Scope of the work*
- 1.14 *Conclusion*
- 1.15 *References*

1.1 Introduction

Ionomers are classes of materials, which are emerging as important commercial polymers having many unique scientific characteristics [1-4]. Typically ionomers consists of low levels of salt groups covalently bonded to the polymer chain. These salt groups consist of metal cations such as those from group 1, group 2 or transition

metals [5-7] and anions such as phosphonate, carboxylate and sulphonate groups. Presence of less than 10 mol % of salt groups chemically combined with a nonpolar polymer backbone can have dramatic influence on polymer properties not observed with conventional homopolymers or with copolymers based on nonionic species. The physical structure of ionomer is distinguished by interchain ionic bonding [8]. Due to the dissociation of the interchain ionic bonding at high temperatures, ionomers can be processed using standard thermoplastic processing methods.

The bulk properties of the ionomers are governed by ionic interactions in the discrete regions of the material (ionic aggregates) [8]. The introduction of a small amount of ionic groups improves the material properties of the polymer, which results in an increased modulus, improved abrasion resistance, better tear resistance and good impact strength [9-11]. The formation of ionomers results in a substantial increase in melt viscosity and physical properties of the polymer [12, 13]. It is generally accepted that the ionic groups interact or associate to form regions rich in ions in the polymer matrix (Fig.1.1).

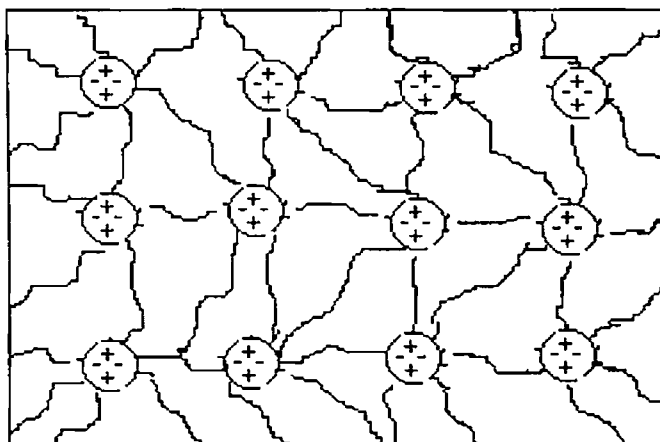


Fig. 1.1 Schematic representation of ionic aggregates in polymer matrix

The ionic interactions and the consequent ionomer properties depend upon various factors [14], which include:

- Type of polymer backbone (plastics or elastomers)

- Level of ionic functionality (ionic content 0 to 10%)
- Type of ionic moiety (carboxylate, sulphonate, phosphonate)
- Degree of neutralization (0 to 100%)
- Type of cation (amine, metal, monovalent or multivalent)

With this range of experimental variables, the spectrum of polymer properties available within the ionomer family may be extremely broad [15-17]. This combination of excellent properties and processing ease has led to the use of ionomers in many high performance material applications and has made this area an extremely fertile one for research and development. Several review articles [18-22] and books [1, 2, 23-25] have been published on ionomers.

1.2 Historical aspects

One of the earlier syntheses of ionomers dates back to 1930s with the work by Littman and Marvel [21] on polymers that were later called ionenes [22]. Shortly thereafter carboxylated elastomers based on butadiene and acrylic acid co-polymers were reported. The polymeric behaviour of halatotelechelic was explored as early as 1944. In 1946 Mc Alevy discovered a family of elastomers [26] with a substantial degree of ionic cross linking, which was introduced commercially in the early 1950s by DuPont under the trade name Hypalon. The 1950s were illuminated with the introduction of ionomers based on butadiene-acrylonitrile-acrylic acid terpolymers by Goodrich and later modified by Brown [27].

A major break through in ionomers occurred in the mid 1960s when DuPont introduced their ethylene-methacrylic acid copolymers, which were partially neutralized with sodium or zinc cation under the trade name Surlyn. In several of their early papers, Rees and Vaughn [28, 29] described the structure, morphology and physical properties of this family of materials. In the 1960s and early 1970s, a number of investigators explored the structure and properties of these ionomers. Specifically McKnight [30], Otocka [31, 32], Cooper [33] and Eisenberg [34-36] were among those who postulated various structures for the ionic cross-links and the resultant morphology. In 1970 Eisenberg undertook the first comprehensive theoretical attempt

to understand the arrangement of salt groups in various ionomers including those of styrene-acrylic acid copolymers.

Table 1.1. *New families of ionic elastomers or flexible plastics of both commercial and experimental type*

a) Commercial Systems

Polymer System	Trade Name	Comments
Ethylene/ Methacrylic acid copolymer	Surlyn (DuPont)	Modified thermoplastic
Butadiene/ Acrylic acid	Hycar (Goodrich)	High strength elastomers
Perfluoro sulphonate ionomers	Nafion (DuPont)	Multiple membrane users
Perfluorocarboxylate ionomers	Flemion (Asahi glass)	Chlor-alkali membrane
Telechelic polybutadiene	Hycar (Goodrich)	Specialty uses
Sulphonated ethylene/ propylene terpolymers	Ionic-elastomers (Uniroyal)	TPE

b) Experimental Systems

Polymer systems
i) Sulphonated Polypentenamer [43]
ii) Telechelic polyisobutylene sulphonate ionomers [44-50]
iii) Alkyl methacrylate/ sulphonate copolymers [51]
iv) Acid- Amine ionomers reaction products [52]

Dasgupta reported ionomers based on polyvinyl butyral [37] in 1992. Reports of other ionomers based on random ethylacrylate zwitter ionic copolymer [38], polyurethane anionomers [39], styrene-coumarin copolymer ionomers [40], poly (1, 4-butylene isophthalate) [41] etc include the valid contributions of the period extending from 1991 to 1993. The year 2000 saw the development and studies of poly (ethylene oxide) ionomers, polyurethane ionomers [42] etc. An overview of new families of ionic elastomers or flexible plastics of both commercial and experimental type is

summarized in table 1.1. Recent developments in the field of ionomers have been incorporated towards the end of this chapter as section 1.12.

1.3 Classification of ionomers

1.3.1. Plastic based ionomers

1.3.1 (a) Styrene ionomers

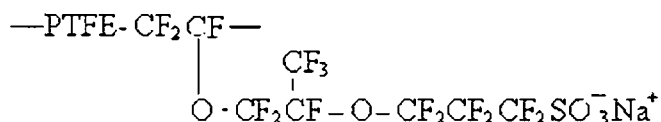
There are five categories of styrene-based ionomers: (a) carboxylated ionomers:- they include poly (styrene-co-methacrylic acid) containing various amounts of metal carboxylate groups [53-59], (b) sulphonated ionomers:- the substitution of a sulphonate group for a carboxylate group changes the properties of the ionomers drastically [60-63]. Although the polymer backbone does not change significantly, extremely strong temperature resistant ionic networks are created at low ionic concentrations. Sulphonate ionic interactions are stronger than carboxylate due to the higher degree of polarity inherent in the sulphonate system, (c) benzyloxy or phenoxy ionomers:- few studies have been performed with alkoxide anions as the ionogenic group. They include copolymers of styrene with 4-phenoxy styrene and styrene with 4-benzyloxy styrene [64-66], (d) vinyl pyridinium methyl iodide ionomers:- they include ionomers based on N-methyl-4-vinyl pyridinium iodide [67, 68] and (e) homoblends - it consists of a mixture of two polystyrene based materials, one of which has pendant cations and the other pendant anions. A typical example includes styrene sulphonic acid and 4-vinyl pyridine [69].

1.3.1 (b) Ethylene ionomers

These were the first family of ionomers commercially manufactured. Owing to the presence of crystallinity, they differ from styrene-based ionomers. Studies include ethylene methacrylic acid based materials [28]. E.I. DuPont de Nemours & Co. Ltd. manufacture ethylene ionomers and market it under the trade name Surlyn [70-71]. Excellent tensile properties, good clarity, high melt viscosity and reduction in haze after neutralization of the ethylene methacrylic acid are the hallmarks of this ionomer

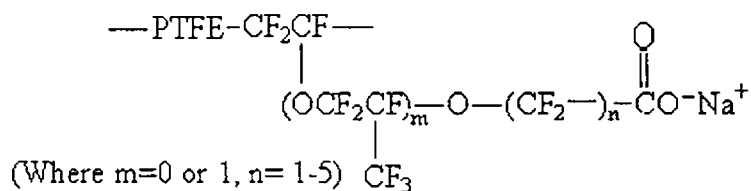
[72-73]. Kutsumizu [74] et al did an exhaustive study on the crystallinity of ethylene ionomers.

1.3.1 (c). Tetrafluoro ethylene ionomers



Scheme 1.1 Nafion (DuPont)

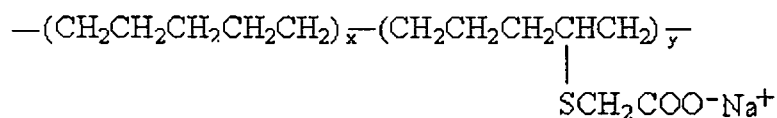
Since these ionomers are used extensively as membranes in the chlor-alkali industry and in fuel cells [75], and also for many industrial applications, they are emerging as one of the important family of ionomers



Scheme 1.2 Flemion (Asahi glass)

Many materials of the family of perfluorosulfonate ionomers (PFSI) [76] are commercialized. For example, Nafion (DuPont) (scheme 1.1), and Flemion (Asahi glass) (scheme 1.2).

1.3.1 (d) Polypentenamer ionomers



Scheme 1.3 A typical carboxylated polypentenamer

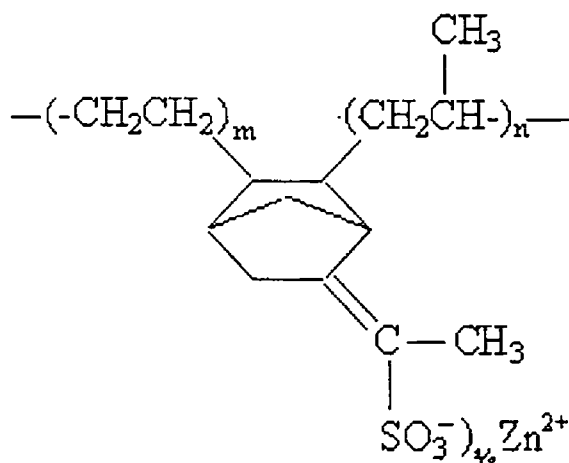
A typical carboxylated polypentenamer is shown below as scheme 1.3. Polypentenamer is a noncrystalline polymer whereas the hydrogenated [77] products are partially crystalline. A series of studies on hydrogenated polypentenamers using materials containing carboxylate, sulphonate and phosphonate groups were done [78, 79].

1.3.2. Rubber based ionomers

1.3.2. (a). Butadiene ionomers

They include the carboxylated rubber [80, 81] neutralized with metal ions such as zinc, magnesium, calcium, cadmium, tin and butadiene-acrylonitrile-methacrylic acid ionomers [82].

1.3.2.(b). Ethylene-propylene-diene terpolymers



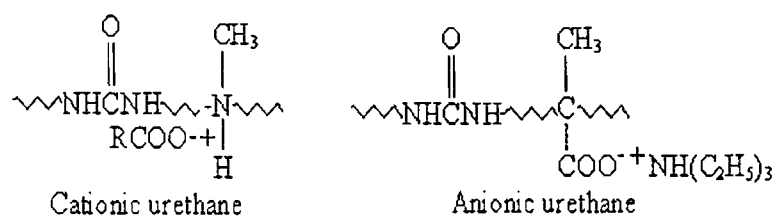
Scheme 1.4. Zinc sulphonated EPDM

A great variety of studies has been performed on the zinc salt of sulphonated ethylene-propylene terpolymers with 5-ethylidene-2-norbornene [83] (ENB). The zinc ion was found to be the most useful counter ion, as it shows excellent ionic cross link properties at low temperatures while preserving a relatively low viscosity at the

processing temperature. This is in contrast to the sodium ion. The zinc sulphonated EPDM has the structure shown in scheme 1.4.

1.3.2 (c). Polyurethane ionomers

Ionomers based on polyurethane emerge in to a class of materials possessing excellent applications. Hence, the synthesis and characterisation of these ionomers [84] become a topic of great interest. An extensive series of investigations on polyurethane [85-88] ionomers are available. The most technically interesting property of polyurethane ionomers is their ability to form stable dispersions in water. Both cationic and anionic type urethane ionomers are shown in scheme 1.5.



Scheme 1.5. Cationic and anionic type urethane ionomers

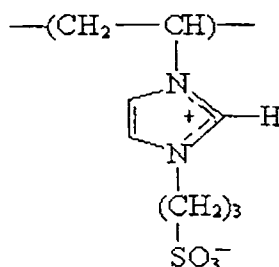
1.3.3. Acrylate and methacrylate ionomers

Synthesis and characterization of acrylate [89-92] and methacrylate [93] ionomers is an area of good interest. The PMMA ionomer has some of the hallmarks of a composite system i.e., longer rubbery plateau and the decrease in the area under loss tangent peak. These materials possess relatively high glass transition temperature.

1.3.4. Zwitter ionomers

The anion and cation in these ionomers are attached to each other and to the main chain. There are two categories of zwitter ionomers: a) siloxane based di-zwitter

ionomers [94-98] in which the ion concentration ranges from 0.5-10-mol percentage and b) hydrocarbon based zwitter ionomers [99-105]. A typical ionomer of the latter type is shown in scheme 1.6



Scheme 1.6 Hydrocarbon based zwitter ionomers

1.3.5. Block copolymer ionomers (BCPI)

These ionomers have a regular architecture. Diblock [106, 107] (AB type), triblock [108] (ABA), bottle brushes [109] or the comb type, star block [110] and dendrimer [111] are the major types. Kennedy and Faust observed the first cationic polymerization of isobutylene monomers [112] in 1986.

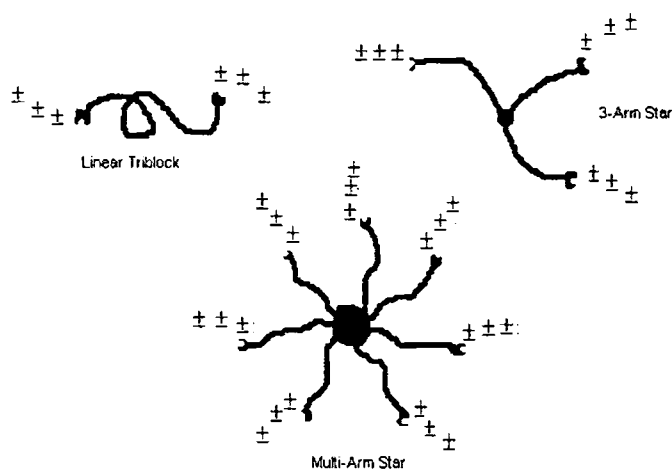
1.3.6 Monochelics, telechelics and star ionomers

In monochelics, an ion or ion pair is placed at only one end of a polymer chain. Large number of studies [113, 114] have been reported, although investigated only briefly. In the telechelics, ion or ion pair is placed at each end of the polymer chain [115, 116]. In stars an ion or ion pair terminates each of the arms emanating from a center point. Three-arm star and multiarm star have been studied extensively for isobutylene-based materials [55].

1.3.7 Ionenes

The ionic groups in these ionomers [117, 118] have a precise spacing along the backbone. An enormous range of ionenes can be synthesized by structures with aliphatic, aromatic or both sequences together [119]. An important paper in the field of ionenes was published by Klun [120] et al and a more recent study of ionenes

came from Wilkes group [121]. The tetra methyl ionene has been evaluated for its pharmacological and antiheparin action. Ionenes with segments of polypropylene oxide in the backbone have been evaluated as thermoplastic elastomers. Linear triblock, 3-arm star and multi arm star ionenes are represented in the scheme 1.7



Scheme 1.7 Linear triblock, 3-arm star and multi arm star ionenes

1.3.8 Polymer salt mixtures

The main reason for the interest in these systems lies in their potential use as solid polymer electrolytes [122]. This is because the low T_g materials exhibit high conductivity in the complete absence of water. Low molecular weight ethers form polymer salt mixtures [123], in which the interactions between polyethylene oxide (PEO) and polypropylene oxide (PPrO) and salts such as lithium per chlorate (LiClO_4) and potassium iodide were studied. Major investigations on polymer salt mixtures include inorganic salt nitrates, PMMA [124], polyvinyl alcohol, polyacrylonitrile [125] etc.

1.3.9 Graft ionomers

Studies include short polyacrylic acid side chains grafted on to a nonionic backbone (eg: polystyrene) and the large family of cellulose with grafted acrylate or methacrylate chains [126]. Ionic chains with nonionic grafts are also possible.

1.4. Synthesis of ionomers

1.4.1. General methods

1.4.1(a). Copolymerization:

A low level of functionalized monomer is copolymerized with an olefinically unsaturated monomer. Carboxyl containing ionomers are synthesized by the direct copolymerization [127] of acrylic or methacrylic acid with ethylene, styrene and similar monomers by free radical copolymerization. The resulting copolymer is obtained as the free acid, which can be neutralized to the intended level with metal hydroxides, acetates and similar salts.

1.4.1 (b). Modification of preformed polymer:

Sulphonation of the copolymer of polystyrene-divinyl benzene [128], EPDM [129], and polychloroprene [130] yield sulphonated derivatives with a level of sulphonic acid groups in proportion to the amount of sulfonating agent [131]. Typically these reactions are conducted in homogenous solutions, permitting the direct neutralization of the acid functionality to the desired level. Isolation of the neutralized ionomer is then effected by conventional polymer isolation techniques.

1.4.1 (c). The extruder reaction technique [132]

Sulphonation of oil extended EPDM can be carried out at 90-100°C for 6-12 minutes followed by the melt extruder neutralization using zinc stearate [133]. Although the preparation of other types of ionomers based on phosphonate [7] are reported, only carboxylate and sulphonate derivatives are useful commercially.

1.4.2. Carboxylated ionomers

Typically less than 6% of acrylic acid and methacrylic acid groups are incorporated in to polymers by free radical polymerization. Styrene-butadiene-acrylic acid, butadiene-acrylonitrile-acrylic acid and butadiene-acrylic acid polymers are the typical examples.

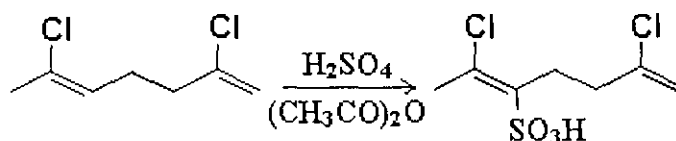
Vast majorities of commercially available carboxylated elastomers are prepared by emulsion polymerization [134]. The typical formulation for the preparation of conventional carboxylated elastomers is shown in the table 1.2. Anionic or free radical initiated polymerization followed by the neutralization with metal alkoxides produces halatotelechelic ionomers [135,136].

Table 1.2 Typical formulation for the preparation of conventional carboxylated elastomers

System	Number of parts
Butadiene (combination with other monomers)	100
Water (deionised)	100
Methacrylic acid	5
Sodium alkyl aryl polyether sulphate	1
Potassium per sulphate	0.4
Temperature	30-50°C

1.4.3. Sulphonated Ionomers

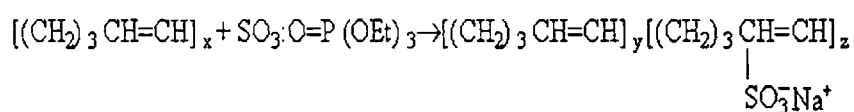
The sulphonation agent that is preferred at ambient temperature is acetyl sulphate, generated by reaction of acetic anhydride and concentrated sulphuric acid. The sulphonation proceeds typically at 95 % conversion of sulphuric acid to polymer-sulphonic acid based on titration of the final product.



Scheme 1.8. Sulphonation reaction in polychloroprene rubber

The free acids possess low strength and are less stable thermally. On being neutralized with metallic bases, the bulk and solution properties of the neutralized

products are changed markedly. Examples include ionic polychloroprene rubber, EPDM, SBR, and NBR. The sulphonation reaction in polychloroprene rubber is represented in the scheme 1.8. The sulphonation procedure was utilized for the preparation of linear telechelic polyisobutylene, diolefins [55] and radial star triolefins. More recently Storey and coworkers have achieved living cationic polymerizations of isobutylene and styrene producing linear triblock, 3-arm star and multi-arm star ionomers [112]. These polymerizations utilize either dicumyl or tricumyl chloride as initiators for two or three-arm star polymers respectively [137].



Scheme 1.9 sulphonation of polypentenamer

The successful sulphonation of polypentenamer in chloroform at room temperature [138] has been reported. The reaction is represented as scheme 1.9. A number of publications [132, 139] have now shown that styrene sulphonates can be copolymerized with a variety of monomers in conventional emulsion polymerizations. In this respect the styrene derivative appears more suitable to successful copolymerization with nonpolar comonomers than a variety of other sulphonate moieties. The copolymerization of sodium styrene sulphonate with alkyl methacrylate has been reported [51]. In the work of Eisenberg [140], he compares the products of emulsion copolymerization of styrene and sodium styrene sulphonate with those prepared by direct sulphonation of polystyrene. The results suggest that emulsion copolymerization routes can lead to non-random incorporation of sulphonate groups in the polymer chain. Zwitter ionomers based on polyurethane are prepared from a prepolymer and a diisocyanate in the presence of a tertiary amine containing diol extender, such as N-methyl diethanolamine, dissolving the polyurethane produced in dimethyl acetamide and adding the suitable amount of gamma - propane sultone. Reaction of zwitter ionomers with the suitable metal acetate results in a metal sulfonyl ion pair, and reduction to the tertiary amine of the ammonium ion, with the generation of methyl acetate.

1.5. Morphology of ionomers

1.5.1. Multiplet-cluster model

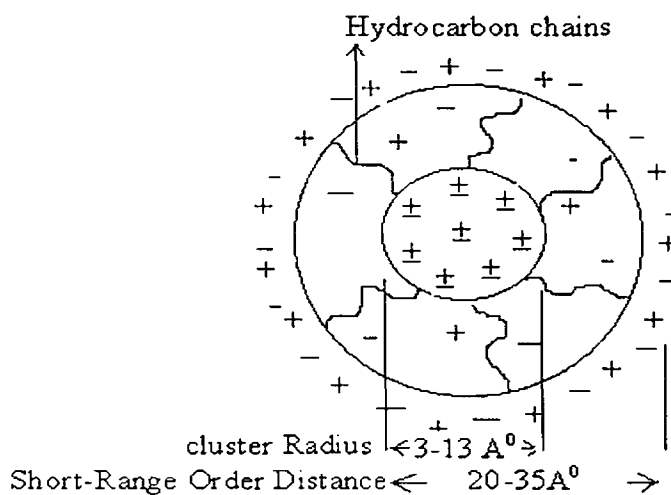
The spatial arrangement of salt groups in ionomers, according to Eisenberg [140], assumes contact ion pairs. Due to the steric considerations only a small number of ion pairs can associate as "multiplet", without the presence of the hydrocarbon matrix. The multiplets have a tendency to associate further in to "clusters" which contain a considerable quantity of hydrocarbon material. This association is favoured by electrostatic interactions between multiplets and opposed by forces arising from the elastic nature of the backbone chains. The assumption that the clustering would not make any dimensional change to the polymer chains was later corrected [141,142]. This model is inadequate for the illustration of the properties of the ionomers. The multiplet-cluster concentration ratio varies with the backbone, acid type and neutralizing species.

1.5.2. Hard-sphere model

Yarusso and Cooper [143] who proposed this model assumes that the multiplets have a liquid like order at a distance of closest approach, determined by the hydrocarbon layer attached to and surrounding each multiplet. This model postulated a distance of closest approach of the multiplets, which was equivalent to a hard sphere diameter somewhat larger than that of the multiplet itself.

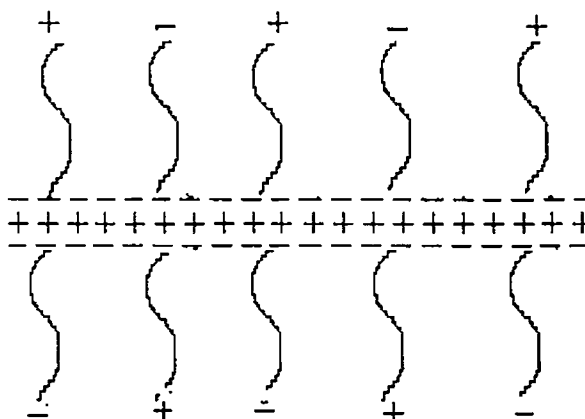
1.5.3. Core shell model

This is an intracluster model (scheme 1.10) proposed by Mc Knight et al. [144]. The ion pairs form a core that is surrounded by a shell of material of low electron density, which in turn, surrounded by another shell of somewhat higher electron density but lower than that of core itself. The core radius is of 8-10Å and contains ~50 ion pairs. The hydrocarbon shell surrounding this multiplet is of the order of 20 Å.



Scheme 1.10 Core shell model proposed by Mc Knight et al.

1.5.4. Intracluster lamellar shell core model



Scheme 1.11 Intracluster Lamellar Shell core model

This model proposed by Roche et al. [145] assumes that the geometry of ion rich phase is lamellar. The model is shown in the scheme 1.11. The central lamella of high electron density is sandwiched between lamella of low electron density

hydrocarbon material, which in turn is sandwiched between layers of intermediate electron density. Interlamellar distance is responsible for the ionic peak.

1.5.5. Eisenberg-Hird-Moore (EHM) model

Since the electrostatic energy released during multiplet formation is considerable and surface energies are also important, a certain amount of crowding in the immediate vicinity of multiplet is to be expected as a result of driving forces, which tend to enlarge the multiplet. A certain amount of chain extension in the immediate vicinity of the multiplet helps to accommodate a large number of chains. All these factors contribute to the reduction in the mobility.

1.5.6. New cluster concept

At higher ion content restricted mobility regions of independent multiples overlap and exceed the threshold size for independent phase behaviour ($50-100 \text{ \AA}^0$) at which they exhibit their own T_g . This overlapped region of restricted mobility is the cluster [146].

1.6. Ionomer behaviour- A generic view

Properties of the ionomer resins vary with the amount and type of metal cation and the proportion of the comonomer. The presence of relatively low levels of metal carboxylate or sulphonate groups pendant to a polymer chain clearly has profound effects on polymer properties. Specific properties such as the polymer glass transition, dynamic mechanical behaviour [147], the rubbery modulus above the glass transition, the melt rheology [148], the relaxation behaviour, dielectric properties and polymer solution behaviour are all modified by the presence of low levels of ionic groups. Ionomers containing zinc cation have better flow, impact strength, tear strength, paint adhesion, and lower moisture absorption. Those containing the sodium cation offer lower haze and improved stress crack resistance, while the addition of the lithium cation increases the modulus. The good thermal stability, outstanding chemical resistance, and low moisture vapor transmission of ionomers

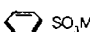

result from their polyolefin like structure. However the interchain ionic cross-linking contributes excellent abrasion, puncture and impact resistance as well as low temperature toughness. More over most ionomers have good optical clarity and the less crystalline grades have superior clarity.

Most commercial grades of ionomers comply with FDA regulations for food contact and food packaging, which leads to their widespread use in this industry as film. Solvent resistance varies with the level of metal cation, but most ionomers are insoluble in common organic solvents at room temperature and resistant to mild acids and bases.

1.7. Investigation on ionomers

1.7.1. Infrared spectroscopy.

Table 1.3 Characteristic ionomer peaks of major interest

Characteristic groups	Wave number (cm ⁻¹)
COO-Na ⁺	230
COO-Li ⁺	450
SO ₃ -Na ⁺ (3.8 mol%)	250
SO ₃ -Na ⁺ >(3.8 mol%)	170
SO ₃ -Cs ⁺	115
SO ₃ -Ba ²⁺	185
C=O _{str}	1750
Tg of styrene based	1700, 1745 kinks
 SO ₃ M	1010
 SO ₃ ⁻	1127
(SO ₃) ₂ Zn sym.str.	1042
SO ₃ ²⁻ asy. Str (doublet)	1172, 1235
COO-Cs ⁺	135

The characteristic FTIR absorbances for styrene sulphonates have been identified [149]. FTIR was used to characterize sulphonated poly (styrene-ethylene/butylene-styrene) ionomers [150], carboxylate ionomers [151], identification of the type of metal

ion neutralized [152, 153], degree of neutralization [154], glass transition temperature [155], surface characterisation [156], micro phase separation [157], plasticizing effect [158], and blend characterisation [159]. Characteristic peaks of major interest are included in the table 1.3.

1.7.2. NMR spectroscopy

Although only few NMR studies have been made on ionomers, important among them are the relaxation phenomena [160], evaluation of ionomers based on ethylene methacrylic acid [161], extent of ion aggregation [162], butadiene-methacrylic acid ionomers [163] and counter ion effect in membranes [164].

1.7.3. Electron microscopy

Owing to the absence of spherulite formation rather than crystallinity, ionomers exhibit a high degree of clarity [28]. This can be made more vivid by comparing the surfaces of ionomer and host polymer [165]. A better insight in to the morphology of ionomers, although not about ionic clusters, was gained from an examination of thin films prepared by casting from solution. Microtomed sections of sulphonated EPDM appeared to contain 300 nm phase separated regions. Osmium tetroxide staining of these EPDM sections showed domains averaging less than 3 nm in size primarily inside those regions.

1.7.4. Thermal studies

Thermogravimetric analysis, differential thermal analysis and differential scanning calorimetry [166] have been extensively used for the investigation of the thermo-oxidative stability of styrene based [167] ionomers. It was found that the softening temperature and thermo-oxidative stability increased with increase in ion content [168]. The neutralization with group 1 metal was found to increase the thermal stability and group 2 metals increased the oxidative stability.

1.8 Properties of ionomer

1.8.1 The glass transition temperature.

An increase in T_g has been noted when the ions reduce the segmental mobility of polymer chain. This has been attributed to: a) copolymer effect; where the ionic groups function as a bulky side group and b) ionic groups act as an interchain cross-link. T_g is influenced by molecular weight (M) and density of cross-links (ρ)

$$T_g = T_g(\alpha) - k/M + k_x \rho$$

$T_g(\alpha)$ for an infinite linear chain, ρ - Density of cross-links in g mol^{-1} , k and k_x are constants. T_g is influenced by water content; more the water content lower [169] will be T_g . Sulphonic acid group has a greater T_g of $\sim 75^\circ\text{C}$ compared to carboxyl ionomers [170]. Recently T_g of electrometric halato telechelic ionomers has been reported [171].

1.8.2 Mechanical properties

The unusual structural features of the ionomers can be revealed from mechanical property studies. Relaxation behaviour of ethylene ionomers, confirmed by X-ray and electron microscopy measurements give striking evidences for the cluster formation [172]. Effect of temperature on the molecular relaxation expressed in terms "shift factor" $\log a_T$ by William, Landel and Ferry (WLF) equation

$$\log a_T = -C_1(T-T_g) / C_2 + (T-T_g)$$

C_1 and C_2 are WLF coefficients, T_g of the polymer is taken as the reference temperature. This equation is useful in the analysis of mechanical properties in the region of glass rubber transition. An elaborate discussion of tri-armed star ionomers, oligomers, polypentenamers [173], EPDM [174] has been reported. The response of different cations to tensile properties indicate that ion pair association and the resulting network formation due to aggregation is more important than cation valency. Stress relaxation studies using dynamical mechanical behaviour i.e., shear modulus and loss tangent peaks broadened with increase in ion content [175].

1.8.3 Electrical properties

The ionic content has direct influence on the conductivity of ionomers. In the case of ethylene copolymer ionomers the dielectric relaxation behaviour parallels the mechanical behaviour. α , β , β' and χ loss peaks were identified. α -peak is the glass transition temperature associated with the ionic clusters, β and β' are low temperature loss peaks which arises due to the motion of hydrocarbon chains to which are attached a small number of salt groups. The electrical properties of the styrene based ionomers have been studied extensively [176].

1.8.4 Dynamic mechanical properties

Unlike the nonionic polymers, the modulus temperature curves show a rubbery plateau for ionomers. So it provides definitive evidence that the salt forms of these systems are different from their host polymers [177]. The zinc sulphonated EPDM systems show a virtual constancy up to 200°C, even at low ionic concentrations, but its nonionic counterpart displays viscous flow above 50°C. For styrene-based systems the DM behaviour shows evidence of micro phase separation. A single loss tangent peak is observed for the parent polymer; where as two such peaks of high intensity appear for the ionomers [178]. This may be due to two-glass transition temperatures (T_{g1} and T_{g2}), one corresponding to the polymer matrix and the other for the phase separated regions containing ionic groups.

1.8.5 Reinforcement by fillers

Ionomers show many properties of filled systems, especially at intermediate ion contents, in which the multiplets and the clusters behave as ultrafine particles of fillers. The use of filler/ionomer composites has been studied elaborately. Precipitated silica has been found to improve the physical properties and melt viscosity of zinc sulphonated EPDM. DMA studies show that silica [179] reinforces the polymer backbone and weakens ionic associations. The effect of clay [180] on the

thermoplastic (TP) property of EPDM salt showed that it enhances the physical properties while the melt viscosity of the clay filled ionomer is reduced by zinc stearate. The influence of zinc stearate and paraffin oil on HAF carbon black filled EPDM [181] based thermoplastic elastomers showed the lowest viscosity. Zinc stearate act both as a plasticizer and reinforcing filler on zinc sulphonated EPDM, and sodium salt of maleated EPDM rubber at ambient temperature [158].

1.8.6 Blend and compatibilising property

A wide range of electrostatic interactions can be used to enhance miscibility in polymer blends. Considering different arsenal of possible interactions, one can choose the best polymer pairs of enhanced miscibility. A large number of ionomer blends have been studied [182-184]. Ionomers can be used to impart sufficient interaction between the blend components to produce useful properties [185-187]. The compatibilising effect of styrene-co-4-vinylpyridine (SVP) random copolymers on the immiscible polystyrene (PS) – polyethylene based ionomer (Surlyn) blends were examined. FTIR results suggest that the compatibilization in this blend system is attributed to the ion-dipole interaction between the polar VP groups of SVP copolymer and ionic groups of surlyn. Blends of polyamide-6 (PA-6) with sulphonated polystyrene ionomers [188] show considerable miscibility enhancement when the counter ion is lithium but are immiscible when the counter ion is sodium. Of late compatibilization of PP/Vectra B “in situ” composites by means of an ionomer [189] has been reported.

1.9. Chemical reactions in ionomers

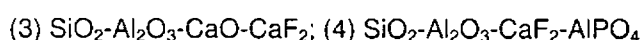
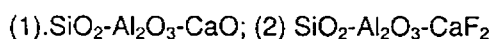
A range of chemical reactions can be performed in the ionic aggregates in ionomers. The multiplets in the ionomers could be used as micro reactors (nanoparticles) after swelling with a suitable solvent such as water [190]. By means of ion exchange process rhodium ions (Rh^{3+}) or ruthenium ions could be inserted in to styrene-co-styrene sulphonate ionomers [191]. The transition metal ions in the ionomer aggregates were used as catalysts in reactions involving carbon monoxide, methanol

or ethanol to give various carbonyls or with hydrogen to form hydrides. Formation of nanoparticle in cadmium methacrylate [192], perfluorosulphonate [193] and ethylene carboxylate ionomers [194] have been reported. The PTFE acid resins [195, 196] can be used as super acid catalysts for various reactions like alkylation of benzene and trans alkylation's of alkyl benzenes, the pinacole rearrangement and deacetylation and decarboxylation of aromatic molecules. The Ag^+ - PTFE ionomer reacts with carbon monoxide to form a silver carbonyl was investigated [197]. However other transition metal-PTFE ionomers do not react with carbon monoxide.

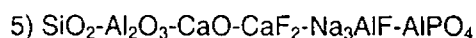
1.10 Glass ionomers

1.10.1 General remarks

They represent the most diverse class of polyelectrolyte cements and are also known as ion-leachable glass. Most glass ionomers are based on calcium aluminosilicate glasses [197]. The aluminosilicate poly (alkenoic acid) (ASPA) ionomer is prepared by fusing a mixture of calcium oxide or fluoride, alumina and silica with aluminum phosphate and cryolite as flux at 1000-1500°C. The product is then shock cooled by pouring the melt on to a metal tray and plunging the hot solidified glass in to water and ground in to a fine powder. Both (1) & (2) show, three components [198] glass ionomers and (3) & (4) represent four phase glasses [199].



The most complex glass used in practical formulations [200] is represented as (5)



The presence of fluoride in the fusion mixture confers certain advantages in preparing the glass and on cement properties, they are:

- a) Lowering of fusion temperature,
- b) Improvement in the strength of cement,
- c) Enhanced working property of cement paste, and
- d) For dental fillings it gives a cariostatic property (i.e. against dental decay).

The other important chemical feature is the $\text{Al}_2\text{O}_3 / \text{SiO}_2$ ratio, which controls the setting time of the cement.

1.10.2. Uses of glass ionomer

1.10.2 a) Dental applications

Glass ionomers were developed in response to the need for improved filling and luting materials. Traditional filling materials, the dental amalgam and the dental silicate cement, and the more recently developed composite resins act as little more than mechanical plugs. They can contain free monomer or stray strong acid, which insult the dental pulp. They are not adhesive, so that cavities have to be under cut, with the loss of sound tooth material, to ensure that the filling is held in place mechanically. Moreover, the lack of adhesion between filling and the cavity wall allows bacteria to penetrate down the margin and initiate secondary caries (dental decay). The glass ionomer is, by contrast, both bland and adhesive, in which the latter property is the most important. It enables a carious lesion to be restored with the minimum of the cavity preparation; trauma caused by drilling is reduced and it is very important in pediatric dentistry. This cement also, by releasing fluoride ions [201], protects adjacent tooth enamel against caries. The glass ionomer can also be used to restore small erosion lesions caused, not by caries, but by abrasion and erosion. These lesions are sensitive yet they are too small to require an under cut cavity needed for conventional materials. They are also used in preventive dentistry to seal or fill naturally occurring pits and fissures found in molar teeth that act as sites for the development of caries. The glass ionomer cement and the opaque zinc polycarboxylate cement are also used as luting cements to attach crowns and inlays to teeth.

1.10.2 b) Surgical applications

A new splint bandage based on glass ionomer cement was successfully introduced [202]. Since plaster of paris is a weak material, in the conventional cases the splint bandages must be bulky enough to obtain sufficient strength. However a coat of a

mixture of borate, phosphate and aluminosilicate glasses together with dry poly acrylic acid powder on cotton gauze hardens in presence of water. Compared with plaster of paris, the glass ionomer bandage is lighter and develops rapidly. The bandage is resistant to water also. The material can be handled similar to plaster of paris.

1.10.2 (c) Miscellaneous

Glass ionomers are useful as a material for sealing for asbestos based materials, which otherwise would be abraded or form dust causing health hazards. It can be used as a substitute for plaster of paris in pottery industry. The use of glass ionomer for forming slip-casting moulds has also been reported. They have also been tested as binders for foundry sands.

1.11 Ionomers in service of mankind

The fast pace in the envious growth of ionomers relies extensively on its innumerable service to the mankind. Most ionomer applications make use of several characteristics, which can be accounted for in terms of ionic aggregation or cluster formation or the interaction of polar group with the ionic aggregates. Properties of the ionomer resins vary with the amount and type of metal cation and the proportion of the comonomer. Applications of ionomers fall in to the following categories:

1.11.1. Permselective membranes

Perfluorosulphonates (Nafion) and perfluorocarboxylates (Flemion) membranes exhibit super perm selectivity [203]. These membranes with exceptional stability allow the cations to pass through the membrane relatively rapidly while limiting the entry of anions. The perfluorinated ionomers are largely used in chlor-alkali industry, which separates chlorine and hydrogen produced during the electrolysis of aqueous sodium chloride at anode and cathode respectively. However sulphonated perfluoro ionomers are used as solid polymer electrolytes [23].

1.11.2. Food and pharmaceutical industry

The unique properties of ethylene ionomers such as oil and chemical resistance, flex resistance, resistance to impact, the ability to be heat sealed under a broad range of conditions, adhesive property, excellent optical properties and high melt strength make it useful for the vacuum packaging of meat, tear-open packages for food and pharmaceutical products, heavy gauge film for electronic products etc.

1.11.3. Shatter proof glass

The direct coating of polyurethane ionomers on to glass objects reduces the danger of breakage. A sandwich coat of the ionomer can be applied from aqueous solutions.

1.11.4. Agriculture

A coating of zinc sulphonated EPDM on the micro spheres of urea can be arranged to produce maximum release of the manure at the height of the growing season [204].

1.11.5. Industrial floor polishes

Zinc cross-linked carboxylated copolymer can be used as a successful floor polish [205] and could be applied from aqueous solution. Once deposited properties such as durability are expected, even when wet footwear comes in to contact with the floor. Removal of the coating can be accomplished in an aqueous solution in the presence of ammonia, which complexes the zinc, softens the coating layer, and allows removal.

1.11.6. Photography

Styrene-n-butyl methacrylate-potassium methacrylate terpolymer was used as a binder in toners involving carbon black in electro photography [206, 207]. Another compound is ionic polystyrene [208] containing cyclopropene unit and the counter ion

such as tetrachloride aluminate. Exposure of this polymer to light produces cross linking, which renders it insoluble, in contrast to the unexposed region from which it can be removed with a solvent. The extensive applications of various ionomers [209] in silver halide photography, as mordent polymers for anionic dye molecules [210, 211] have been reported.

1.11.7. Magnetic recording tapes

Ionic polyurethane made from polyisocyanate and polyhydroxy compounds serve both as a binder and as a dispersing agent in magnetic tape formation [206].

1.11.8. Adhesives

Owing to the high melt strength and their amphiphilic nature, the carboxylated and sulphonated ionomers have been widely used as adhesives [212].

1.11.9. Sporting goods

As a plastic material ionomers are useful for making sporting goods such as golf balls, bowling pins, ice skates, ski boots, wrestling mats and shoe parts, especially for athletic footwear [213]. The moldability and toughness are the two properties of the ionomers, which are made use of in all these applications. The golf ball with ethylene ionomer covers has been used extensively in the amateur market.

1.11.10. Automobile industry

Ionomers have found extensive applications as bulk plastic materials [214] in making automobile parts such as bumper guards, side molding strips, exterior trim etc.

1.11.11. Thermoplastic elastomers

Zinc sulphonated EPDM plasticized with zinc stearate can be injection molded like any other thermoplastic elastomers [212]. It can also be used as a roofing membrane [208].

1.11.12. Drilling fluids

Sulphonated polystyrene ionomers are used as oil based drilling fluids [215] to enhance the suspension of the various agents in the drilling operation. The interaction of the functional groups with solid particles produced during drilling also appears to be advantageous in preventing settling of the material, which might result in damage to the drill bit.

1.11.13 In chemistry

Ionomers can be used catalytically. Perfluoro sulphonic acid catalyses organic reactions such as pinacole-pinacolone rearrangement, deacetylation and decarboxylation of aromatic rings [216]. The use of metal ions in ionomers as catalyst [217] has also been published.

1.11.14 Medical uses

Glass ionomers have been used as a dental filling in dentistry [201]. Split bandages based on glass ionomers [202] are useful in surgical applications.

1.12. Recent studies on ionomers

A number of reviews on ionomers, a promising and challenging area of modern polymer science and technology, are available. Ionomers based on chloroprene, polyurethane, telechelics, sulphonated EPDM, besides liquid crystalline ionomers are gaining momentum, of late. Copolymers of styrene and acrylic acid, perfluorinated ionomers and its silicate hybrid membranes along with polypyrrole coated polystyrene sulphonic acid micro spheres, a proton electrolyte [218] are few among the reported studies. Reactive compatibilization of blends containing liquid crystalline polymers [219], electrochemical characterisation of PAN ionomer [220] and ionomers based on block copolymer poly (styrene isobutylene styrene) [221] have been studied extensively. The proton conduction and methanol permeation in ionomer membranes

based on partially sulphonated polystyrene [222], crystallization kinetics of maleic anhydride grafted polypropylene ionomers [223], crystal phase and crystallinity of polyamide 6/ functionalized poly olefin blends [224] and studies on the fluorescence behaviour [225] are some of the notable contributions in ionomers. Other contributions to the family of ionomers include the swelling behaviour of per fluorinated ionomer membranes in ethanol/water mixtures and a large number of studies on the solution behaviour [226] and miscibility studies [227-229]. Recent studies on ionomers include membrane property of sulphonated naphthalenic polyimides [230], dual polyelectrolyte/ ionomer behaviour [231], insitu rehydration of Perfluoro sulphonated ion exchange membranes [232], SAN study of blends [233], liquid crystalline polymer compatibilization [234-236] and comparison of clustering in various acrylate ionomers [237].

The most important investigations in the field of ionomers, during the year 2001, include the synthesis and characterisation of ion-conducting polymer systems based on EPDM blends [238], kinetic study and characterisation of sulphonated poly (ether ether ketone) (PEEK) [239] etc. The current year, i.e., 2002 has been witnessing a large number of studies on ionomer systems. Online search of the most recent publications in the category of ionomers has been done. The influence of carboxylic group content on properties of ionic elastomers based on carboxylated nitrile rubber (XNBR) and zinc peroxide [240], ion aggregation in the polysiloxane ionomers bearing pendant quaternary ammonium groups [241] are some of the most recent publications. Wetting properties of polystyrene ionomers treated with plasma source ion implantation [242] and simulation study on molecular relaxation in ionomer melts [243] also have been reported of late.

1.13 Scope of the work

The industrial importance of natural rubber, for making rubber products of good resilience combined with good physical properties, is growing up. Unvulcanised natural rubber, however, is not used for the manufacture of rubber products, as it has very poor strength, and very poor resistance against thermo-oxidative degradation.

Requirement of rubber products with the specifications of reprocessability, thermo-oxidative stability etc, therefore, necessitates suitable modification for the natural rubber.

Several techniques have been resorted to the modification of NR to improve its properties. Vulcanization appears to be one of the effective chemical techniques for improving the properties of the rubber. Although several alternatives have been proposed, none could effectively replace vulcanization. Vulcanization, though, forms the backbone of rubber industry, suffers from the major drawback of producing only thermoset products. Being non-biodegradable, the worn out vulcanized rubber products pose a very serious threat to the environment. Resistance to thermo-oxidative degradation is an important criterion to be satisfied for rubber products used in outdoor applications. Introduction of suitable ionic groups in to an elastomer produces ion aggregated centers within the polymer matrix, which act as heat fugitive crosslinks and brings about enhancement in the properties and makes the material reprocessable.

Ionomer modification of natural rubber is an attempt to improve its physical properties using the technique avoiding vulcanisation and to make the elastomer reprocessable. Zinc salt of sulphonated styrene grafted natural rubber (ionomer) could find application as a compatibilizer in blends of SBR with other polar rubbers like NBR in the production of useful rubber products. Presence of polar ionic centers in these ionomers polarisable in the microwave frequencies may help them to be useful as components in microwave devices. The effect of fillers on the ionic form of the modified natural rubber, to improve its properties further, may be carried out using carbon black (HAF), silica, zinc stearate, nylon fibers and glass fibers.

1.14 Conclusion

Review of the literature on ionomers revealed that ionomers are polymers having a promising, scopeful, challenging and enviable list of uses. Although many synthetic rubbers were chemically modified in to ionomers, no attempt was made on natural rubber. The scope of the ionomeric modification of NR was envisaged in this chapter.

1.15 References

1. Eisenberg, A.; Ed. "*Ions in Polymers*", Wiley, New York, 1974. Advances in Chemistry, 187. American Chemical Society. Washington. D.C. (1982).
2. Holliday, L.; Ed. "*Ionic Polymers*", Applied Science. London (1975).
3. Wilson, F. C., Long worth, R. and Vaughan, D.J; *ACS Polymer Preprints*, 9, 505, (1968).
4. Eisenberg, A.; *Macromolecules*, 3,147, (1970).
5. Eisenberg, A. and King, M.; "*Ion-Containing Polymers*", Ch.1; New York, Academic Press, (1977).
6. Pineri, M.; In "*Developments of Ionic Polymers*",(Ed. Wilson, A.D. and Prosser, H.J.), vol.2, ch.3; London, Elsevier Science, (1986).
7. Macknight, W.J. and Earnest, T.R. Jr.; *J.Polym.Sci.Macromol.Rev.* 16, 41, (1981).
8. Eisenberg, A. and Rinaudo, M.; *Polym. Bull.*, 24, 671, (1990).
9. Pineri, M; Eisenberg, A.; Eds. "*Structure and Properties of Ionomers*"; NATO ASI series C, 198; Reidel: Dordrecht, The Netherlands, (1987).
10. Salmen, L.; Htun, M., Eds; "*Properties of Ionic Polymers, Natural & Synthetic*", STFI meddelande; Stockholm, (1991).
11. Lundberg, R.D. In: "*Encyclopedia of Chemical Technology*"; Grayson, M., Ed.; Wiley: NewYork, 3rd ed., Vol. Suppl., 546, (1984).
12. Hara, M. and Sauer, J.A.; *J. Macromol. Sci.Rev. C Macromol. Chem.Phys.* 34, 325, (1994).
13. Lantman,C.W, Macknight.W.J, and Lundberg, R.D.; In: "*Comprehensive Polymer Science: The Synthesis, Characterisation, Reactions & Applications of Polymers*"; Booth, C.; Price, C., Eds; Pergamon: Oxford, UK, Vol. 2, Chapter 25, (1989).
14. Mauritz, K.A.; *J. Macromol.Sci. Rev.Macromol.chem..Phys.*, C28, 65-98, (1988).
15. Bazuin, C.G.; In: "*Polymeric Materials Encyclopedia*"; Salamone, J.C., Ed.; CRC; Boca Raton, FL, 3454, (1996).
16. M.Hara; In: "*Polymeric Materials Encyclopedia*"; Salamone, J.C., Ed.; CRC; Boca Raton, FL; 3473-3481(1996)
17. Longworth, R., In: "*Ionic Polymers*"; Holliday, Ed., Applied Science Publishers, London, ch. 2, (1973).
18. Longworth, R., "*Plastics and Rubber: Materials and Applications*", August 75 (1978).
19. Otocka, E. P., *Macromol. Sci.-Revs. Macromol. Chem.*, C5 (2) 275, (1971).
20. Eisenberg, A., *ACS Polymer Preprints* 14, 871, (1973).
21. Littman, E.R.; and Marvel, C.S.; *J. Am. Chem. Soc.*, 52, 287-294, (1930).

22. Rembaum, A.; Baumgartner, W.; Eisenberg, A. *J. Polym. Sci. Polym. Lett.*, 6, 159,(1968).
23. Schlick, S. Ed: "*Ionomers, Characterisation, Theory and Appl*". CRC Press: Boca Raton, FL, (1996).
24. Tant, M.R.; Mauritz, K.A.; Wilkes, G.L. Eds. "*Ionomers: Synthesis, Structure, Properties, and Applications*"; Chapman & Hall, New York, (1997).
25. Eisenberg, A.; Kim, J.-S.; "*Introduction to Ionomers*"; Wiley Interscience Publication, USA, (1998).
26. McAlevy, A.; *Halogenated Polyethylene, U.S. Patent* 2,405,971, Aug. 29, (1946).
27. Brown, H. P.; *Rubber Chem. Technol.* 35, 1347 (1957).
28. Rees, R. W. and Vaughan, D. J.; *Polym. Prepr. Am. Chem. Soc., Div. Polym. Chem.* 6a, 287 (1965).
29. Rees, R. W. and Vaughan, D. J.; *Polym. Prepr. Am. Chem. Soc., Div. Polym. Chem.* 6b, 296 (1965).
30. Macknight, W. J.; *Polym. Prepr. Am. Chem. Soc., Div. Polym. Chem.* 11, 504 (1970).
31. Otocka, E. P. and Eirich, F.R; *J. Polym. Sci., Part A-2* 6, 921 (1968).
32. Otocka, E. P. Hellman, M.Y. and Blyler, L. L.; *J. Appl. Phys.* 40, 4221 (1969).
33. Marx, C. L., Caulfield, D.F. and Cooper, S.L.; *Macromolecules* 6, 344 (1973).
34. Eisenberg, A, Ed., *J. Polym. Sci., Polym. Symp.* 45 (1974).
35. Eisenberg, A and Navaratil, M.; *Macromolecules* 6, 604 (1973).
36. Eisenberg, A and Navaratil, M.; *Macromolecules* 7, 90 (1974).
37. Dasgupta, A.M; David, D.J.; Misra, A.; *J. Appl. Polym. Sci.*, 44, 1213 (1992).
38. Mathis, A.; Zhng, Y.L.; Galin, J.C.; *Polymer* 32, 3080 (1991).
39. Chen, -show-An; Hsu, --Jen-sung. *Polymer* 34, 2776 (1993).
40. Chen, -Yun; Chen, -yun-Hsiu, *J. Appl. Polym. Sci.* 57, 255 (1995).
41. Pilati,-F.; Manaresi,-P.; Ruperto,-M.G.; Bonora,-V.; Munari,-A.; Fiorini,-M. *Polymer* 34, 2413 (1993).
42. Xinling Wang, Lei Wang, Hui Li, Xiaozhen Tang, and Feng-Chich Chang: *J. Appl. Polym. Sci.* 77, 184 (2000).
43. Rahrig, D.; Macknight, W. J. and Lenz, R. W.; *Macromolecules.* 12, 195 (1979).
44. Kennedy, J. P. and Story, R. F.; *Organic coatings and Appl. Polym. Sci. Proceedings*, 46, 182 (1982).
45. Mohajer, Y.; Tyagi, D.; Wilkes, G.L.; Storey R. F., and Kennedy, J. P.; *Polym. Bull.* 8, 47 (1982).
46. Bagrodia, S.; Mohajer, Y.; Wilkes, G. L.; Storey R. F., and Kennedy, J.P.; *Polym. Bull.* 8, 281 (1982)

47. Bagrodia, S.; Mohajer, Y.; Wilkes, G. L.; Storey R. F., and Kennedy, J. P; *Polym. Bull.* 9, 174 (1983).
 48. Bagrodia, S.; Wilkes, G. L. and Kennedy, J.P; *J. Rheol.*, 28,474 (1983).
 49. Mohajer, Y.; Bagrodia, S.; Wilkes, G. L.; Storey R. F., and Kennedy, J. P; *J. Appl. Polym. Sci.*29, 1943, (1984)
 50. Tant, G.; Wilkes, G. L. and Kennedy, J. P; *Polym. Preprints*, 26, 32 (1985).
 51. McGrath, J. E., *Polym. Prepr.* 24, 37 (1983).
 52. Eisenberg, A.; Smith P., and Zhou, L. L.; *Polym. Eng. and Sci.*, 22, 1117 (1982).
 53. Erdi, N. Z.; Morawetz, H.; *J. Colloid Sci.*, 19, 708 (1964).
 54. Fitzgerald, W. E.; Nielsen L. E.; *Proc. R. Soc. Ser. A.*, 282, 137, (1964).
 55. Ide, F.; Kodama, T.; Hasegaawa, A.; Yamamoto, O. *Kobunshi Kagaku*, 26, 873 (1969).
 56. Kim, J. -S.; Jackman, R. J.; Eisenberg, A.; *Macromolecules*, 27, 2789, (1994).
 57. Kim, J. -S.; Wu, G.; Eisenberg, A.; *Macromolecules*, 27, 814 (1994).
 58. Hird, B.; Eisenberg, A.; *Macromolecules*, 25, 6466 (1992).
 59. Gauthier, M.; Eisenberg, A.; *Macromolecules*, 23, 2066 (1990).
 60. Rigdal, M.; A. Eisenberg; *J. Polym. Sci. Polym. Phys. Ed.*, 19, 1641 (1981).
 61. Ludberg, R. D.; Makowski, H. S. In: " Ions in Polymers"; Eisenberg, A., Ed.; Advances in chemistry 187; American Chemical Society: Washington, DC, chapter 2, (1980).
 62. Weiss, R. A.; Fitzgerald, J. J.; Kim, D. *Macromolecules*, 24, 1071(1991).
 63. Hara, M.; Jar; Sauer, J. A.; *Polymer*, 32, 1622 (1991).
 64. Clas, S. -D.; Eisenberg, A.; *J. Polym. Sci. B Polym. Phys.*, 24, 2743 (1986).
 65. Clas, S. -D.; Eisenberg, A. *J. Polym. Sci. B Polym. Phys.*, 24, 2757 (1986).
 66. Clas, S. -D.; Eisenberg, A. *J. Polym. Sci. B Polym. Phys.*, 24, 2767 (1986).
 67. Gauthier, S.; Duchesne, D.; Eisenberg, A. *Macromolecules*, 20, 753 (1987).
 68. Wollmann, D.; Williams, C. E.; Eisenberg, A.; *Macromolecules*, 25,6775 (1992)
 69. Smith, P. *Ph.D. Dissertation*, McGill University (1985).
 70. Wilson, F. C.; Long worth, R.; Vaughan, D. J.; *Polym. Prepr. Am. Chem. Soc. Div. Polym. Chem.*, 9, 505 (1968).
 71. Macknight, W. J.; McKenna, L. W.; Read, B. E *J. Appl. Phys.*, 38,4208 (1967).
 72. Otocka, E. P.; Davis, D. D.; *Macromolecules*, 2, 47 (1969).
 73. Yano, S.; Yamashita, H.; Matsushita, K.; Aoki, K.; Yamauchi; *J. Colloid Polym. Sci.*, 259, 514 (1981).
 74. Hideki Hashimoto, Shoichi Kutsumizu, Kenji Tsunashima, and Shinichi Yano.; *Macromolecules*, 34, 1515 (2001).
 75. Eisenberg, A.; Yeager, H.L., Eds; "Perfluorinated Ionomer Membranes"; ACS Symposium Series 180; American Chemical Society: Washington, DC(1982).
-

76. Sanui, K.; Ienz, R. W.; Macknight, W. J.; *J. Polym. Sci. Polym. Chem. Ed.*, 12, 1965 (1974).
77. Sanui, K.; Macknight, W. J.; Ienz, R. W.; *Macromolecules*, 7, 101 (1974).
78. Earnest, T. R. jr.; Macknight, W. J. *Macromolecules*, 10, 206 (1977).
79. Azuma, C.; Macknight, W. J.; *J. Polym. Sci. Polym. Chem. Ed.*, 15, 547 (1977).
80. Brown, H. P.; *Rubber Chem. Technol.*, 30, 1347 (1957).
81. Cooper, W. *J. Polym. Sci.*, 28, 195 (1958).
82. Tobolsky, A. V.; Lyons, P. F.; Hata, N.; *Macromolecules*, 1, 515 (1968).
83. Agarwal, P. K.; Makowski, H.S.; Lundberg, R. D.; *Macromolecules*, 13, 1679 (1980).
84. Miller, J.A.; Hwang, K.K.S.; Yang C. Z., and Cooper, S. L.; *J. Elastomers and Plastics*, 15, 174 (1983).
85. Dieterich, D.; Keberle, W.; Witt, H. *Angew. Chem. Int. Ed. Engl.* 9, 40 (1970).
86. Hwang, K. K. S.; Yang, C. -Z.; Cooper, S. L.; *Polym. Eng. Sci.*, 21, 1027 (1981)
87. Yang, C. -Z.; Hwang, K. K. S.; Cooper, S. L.; *Makromol. Chem.*, 184, 651 (1983).
88. Lee, J. C.; Kim, B. K.; *J. Polym. Sci. A Polym. Chem.*, 32, 1983 (1994).
89. Matsuura, H.; Eisenberg, A.; *J. Polym. Sci. Polym. Phys. Ed.*, 14, 1201 (1976).
90. Eisenberg, A.; Matsuura, H.; Tsutsui, T. *J. Polym. Sci. Polym. Phys. Ed.* 18, 479 (1980).
91. Duchesne, D. *Ph.D. Thesis*, McGill University (1985).
92. Wollmann, D.; Williams, C.E.; Eisenberg, A. *Macromolecules*, 25, 6775 (1992).
93. Ma, X.; Sauer, J.A.; Hara, M. *Macromolecules*, 28, 3953 (1995).
94. Graiver, D.; Baer, E.; Litt, M.; Baney, R. H.; *J. Polym. Sci. Polym. Chem. Ed.*, 17, 3559 (1979).
95. Gravier, D.; Litt, M.; Baer, E.; *J. Polym. Sci. Polym. Chem. Ed.*, 17, 3573 (1979).
96. Gravier, D.; Litt, M.; Baer, E.; *J. Polym. Sci. Polym. Chem. Ed.*, 17, 3589 (1979).
97. Gravier, D.; Litt, M.; Baer, E.; *J. Polym. Sci. Polym. Chem. Ed.*, 17, 3607 (1979).
98. Gravier, D.; Litt, M.; Baer, E.; *J. Polym. Sci. Polym. Chem. Ed.*, 17, 3625 (1979).
99. Salomone, J. C.; Volksen, W.; Olson, A. P.; Israel, S. C.; *Polymer* 1978, 19, 1157 (1979).
100. Schilz, D. N.; Peiffer, D. G.; Agarwal, P. K.; Larabee, J.; Kaladas, J. J.; Soni, L.; Handwerker, B.; Garner, R. T. *Polymer*, 27, 1734 (1986).
101. Liaw, D. -J.; Lee, W. -F.; Whung, Y. -C.; Lin, M. -C.; *J. Appl. Poly. Sci.*, 34, 999 (1987).
102. Monroy Soto, V. M.; Galin, J. C. *Polymer*, 25, 121 (1984).
103. Zheng, Y. -L.; Galin, M.; Galin, J. -C.; *Polymer*, 29, 724 (1988).
104. Pujol-Fortin, M. -L.; Galin, J. -C.; *Macromolecules*, 24, 4523 (1991).
105. Ehmann, M.; Galin, J. -C.; *Polymer*, 33, 859 (1992).
106. Selb, J.; Gallot, Y. *J. Polym. Sci. Polym. Lett. Ed.*, 13, 615 (1975).

107. Allen, R. D.; Yilgor, I.; McGrath, J. E. In: "Coulombic Interactions in Macromolecular Systems"; Eisenberg, A.; Baily, F.E.; Eds; ACS Symposium Series 302; American Chemical Society: Washington, DC; Chapter 6 (1986).
 108. Weiss, R.A.; Sen, A.; Willis, C.L.; Pottick, L. A.; *Polymer* 32, 1867 (1991).
 109. Wollmann, D.; Williams, C. E.; Eisenberg, A.; *J. Polym. Sci. Polym. Phys. Ed.*, 28, 1979 (1990).
 110. Storey, R. F.; George, S.E.; Nelson, M.E.; *Macromolecules*, 24, 2920 (1991).
 111. Vanhest, J. C. M.; Baars, M. W. P. L.; Elissan-Roman, C.; Van Genderen, M.H. P.; Meijer, E. W. *Macromolecules*, 28, 6689 (1995).
 112. Faust, R.; Kennedy, J. P.; *J. Polym. Sci. Polym. Chem. Ed.* 25, 1847 (1987).
 113. Moller, M.; Omeis, J.; Mohleisen, E. In: "Reversible Polymeric Gels and Related Systems"; Russo, P.S.; Ed.ACS symposium series 350, American Chemical Society, Washington DC, chapter 7, (1987).
 114. Jalal, N.; Duplessix, R.; *J.Phys. France*, 49, 1775 (1988).
 115. Jerome, R.; In: "Telechelic Polymers: Synthesis and Applications"; Goethals, E. J.; Ed.; CRC: Boca Raton, FL, Chapter 11 (1989).
 116. Vanhooime, P.; Jerome, R.; In: "Ionomers: Characterisation, Theory and Applications"; Schlick, S., Ed.; CRC: Boca Raton, FL; Chapter 9 (1996).
 117. Tsutsui, T.In: "Development in Ionic Polymers 2"; Wilson, A. D., Ed.; Elsevier: NewYork, Chapter 4 (1980).
 118. Rembaum, A., Baumgartner, W.; Eisenberg, A.; *J. Polym. Sci. B Polym. Lett.* 6, 159 (1968).
 119. Eisenberg, A.; Matsuura, H.; Yokoyama, T.; *Polym. J.* 2, 117 (1971).
 120. Klun, T.P.; Wendling, L. A.; Van Bogart, J. W. C.; Robbins, A. F.; *J. Polym. Sci. A Polym.Chem.* 25, 87 (1987).
 121. Feng, D.; Wilkes, G. L.; Leir, C. M.; Stark, J. E.; *J. Macromol. Sci.Chem.*,A26, 1151(1989).
 122. Watanabe, M.; Sanui, K.; Ogata, N.; Inoue, F.; Kobayashi, T.; Ohtaki, Z.; *Polym. J.*, 16,711 (1984).
 123. Moacanin, J.; Cuddihy, E.F.; *J. Polym. Sci. C*, 313 (1966).
 124. Wissbrun, K.F.; Hannon, M.J. *J. Polym. Sci. Polym.Phys. Ed.*, 13, 2239 (1975).
 125. Reich, S.; Michaeli, I.; *J.Chem. Phys.*, 56, 2350 (1972).
 126. Vitta, S. B.; Stahel, E. P.; Stannct, V. T. *J. Macromol. Sci.Chem.*, A22, 579 (1985).
 127. Rees, R.W. (to E.I. Dupont de Nemours and Co.), U.S. 3322, 734(August 2, (1966).
 128. Rodriguez, S.; Linares, A.; Acosta, J.I.; *Macromol. Mater. Eng.*, 283 (2000).
 129. Ludberg, R. D.; Makowski, H.S. and Westerman, L.; *Adv. Chem. Ser.* 187, 67 (1980).
-

130. Chakravarthy, D.; Mal, D; Konar, J. and Anil K. Bhowmick; *J. Elastomers and Plastics*, 32 (2000).
131. *U S Patent* 3.870.841 (1995), invs: Makowski, H.S.; Lundberg, Singha,G.H.
132. Siadat, B.; Oster, B. and Lenz, R.W; *J.Appl. Polym. Sci.*, 26, 1027 (1981).
133. Lundberg, R. D.; Mackowski, H.S.; Bock, Zawadski, J T.; *U.S.Patent* 4, 157, 432 Assigned to Exxon and Research and Engineering Co., June 5 (1979).
134. Jenkins, D.K. and Duck, E.W. In: "*Ionic Polymers*", L. Holliday, Ed., Halstead Press, Wiley, New York, ch. 3 (1975).
135. Schulz, D.N. ; Sandra, J.C. and Willoughby B.G.; In: "*Anionic Polymerization: Kinetics Mechanisms, and Synthesis*", J.E. McGrath, Ed., A.C.S. Symposium Series 166, chapter 27, p. 427 (1981).
136. Jerome, R.; Horrión, J.; Fayt R., and Teyssie, P. *Macromolecules*. 17, 2447 (1984).
137. Storey, R.F.; *J.Mater. Sci.*, A29, 11, 1017 (1992).
138. Rahrig, D.; Macknight, W.J. and Lenz, R.W.; *Macromol.* 12, 195, (1979).
139. Weiss, R.A.; Ludberg, R.D. and Turner, S.R.; *J.Polym. Sci., Polym.Chem. Ed.* 23, 525 (1985).
140. Eisenberg, A.; *Macromolecules* 3, 147 (1970).
141. Forsman, A.; *Macromol.* 15, 1032 (1982).
142. Earnest, T.R.; Higgins, J.S.; Handlin D.L., and Macknight, W.J.; *Macromol.* 14, 192 (1981).
143. Yarusso, D.J.; Cooper, S.L. *Macromolecules*, 16, 1871 (1983).
144. Macknight, W.J.; Taggart, W.P.; Stein, R.S; *J. Polym. Sci. Symp.*, 45, 113 (1974).
145. Roche, E.J.; Stein, R.S.; Russel, T.P.; Macknight, W.J.; *J. Polym. Sci. Polym. Phys. Ed.* 18, 1497 (1980).
146. Eisenberg, A.; Hird, B.; Moore, R.B.; *Macromolecules*, 23, 4098 (1990).
147. Earnest, T.R. Jr.; Higgins, J.S. and Macknight, W.J.; *J. Polym. Sci.Polym. Phys. Ed.* 16, 143, (1978)
148. Shohami, E. and Eisenberg, A.; *J. Polym. Sci. Polym. Phys. Ed.* 14, 1211(1976)
149. Fitzgerald. J.J and Weiss, R.A, In:"*Coulombic Interactions in Macromolecular Systems*" (Eds. Eisenberg, A. and Fitzgerald) ACS Symp. Ser. 302: American Chemical Society, Washington, DC, P. 35 (1986).
150. Weiss. R.A. and Fitzgerald, J.J. In: "*Structure and Properties of Ionomers*"(Eds. Pineri, M. and Eisenberg, A.) Dordrecht. p. 361(1987).
151. Rouse, G.B.; Risen, W.M.Jr.; Tsatsas, A.T.; Eisenberg, A.; *J.Polym. Sci. Polym. Phys. Ed.*, 17, 81 (1979).
152. Tsatsas, A.T.; Risen, W.M.Jr. *Chem. Phys. Lett.*: 7, 354 (1970).

153. Padmavathy Rajagopalan, Andreas T. Tsatsas and Riscn, W.M. Jr.; *J. Polym. Sci. Polym. Phys. Ed.*, 34,151 (1996).
154. Macknight, W.J.; McKenna, L.W.; Read, B.E.; Stein, R.S. *J. Phys. Chem.*, 72, 1122 (1968).
155. Ogura, K.; Sobue, H.; Nakamura, S. *J. Polym. Sci. Polym. Phys. Ed.*, 11, p 2079 (1973).
156. Belfer, S.; Fainchtain, R.; Purinson, Y. and Kedem, O; *J. Membrane Sci.*, 172,113 (2000).
157. Peiffer, D.G.; Hager, B.L; Weiss, R.A.; Agarwal, P.K. and Ludberg, R.D.; *J. Polym. Sci. Polym. Phys. Ed.* 23, 1869-1881 (1985).
158. Ghosh, S.K.; Bhattacharya, A.K.; De, P.P.; Khastgir, D. and De, S.K.; *Plast. Rubb. Compos.* 30, 16 (2001).
159. Kim, D.H.; Jo, W.H.; Lee, S.C. and Kim, H.C.; *J. Appl. Polym. Sci.*, 69, 807 (1998).
160. Powels, D.G. *Polymer* 1, 219 (1960).
161. Read, B.E.; Carter, E.A.; Connor, T.M. and Macknight, W.J.; *British Polymer J.*, 1,123 (1969).
162. Otocka, E.P. and Davis, D.D.; *Macromolecules*, 2, 437 (1969).
163. Pinceri, M.; Meyer, C.; Levulet, A.M. and Lambert, M; *J. Polym. Sci. Polym. Phys.* 12, 115 (1974).
164. Kang, H.W and Moran, G.; *J. Membrane Sci.*, 148, 173 (1998).
165. Davis, H.A.; Long worth, R and Vaughan, DJ. *Ibid.* 515
166. Charlier, P.; Jerome, R.; Teyssie, P.; Prud'homme, R.E.; *J. Polym. Sci. A. Polym. Chem.*, 31, 129 (1993).
167. Suchoka-Galas, K.; *Polimery Warsaw*, 27, 383 (1982).
168. Bukin, I.I.; *Plast. Massy*, 6, 33 (1977).
169. Reich, S. and Michaeli, I.; *J. Polym. Sci., Polym. Phys.*, 13, 9 (1975).
170. Ludberg, R.D. and Makowski, H.S., *ACS Polymer Preprints*, 19 287 (1978).
171. Noshay, A. and Robeson, L.M.; *J. Appl. Polym. Sci.*, 20, 1885 (1976).
172. Long worth, R. and Vaughan, D.J., *ACS Polym. Preprints*, 9, 525 (1968).
173. Rahrig, D. and Macknight, W.J.; " *Advances in Chemistry, Series* " No. 187, Eisenberg, A. Ed., ACS, Chapter 6 (1980).
174. Makowski, H.S.; Ludberg, R.D.; Westerman, L. and Bock, J.; *Adv. Chem. Series* 187, 3 (1980).
175. Meyer, C.T. and Pinceri, M.; *J. Polym. Sci. Phys. Ed.*, 13, 1057, (1975)
176. Hodge, I.M. and Eisenberg, A., *Macromolecules*, 11 283, (1978)
177. Agarwal, P.K.; Makowski, H.S. and Ludberg, R.D.; *Macromolecules* 13, 1679 (1980).
178. Samuel J., Manjooran, K.B and Kurian, T. *Inter. J. Polym. Mater.* (2000).

179. Kurian, T.; Bhattacharya, A.K.; De, P.P.; Tripathy, D.K.; De, S. K. and Peffier, D.G.; *Plast. Rub. Compos. Proc. Appl.* 25, 2075 (1995).
180. Kurian, T.; Khastgir, D.; De, P.P.; Tripathy, D.K.; De, S.K. and Peiffer, D.G.; *Polymer*, 37, 5597 (1996)
181. Kurian, T.; De, P.P.; Tripathy, D.K.; De, S.K. and Peiffer, D.G.; *J. Appl. Polym. Sci.*, 62, 1729 (1996).
182. Shengqing Xu, Tao Tang, Bin Chen & Baotong, *Polymer*, 40, 2239 (1999).
183. Antony, P.; Bandyopadhyay, S. & De, S.K.; *Polymer*, 41, 787 (2000).
184. Storey, R.F. & Baugh, D.W.; *Polymer*, 42, 2321 (2001).
185. Eisenberg, A.; Smith, P. and Zhou, L.L.; *Polym. Eng. and Sci.*, 223, 1117 (1982).
186. Smith, P. and Eisenberg, A.; *J. Polym. Sci. Polym. Letters*, 21, 223 (1983).
187. Zhou, L.L. and Eisenberg, A.; *J. Polym. Sci. Phys. Ed.* 21, 595 (1983).
188. Molnar, A. and Eisenberg, A.; *Macromolecules*, 25, 5774 (1992).
189. Vallejo, F.J.; Eguiazabal, J.I. & Nazabal, J. *Polymer*, 41, 6311 (2000).
190. Wang, Y.; Suna, A.; McHugh, J.; Hilinski, E.F.; Lucas, P.A.; Johnson, R.D. *J. Chem. Phys.*, 92, 6927 (1990).
191. Shim, I.W.; Mattera, V.D.Jr.; Risen, W.M. Jr. *J. Catal.* 94, 531 (1985).
192. Moffitt, M. and Eisenberg, A. *Chem. Mater.* 7, 1178 (1995).
193. Hilinski, E.F.; Lucas, P.A. and Wang, Y. *J. Chem. Phys.*, 89, 3435 (1988).
194. Wang, Y.; Suna, A.; Mahler, W.; Kasowski, R.; *J. Chem. Phys.* 87, 7315 (1987).
195. Olah, G. A.; Meidar, D.; *Synthesis*, 358 (1978).
196. Barnes, D. M.; Chaudhuri, S. N.; Chryssikos, G. D., Mattera, V. D. Jr.; Peluso, S. L.; Shim, I. W.; Tsatsas, A.T.; Risen, W. M. Jr. In: "Coulombic Interactions in Macromolecular Systems"; Eisenberg, A.; Bailey, F. E., Eds.; ACS Symposium Series 302; ACS: Washington, DC, Chapter 5 (1986) Ameduri, B.; Boutevin, B. and Kostov, G.; *Prog. Polym. Sci.*, 26, 105 (2001).
197. Wilson, A.D. and Kent, B.E. *J. Appl. Chem.* 21, 313 (1971).
198. Wilson, A.D.; Crisp, S.; Prosser, H.J.; Lewis, B.G. and Merson, S.A. *Ind. Eng. Chem. Prod. Res. Dev.* 19, 263 (1980).
199. Potter, W.D.; Barclay, A.C.; Dunning, R. and Parry, R.J; *British Patent* 1, 554, 553; 1,554, 555 (1979); US Patent 4, 043,327 (1977).
200. Kent, B.E.; Lewis, B.G. and Wilson, A.D.; *J. Dent. Res.* 58 1607 (1979).
201. Maldonado, A., Swarz, M. N. and Phillips, R.W., *J. Am. Dent. Assoc.*, 96, 785 (1978).
202. Potter, W. D. and Drake, C. F.; *Ger. Offen.* 2, 753,663 (1978).
203. Eisenberg, A.; Yeager, H. L., Eds; "Perfluorinated Ionomer Membranes"; ACS Symposium Series 180; ACS: Washington, DC (1982).

204. Drake, E. N. *Polym. Prepr. Am. Chem. Soc. Div. Polym. Chem.*, 35, 14 (1994).
 205. Rogers, J. R.; Randall, F. J. *Polym. Prepr. Am. Chem. Soc. Div. Polym. Chem.*, 29, 432 (1989).
 206. Tan, J. S. In: "Structure and Properties of Ionomers"; Pineri M.; Eisenberg, A., Eds. NATO ASI Series C: Mathematical and Physical Sciences 198; Reidel: Dordrecht, 439 (1987).
 207. Diaz, A.; Fenzel-Alexander, D.; Miller, D. C.; Wollmann, D.; Eisenberg, A.; *J. Polym. Sci. C Polym. Lett*, 28, 75 (1990).
 208. Wadsworth, D. H. and co-workers. *U.S. Patent 4 3779 989* (1973).
 209. Hanson, W. T. Jr. *J. Photogr. Sci. Eng.*, 20, 155 (1976).
 210. Hanson, W. T. Jr. *J. Photogr. Sci. Eng.*, 25, 189 (1977).
 211. Fleckenstein, L. J. In: "The Theory of Photographic Process"; James, T.H. Ed.; Macmillan: New York, 366 (1977).
 212. Lundberg, R. D. In: "Structure and Properties of Ionomers"; Pineri M.; Eisenberg, A., Eds. NATO ASI Series C: Mathematical and Physical Sciences 198; Reidel: Dordrecht, 429 (1987).
 213. Risen, W. M. Jr. In; "Ionomers: Characterisation, Theory, and Applications"; Schlick, S., Ed.; CRC; Boca Raton, FL.; Chapter 12(1996).
 214. Statz, R. J. *Polym. Prepr. Am. Chem. Soc. Div. Polym. Chem.*, 29, 435 (1989).
 215. Portnoy, R. C.; Lundberg, R. D.; Peiffer, D. G. *Polym. Prepr. Am. Chem. Soc. Div. Polym. Chem.*, 29, 433 (1989).
 216. Krishnan, M.; White, J.R.; Fox, M.A.; Bard, A.J. *J. Am. Chem. Soci.*, 105, 7002 (1983).
 217. Mau, A.W.H.; Huang, C. B.; Kakuta, N.; Bard, A.J.; Campion, A.; Fox, M. A.; White, J.M.; Webber, S.E. *J. Am. Chem. Soci.* 106, 6537 (1984).
 218. Chen, N. and L. Hong, *Europ. Polym. J.*, 37, 1027 (2001).
 219. Zhang, H.; Weiss, R. A.; Kuder, J. E. and Cangieno, D.; *Polymer*, 41, 3069,(2000).
 220. Lee, K.H.; Oark, J.K. & Kim, W.J.; *Electrochimica Acta*, 45, 1301 (2000).
 221. Storey, R.F. and Baugh, D.W; *Polymer*, 42, 2321 (2001).
 222. Caretta, N.; Tricoli, V. and Picchioni, F.; *J. Membrane. Sci.*, 166, 189 (2000).
 223. Yu, J. & He, J.; *Polymer*, 41, 891(2000).
 224. Pisarski, M.; Pracella, M. & Galeski, A.; *Polymer*, 41, 4923 (2000).
 225. Ren, B.; Tong, Z.; Gao, F.; Liu, X. & Zeng, F.; *Polymer*, 42, 2001 (2001)
 226. Elliott, J.A.; Hanna, S.; Elliott, A.M.S. and Coolley, G.E.; *Polymer*, 42, 2251, (2001)
 227. Agar, E. and Igon, M.; *Polymer*, 41, 3513 (2000).
 228. Leung, L.M.; Lau, C.T.; Chang, L.; Huang, Y.; Liao, B.; Chen, M. and Gong, G.; *Polymer*, 42, 539 (2001).
-

-
229. Deimede, V.A.; Fragou, K.V.; Koulouri, E.G.; Kallitsis, J.K. and Voyiatzis, G.A.; *Polymer*, 41, 9095 (2000)
230. Genies, C.; Mercier, R.; Sillion, B.; Cornet, N.; Gebel, G. and Pineri, M.; *Polymer*, 42, 359 (2001)
231. Tong, Z. and Gao, B.R.; *Polymer*, 42, 143 (2001).
232. James, P.J.; Mac Master, T.J.; Newton, J.M. and Miles, M.J.; *Polymer*, 41, 4223 (2000).
233. Kalhor, M.S.; Gabrys, B.J.; Zajac, W.; King, S.M. and Peiffer, D.G.; *Polymer* 42, 1679 (2001).
234. Zhang, H.; Weiss, R.A.; Kudcr, J.E. and Kangiano, D.; *Polymer*, 41, 3069 (2000).
235. Weiss, R.A.; Ghebremeskel, Y. and Charbonneau, L.; *Polymer*, 41, 3471 (2000)
236. Samios, C.K. and Kalfoglou, N.K.; *Polymer*, 42, 3687 (2001).
237. Kim, J.S.; Nah, Y.H. and Jamg, S.S.; *Polymer*, 42, 5567 (2001).
238. Bashir, H.; Linares, A.; Acosta; J. L. *J. Appl. Polym. Sci.* 82: 3133- 3141 (2001):
<http://www3.interscience.wiley.com/locate/japs>.
239. Huang, R. Y. M.; Pinghai Shao, Burns, C. M.; Feng, X., *J. Appl. Polym. Sci.* 82: 2651-2660 (2001): <http://www3.interscience.wiley.com/locate/japs>.
240. Ibarra, L.; Alzoriz, M., *J. Appl. Polym. Sci.* 84: 605-615 (2002):
<http://www3.interscience.wiley.com/locate/japs>.
241. Zuoxin Huang, Yunzhao Yu, Ying Huang; *J. Appl. Polym. Sci.* 83: 3099-3104 (2002):
<http://www3.interscience.wiley.com/locate/japs>.
242. Kim, J.-S.; Min-Chul Hong, Yeon Hwa Nah, Yeonhee Lee, Seunghee Han, Hyun Eui Lim, *J. Appl. Polym. Sci.* 83: 2500-250 (2002):
<http://www3.interscience.wiley.com/locate/japs>.
243. Simulation study on molecular relaxation in ionomer melts, *Polymer* 43 (2002) 239 – 242, www.elsevier.com/locate/polymer: www.elsevier.com/locate/polymer.
-

Chapter 2

Materials and Measurements

- 2.1 *Materials*
 - 2.1.1 *Elastomers*
 - 2.1.2 *Chemicals*
 - 2.1.3 *Fillers*
- 2.2 *Measurements*
 - 2.2.1 *X-ray fluorescence spectroscopy*
 - 2.2.2 *Inductively coupled atomic emission spectroscopy*
 - 2.2.3 *Fourier transform infrared spectroscopy*
 - 2.2.4 *Fourier transform nuclear magnetic resonance spectroscopy*
 - 2.2.5 *Scanning electron microscopy*
 - 2.2.6 *Thermal studies*
- 2.3 *Mixing and homogenization*
- 2.4 *Determination of cure characteristics of rubber compounds*
- 2.5 *Molding of test sheets*
- 2.6 *Physical test methods*
- 2.7 *Microwave measurement*
- 2.8 *References*

2.1. Materials

2.1.1. Elastomers

2.1.1. (a). Natural rubber (NR)

ISNR-5 was supplied by Rubber Research Institute of India (RRII), Kottayam. The Mooney viscosity ML (1+4) at 100°C was 85.3 and $M_w = 7.70 \times 10^5$. The Bureau of Indian Standards (BIS) specifications for this grade of rubber is given in table 2.1.

Table 2.1 Typical composition of ISNR-5

<i>Parameters</i>	<i>Limits</i>
Dirt content, % by mass, max.	0.05
Volatile matter, % by mass, max.	1.00
Nitrogen, % by mass, max.	0.70
Ash, % by mass, max.	0.60
Initial plasticity, P ₀ , min.	30.00
Plasticity retention index (PRI), min.	60.00

2.1.1. (b). Acrylonitrile butadiene rubber or Nitrile rubber (NBR)

Nitrile rubber was supplied by Gujarat Apar polymers limited, N 553 NS had an acrylonitrile content of 33% and mooney viscosity (ML (1+4), 100°C): 40.9.

2.1.1. (c). Styrene butadiene rubber (SBR)

Styrene butadiene rubber (Synaprene-1502) was obtained from Synthetics and Chemical Ltd., U.P., India. The Mooney viscosity (ML (1+4) at 100°C) was 49.2.

2.1.1. (d) Radiation induced styrene grafted natural rubber

Radiation induced styrene grafted natural rubber [1] was obtained from Rubber Research Institute of India, Kottayam, India. Which had, $M_w = 3.95 \times 10^5$, Density = 0.94 g/cm³; Grafted styrene is 20 %

2.1.2. Chemicals

2.1.2. (a). Zinc oxide

Zinc oxide was supplied by M/S. Meta zinc Ltd., Bombay. It had the following specifications

Specific gravity	-	5.5
ZnO content	-	98%
Acid content	-	0.4% max.
Heat loss (2hrs at 100°C)	-	0.5% max.

2.1.2. (b). Stearic acid

Stearic acid used in this study was supplied by Godrej soaps Ltd., Bombay and had the following specifications

Melting point	-	50-69°C
Acid number	-	185-210
Iodine number	-	95 max.
Specific gravity	-	0.85 ± 0.01
Ash	-	0.1 max %

2.1.2. (c). Tetra methyl thiuram disulphide (TMTD)

It was supplied by NICIL, Bombay. It had the following specifications.

Melting point	-	136°C
Specific gravity	-	1.4

2.1.2. (d). Sulphur

Sulphur was supplied by Standard Chemical Company Pvt. Ltd., Chennai and had the following specifications.

Specific gravity	-	2.05
Acidity	-	0.01% max.
Ash	-	0.01% max.
Solubility in CS ₂	-	98% max.

2.1.2. (e). CBS

N-cyclo hexyl-2-benzthiazyl sulphonamide (CBS) used in the study was PIL cure CBS supplied by polyoleffins Industries, Bombay, having the following specifications.

Ash	-	0.5% max
Moisture	-	0.5% max
Specific gravity	-	1.27

2.1.2. (f). Aromatic oil

Aromatic oil was supplied by Hindustan Petroleum Corporation Ltd. It had the following specifications.

Specific gravity	-	0.95-0.98
Aniline point	-	25°C
Flashpoint	-	245°C

2.1.2. (g). Reagents

Toluene, chloroform, isopropyl alcohol, concentrated sulphuric acid, methanol, isopropanol, and n-heptane were procured from E. Merck India Ltd., Mumbai. Acetic anhydride, zinc acetate, and 1,2-dichloroethane (DCE) were obtained from S.D. Fine Chemicals Ltd, Mumbai, India.

2.1.3. Fillers

2.1.3. (a) HAF:

High abrasion furnace carbon black (N330) was obtained from M/s. Carbon and Chemicals (India) Ltd., Cochin. It had the following specifications:

Iodine adsorption	-	80 mg/g
DBP absorption	-	105-cm ³ /100 g
Mean particle diameter	-	32 nm
Surface area	-	80 m ² /g
pH	-	7.6

2.1.3. (b) Silica:

Precipitated silica manufactured by Degussa, Germany, had the following characteristics:

Surface area	-	234-m ² g ⁻¹
Oil absorption	-	240 g per 100 g
pH	-	6.0
Mean particle diameter	-	20 nm

2.1.3. (c) Nylon-6

Nylon-6 fibers obtained from SRF Ltd., Chennai was chopped to 6 mm and had the following specifications:

Breaking Strength (Kg/m ²)	-	28.3 - 31.5
Elongation at break (%)	-	27.5 - 36.5
Twist	-	S 392 - 374
Denier (g)	-	3656 - 3886
Diameter (mμ)	-	10-15

2.1.3. (d) E-glass

Untwisted continuous filament of E-glass chrome-free silane sized roving obtained from Binani Industries Ltd; Mumbai, India was chopped to 6 mm length and had the following specifications:

Linear weight (Tex)	-	150-300 (±10%)
Size content	-	0.40 ± 0.20
Moisture content (%)	-	< 0.20
Diameter (micron)	-	13

2.1.3. (e) Zinc stearate

Zinc stearate of rubber grade was obtained locally

Melting point	-	128-130°C
---------------	---	-----------

2.2. Measurements

2.2.1. X-ray fluorescence spectroscopy

The estimation of the sulfur content of the ionomer was conducted as per ASTM D - 4294 (1995). The measurement was done using Oxford Lab X-3000 bench top XRF analyzer supplied by Oxford Instruments, U.K., using thin films molded in an electrically heated hydraulic press at 10 MPa.

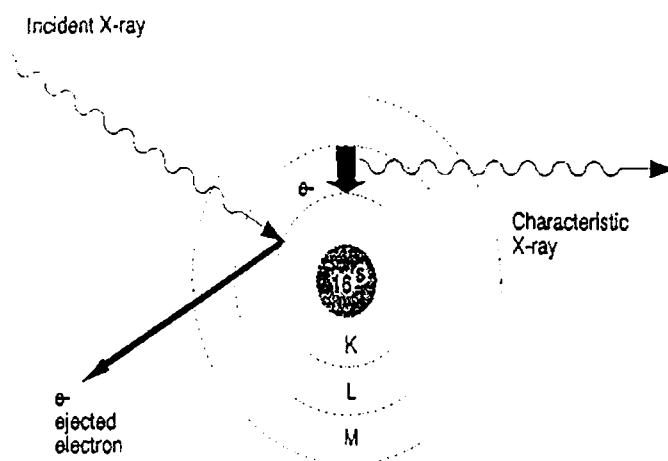


Fig. 2.1 Diagrammatic representation of K, L, M, N and O levels

In this method, the sample is taken in a hollow cup at the bottom of which a polycarbonate film of six micrometers thickness is fixed. Primary X-rays then irradiate the sample. Under the effect of the radiation, some electrons orbiting in internal shells are torn away. Electrons coming from higher levels fill the holes created by departing electrons. The discrete energy difference give rise to characteristic emission of what are called secondary X-rays, as shown in figure 2.1, the wavelength of which is characteristic of the element being bombarded. The energy of the X-ray emission lines in keV increase with increase in atomic number. The relationship between energy and wavelength is as follows: n as a function of wavelength is established using a crystal analyzer based on Bragg's law. The spectral lines produced are described in figure 2.2 and 2.3 using the classical Siegbahn system i.e., K_{α} , K_{β} etc.

Sulphur is analyzed as the K_{α} emission (resulting from the movement of the electron arriving at the K-shell and coming from the L-shell) at 5.573 \AA^0 . The phenomenon of excitation of atoms using X-rays is known as X-ray fluorescence.

$$E \text{ (keV)} = 12.4 / \text{wavelength } (\lambda)$$

The spectrum of the secondary emission, i.e., the intensity of X-ray radiation.

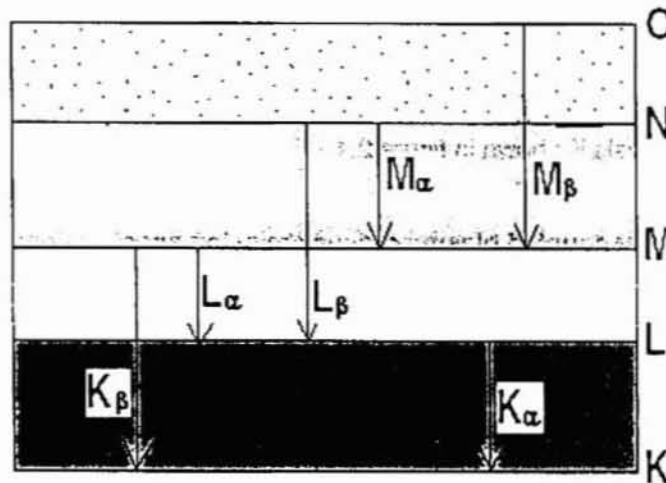


Fig. 2.2 Representation of the various spectral lines; K_{α} and K_{β} are the most sensitive lines emitted as X-rays.

The fluorescence of sulphur atom has been represented here. This apparatus works on the principle of energy dispersive X-ray fluorescence (EDXRF) spectroscopy. The EDXRF spectrometer has a single detector, which sees X-rays of all energies simultaneously. This advantage has to be used carefully to ensure a maximum count rate of, typically, 30,000 counts per second, which the detector will accept. Helium purging is given for concentrations of sulphur up to 0.05%. Knowledge of the nature of absorption of X-rays is fundamental to the understanding of nearly everything that happens in X-ray analysis. Two basic facts need to be grasped as follows:

1. X-rays are absorbed exponentially according to Beer's law.

$$I_x = I_0 e^{-\mu x}$$

Where

I_x	=	the intensity passing through a thickness x
I_0	=	the initial incident intensity
μ	=	the mass absorption coefficient

ρ = the density
 x = the thickness of the absorber

2. The value of the mass absorption coefficient changes with wavelength and a plot of the variation between absorption and wavelength shows maxima followed by a sharp drop as represented in figure 2.3.

Since the apparatus requires helium gas supply for optimum analytical performance at low concentrations, samples whose expected sulphur concentrations were below 0.05% were analyzed in helium purging mode. The sample cup assembly used for the sulphur analysis is shown in figure 2.4.

2.2.2. Inductively coupled plasma-atomic emission spectroscopy

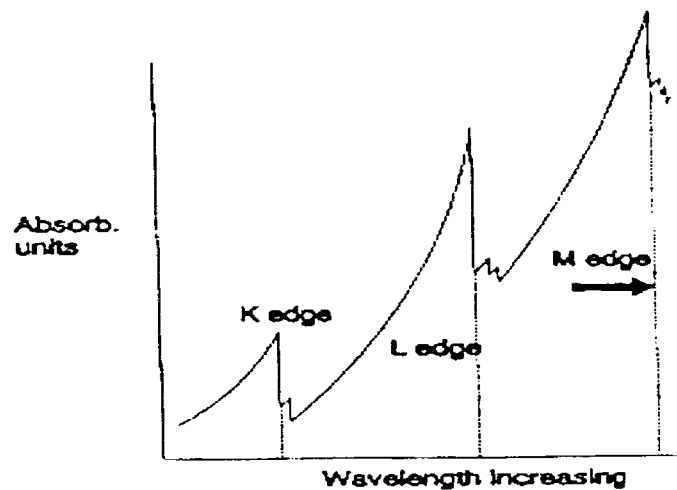


Fig. 2.3 plot of the variation between absorption and wavelength

Zinc analysis was performed using Inductively coupled plasma-atomic emission spectroscope [2] (ICPAES) model Labtam Plasmascan-8410. 0.5 g of the sample digested with 15 ml of 9:4 mixtures of nitric acid and perchloric acid and diluted to 100 ml was analyzed in ICPAES.

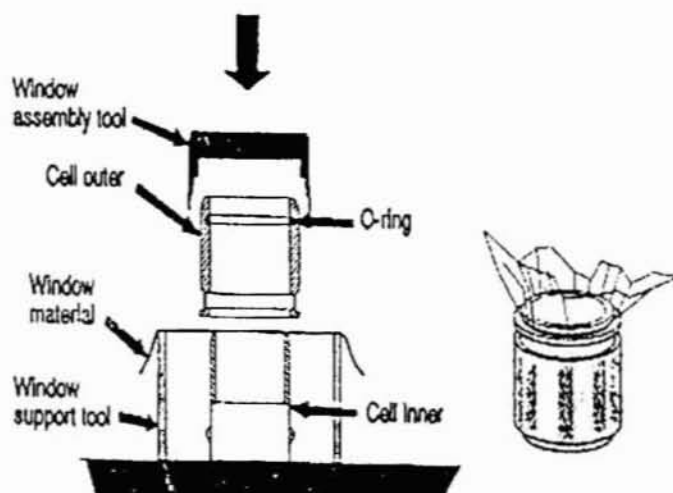


Fig. 2.4 Sample cup assembly used for the sulphur analysis

This method involves the identification of the spectral lines originating from the neutral atom and ionized states at the plasma state of the material. The inductively coupled plasma spectrum of zinc metal ion has the forms shown in the figures 2.5 and 2.6. The emission spectra provide a convenient means for estimation of the trace element analytical capabilities of the various lines for each element.

Spectral lines of impurity elements, particularly the ubiquitous elements that have very intense lines, such as the alkaline earth elements, appear in a number of scans. The strongest silicon lines appear at low intensity in some of the scans. The two carbon lines are present in all of the scans, and probably arise from the presence of a carbon containing species in the argon plasma support gas. The analyst should become familiar with the locations of the carbon lines and the strongest lines or groups of lines of calcium, magnesium, and silicon so that these lines can be distinguished in the scans of other elements.

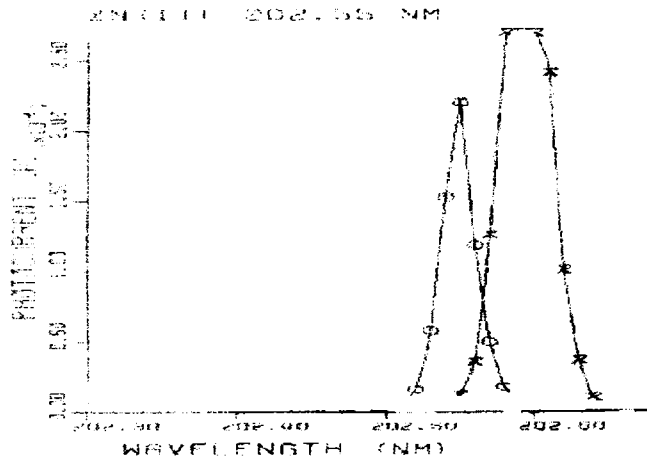


Fig. 2.5 Inductively coupled plasma atomic emission spectrum of zinc metal ion at high resolution

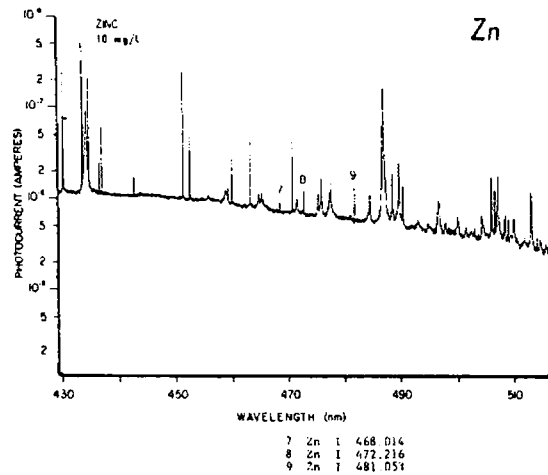


Fig. 2.6 Inductively coupled plasma atomic emission spectrum of zinc metal ionomers

2.2.3. Fourier transform infrared spectroscopy.

Infra red spectra are generated by the absorption of electromagnetic radiation in the frequency range 400 to 4000cm^{-1} by organic molecules. Different functional groups

and structural features in the molecule absorb at characteristic frequencies. The frequency and intensity of absorption are indication of the bond strengths and structural geometry in the molecule. FTIR spectra of the compression-molded films of the samples were taken in Nicolet Avtar 360 ESP FTIR Spectrometer.

2.2.4. Nuclear magnetic resonance spectroscopy

NMR spectra of the samples were taken in a Bruker Avance DPX 300 FTNMR spectrometer operating at a proton resonance frequency of 300.13 MHz.

2.2.5. Scanning electron microscopy

Scanning electron microscope (SEM) was first introduced in 1965 and it has since become a very useful tool in polymer research for studying morphology [3-5] Scanning electron microscope model S -2400 Hitachi, Japan, was used to investigate the morphology of fractured surfaces.

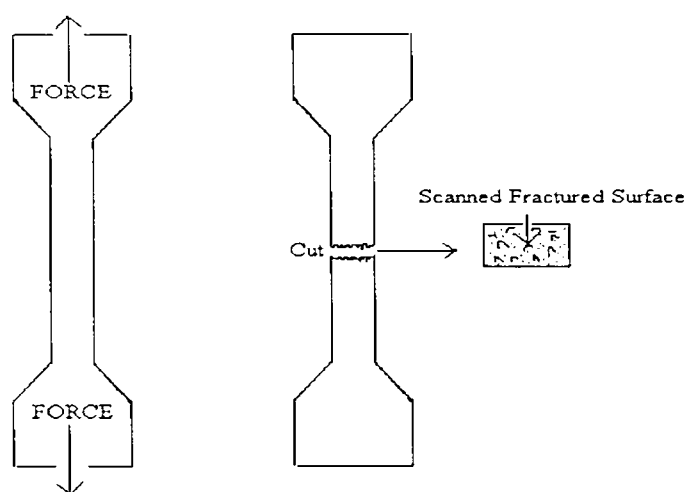


Fig. 2.7 SEM scan area of the tensile fracture surface

In this technique, an electron beam is scanned across the specimen resulting in back scattering of electrons of high energy, secondary electrons of low energy and X-rays. These signals are monitored by detectors (photo multiplier tube) and magnified.

An image of the investigated microscopic region of the specimen is thus observed in cathode ray tube (CRT) and photographed using 120- roll black and white film.

The SEM observations reported in the present study were made on the fracture surface of tensile specimens. Thin specimen of the sample was prepared and mounted on a metallic stub with the help of a silver tape and conducting paint in the upright position. The stub with the sample was placed in an E-101 ion sputtering unit for gold coating of the sample to make it conducting. Gold-coated sample was observed in the SEM. The shapes of the tensile test specimens, direction of the applied force and portions from where the surfaces have been cut out for SEM observations are shown in the figure 2.7.

2.2.6. Thermal studies

Thermal analysis was carried out using thermogravimetric analyzer (TGA), differential scanning calorimeter (DSC), and dynamic mechanical thermal analyzer (DMTA).

2.2.6. (a). Thermogravimetric analysis (TGA)

Thermogravimetric analyzer was used to measure the thermal stability of the polymer. The measurements were taken under nitrogen atmosphere from 0 °C to 700 °C using Netzsch STA 409 with a data acquisition system 414/1. Samples of about 10 mg were heated under an inert atmosphere of 75 ml/min nitrogen gas stream at a heating rate of 10 °C / min.

2.2.6. (b). Differential scanning calorimetry (DSC)

For the thermal analysis studies, a differential scanning calorimeter (DSC) (Thermal Analysis Co. Model DSC 2010) was used. It was calibrated with indium. The sample cells, which contained about 10 mg of material, were stored under a dry nitrogen atmosphere, the flow rate of which was 50 mL/min. To ensure a uniform thermal history, the material was first scanned at 20 °C/min from –80 to 250 °C, and then they

were quenched with liquid nitrogen to -80 °C. The glass transition temperatures were taken as the midpoint of the heat capacity plot between two base lines.

2.2.6 (c). Dynamic mechanical thermal analysis (DMTA)

To measure dynamic mechanical properties of samples, a Polymer Laboratories dynamic mechanical thermal analyzer (DMTA, Mark II model) was used. The dual cantilever bending mode, at frequencies of 10 Hz was utilized. The heating rate was 1 °C/min. For each sample, the storage moduli (E') and loss tangents were obtained as a function of temperature.

2.3. Mixing and homogenization

2.3. (a). Using the Brabender plasticorder

The samples were masticated in a Brabender plasticorder model PL-3S. Mixing was done for five minutes at a rotor speed of 60 rpm, and at a temperature of 120°C.

2.3. (b) Using the mixing mill

Mixing and homogenization of elastomers and compounding were done on a laboratory size (15cm × 33cm) two-roll mill at a friction ratio of 1:1.2.

2.4. Determination of cure characteristics of rubber compounds

A Gottfert elastograph model 67.85 was used in the study for the determination of curing behavior of rubber compounds. This is a rotorless cure meter and the torque time curve (vulcanization curve) is generated by the oscillation of the lower half of the cavity in which the rubber compound is charged. The reaction chamber is biconical in shape, so that the shear angle remains constant throughout the specimen. Further, by using a specimen of a defined size obtained by means of a special stamping press, the chamber can be filled completely restricting oxidative breakdown as well as

ensuring greater reproducibility. The upper platen is brought to the lower by means of a ram actuated by compressed air. A cure curve has the form similar to figure 2.8

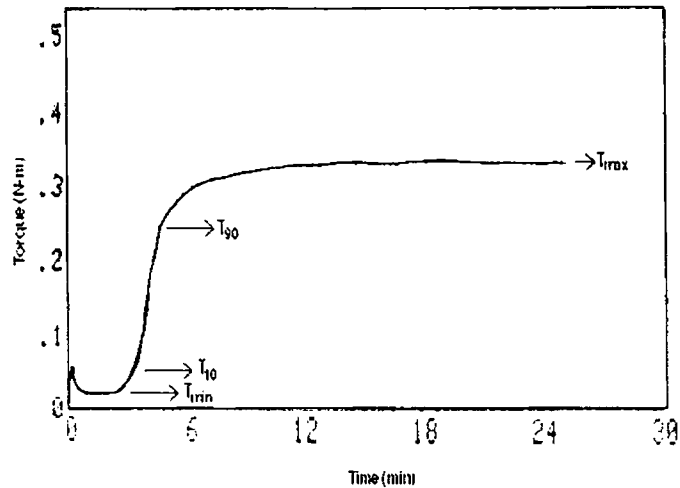


Fig. 2.8 Typical cure curve

The relevant data that could be taken from the torque-time curve are

1. Minimum torque: This is the torque attained by the mix after homogenizing at the test temperature before the onset of cure.
2. Maximum torque: This is the torque recorded after the curing of the mix is completed.
3. Optimum cure time: This is the time taken for attaining 90% of the maximum torque (90% vulcanization)
4. Scorch time: This is the time taken for 2 units (0.02Nm) rise above the minimum torque (about 10% vulcanization).

The computer evaluates the vulcanization curve and prints out these data after each measurement. It is also capable of generating many other data such as the cure rate curve.

2.5. Molding of test sheets

The test sheets for determining the physical properties were prepared in standard moulds by compression moulding in an electrically heated hydraulic press having 30

cm×30 cm platens at a pressure of 10 MPa on the mould. The rubber compounds were vulcanized up to their respective optimum cure times at 150°C unless otherwise specified. At the end of the curing cycle moldings were cooled quickly and stored in a cold and dark place for 24 hours and were used for subsequent physical tests. For samples having thickness more than 6mm (compression set, abrasion resistance etc.) additional curing time based on the sample thickness was given to obtain satisfactory moldings. The test specimens of ionomers were prepared by molding in an electrically heated hydraulic press for 5 minutes at 120°C and at a pressure of 10 MPa.

2.6. Physical test methods

2.6.1. Tensile strength and elongation at break

These tests were carried out according to ASTM D 412 (1987) [6] at 25 °C using dumb-bell specimens in an Instron universal testing machine (UTM) model 4206. Samples were punched from compression-moulded sheets parallel to the mill grain. The sample was held tight by the two grips, the upper grip of which was fixed. The rate of separation of the power actuated lower grip was 500 mm/minute. The computer attached to the machine calculates the tensile strength and elongation at break and prints out these data after each testing.

2.6.2. Tear resistance

The tear resistance [7] was determined as per ASTM D 624 (1986) using unnicked 90° angle test pieces (die C) at 25 °C, using a crosshead speed of 500 mm per minute in an Instron UTM, model 4206.

2.6.3. Hardness

The hardness [8] (Shore A) of the molded samples was tested using Zwick 3114 hardness tester in accordance with ASTM D 2240 (1986). The tests were performed on mechanically unstressed samples of 300mm diameter and minimum 6mm

thickness. A load of 12.5 N was applied and the readings were taken after 10 seconds of indentation after firm contact had been established with the specimens.

2.6.4. Abrasion resistance

The abrasion resistance was determined using Zwick abrader as per DIN standard 531516.

2.6.5 Density

Density of the samples was measured as per ISO 2781 (method A). Samples weighing about 2.5 g with smooth surface were used. Weight of the specimen in the air and water was taken. Density of the sample was calculated as

$$\text{Density} = W_1/W_2 \times D$$

Where,

W_1	=	weight of the sample in air
W_2	=	loss of weight in air
D	=	density of water, (1 g/cm ³)

2.6.6. Reprocessability studies

The reprocessability of the ionomer was studied by masticating the moulded samples in the Brabender Plasticorder PL - 3S for 5 minutes at a rotor speed of 60 rpm at 120°C. The sample was molded in an electrically heated hydraulic press for 5 minutes at 120°C, under a pressure of 10 MPa. The process of mastication and molding was repeated up to three cycles. The stress-strain properties of the moulded specimen after each cycle were determined.

2.7 Microwave measurement.

Cavity perturbation technique [9], the most accurate dielectric measurements of its type, was employed for the study. A closed section of a wave-guide constitutes wave-guide cavity resonator. The cavity resonator can be of transmission or reflection type. The electromagnetic energy is coupled to the cavity through coupling holes at the

ends of the cavity. A non-radiating slot is provided at the broad wall of the cavity for the introduction of the sample.

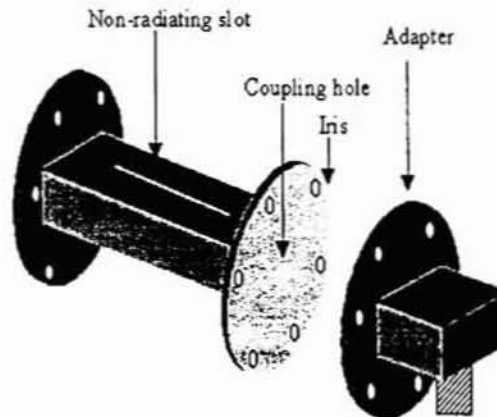


Fig. 2.9 Schematic diagram of the transmission type cavity used in the cavity perturbation technique for the Microwave measurement.

The cavity resonates at different frequencies depending on the dimensions of the cavity. The schematic diagram of the transmission type cavity is shown in figure 2.9. The basic principle involved in the technique is that the field within the cavity resonator is perturbed by the introduction of the dielectric sample through the non-radiating slot. The perturbation shifts the resonant frequency and the quality factor of the cavity. The shift in the frequency is a measure of dielectric constant and that in quality factor gives the loss factor. The conductivity of the sample can be found out from the loss factor.

The experimental set-up consists of a transmission type S-band rectangular cavity resonator, HP 8714 ET network analyzer and an interfacing computer as shown in figure 2.10. The cavity resonator is excited in the TE_{10p} mode. A typical resonant frequency spectrum of the cavity resonator is shown in figure 2.11. Initially, the resonant frequency f_0 and the corresponding quality factor Q_0 of each resonant

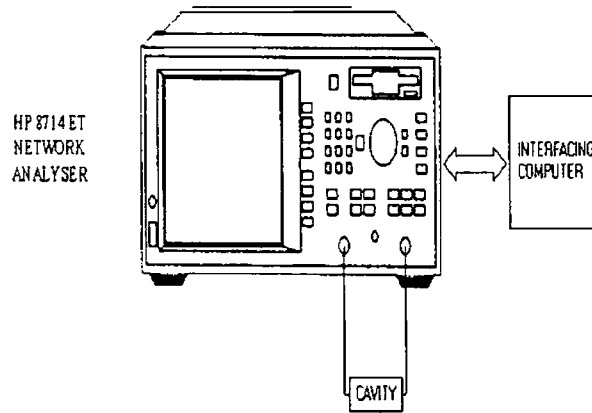


Fig. 2.10. Schematic diagram of the experimental set-up consisting of a transmission type S-band rectangular cavity resonator, HP 8714 ET network analyser and an interfacing computer.

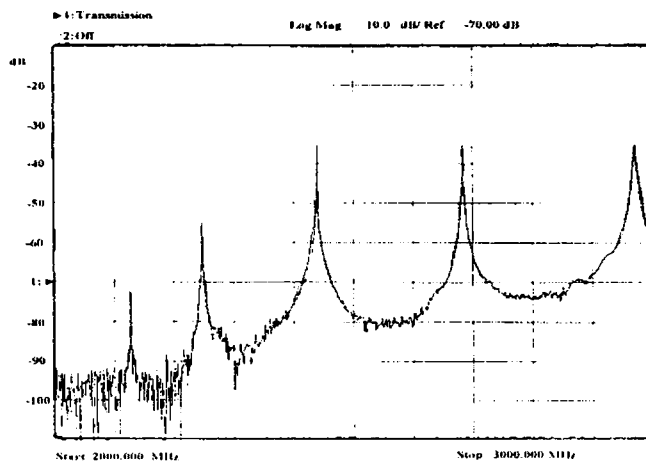


Fig. 2.11 A typical resonant frequency spectrum of the cavity resonator

peak of the empty cavity are determined. Samples prepared in the form of thin strip are introduced into the cavity resonator through the non-radiating slot. One of the resonant frequencies of the loaded cavity was selected and the position of the sample

was adjusted for maximum perturbation (i.e. maximum shift of resonant frequency with minimum amplitude for the peak). The new resonant frequency f_s , 3dB bandwidth and hence the quality factor Q_s were determined. The procedure was repeated for all other resonant frequencies.

2.8. References

1. Claramma, N. M.; Varghese, L.; Thomas, K.T.; Mathew, N. M. *Radiation Induced Graft Co polymerization of Styrene on to Natural Rubber*. IRMRA, 18th Rubber Conference, 165, (2000)
2. Winge, R. K.; Fassel, V. A.; Peterson, V.J.; Floyd, M. A. *Inductively Coupled Plasma Atomic Emission Spectroscopy. An Atlas of spectral Information (Physical Sciences data 20)*. Elsevier Science Publishers B.V, Molenwerf 1, Netherlands
3. De, S.K.; Dhindaw, B.K. *J. Scanning Electron Micros.* 3, 973 (1982).
4. Sawyer, L.C.; Grub, D.T. *'Polymer Microscopy'* Chapman & Hall, London, U.K. Second Edition (1996).
5. Goodhew., *Elastomer Microscopy Analysis.*, Wykehem Publication Ltd., London, (1975).
6. Annual Book of ASTM Standard, D 412 – 1992.
7. Annual Book of ASTM Standards, D 2240 – 1981.
8. Annual Book of ASTM Standards, D 624 – 1991.
9. Mathew, K. T.; Raveendrannath, U. In: "*Sensors Update*" Baltes, H.; Gopel, W.; Hesse, J. Eds. WILEY-VCH (Germany), chapter 7, 185-210, (2000).

Chapter 3

Ionomers based on radiation induced styrene grafted natural rubber

Part of the work presented in this chapter has been published in *Macromol. Mater.*

Eng. 286, 507 (2001)

- 3.1 *Introduction*
- 3.2 *Synthesis*
- 3.3 *Characterisation*
 - 3.3.1 *Estimation of sulphur content*
 - 3.3.2 *Characterisation of ionic groups using FTIR spectroscopy*
 - 3.3.3 *FTNMR spectroscopy*
 - 3.3.4 *Thermogravimetric analysis*
 - 3.3.5 *Differential scanning calorimetry*
 - 3.3.6 *Dynamic mechanical thermal analysis*
 - 3.3.6 (i) *Loss tangent-temperature plot*
 - 3.3.6 (ii) *Storage modulus- temperature plot*
 - 3.3.7 *Influence of ionic groups on physical properties*
 - 3.3.8 *Reprocessability studies*
- 3.4 *Conclusion*
- 3.5 *References*

3.1. Introduction

Chemical modification of natural rubber aims at improving its mechanical properties. Vulcanization and grafting are some of the viable techniques for modifying the properties of natural rubber. The incorporation of reactive aromatic molecules like

styrene in to the natural rubber backbone, through grafting, produces natural rubber with improved mechanical properties [1]. The grafting of monomers such as styrene, methyl methacrylate etc. to the natural rubber backbone has been reported [1-4]. The subsequent modification of grafted natural rubber into ionomers would yield a material with improved mechanical properties compared to plain rubber. Ionomers are copolymers having ionic pendant groups attached to the hydrocarbon backbone. It is well known that such ionic groups tend to form phase-separated ionic aggregates through metal bridges in the hydrophobic polymer matrix resulting in physical properties superior to the host polymer [5]. Ionic thermoplastic elastomers combine the processing characteristics of thermoplastics with the physical properties of vulcanized rubbers. This unique feature of ionic thermoplastic elastomers to provide products with most of the physical properties of conventional vulcanized rubbers, but without going through the process of vulcanization is so attractive that they become commercially very important. To date, many types of ionic thermoplastic elastomers have been developed and examined. Among them ionomers based on EPDM, nitrile rubber, polychloroprene rubber, and ethylene methacrylic acid copolymers are very important [6-8]. There is no report, so far, on reprocessable ionomers based on natural rubber or styrene grafted natural rubber.

This chapter presents:

- (a) Introduction of ionic groups into radiation-induced styrene grafted natural rubber (RISGNR).
- (b) Characterisation of zinc sulphonated radiation-induced styrene grafted natural rubber (ZnS-RISGNR).
- (c) Evaluation of the effects of ionic groups on the mechanical properties of the ZnS-RISGNR, and
- (d) Study of the reprocessability of the ionic polymer.

3.2. Synthesis

The graft copolymer (RISGNR) was dried under vacuum at 50 °C for 72 hrs before use. In to 250 ml of stirred 1, 2, dichloroethane (DCE), 10 g of polymer (RISGNR) was dissolved. The sulfonating reagent (acetyl sulphate) was generated [9] in a

separate vessel at the molar ratio of acetic anhydride to sulphuric acid of 1.4:1. The reactor was cooled in an ice bath, whose temperature was not allowed to surpass 0°C. Subsequently the solution was diluted to 150 ml of DCE. After stirring the polymer solution for 30 minutes, under nitrogen atmosphere, the sulphonating reagent was added slowly; drop wise, under stirring at 0°C. After complete addition, the cooling bath was removed and the solution was vigorously stirred for one hour. The reaction was terminated after 10 minutes by adding isopropanol. Stirring was continued and a stoichiometric amount of zinc acetate in methanol was added for the neutralization of the polymer sulphonic acid. The product was recovered by steam stripping, and was washed several times with deionised water (until reaching neutral pH).

Table 3.1 Results of XRF analysis of sulphur

Samples	Sulphur (wt.- %)	Ion content [meq]
1	0.46	14.5
2	0.67	21.2
3	0.84	26.5
4	1.28	40.0

The zinc sulfonated styrene grafted natural rubber was then vacuum dried at 50 °C for 72 hrs. RISGNR of various concentrations of sulfonic acid contents could be prepared by varying the acetyl sulphate concentrations. The ionic polymer is hereafter represented as x.y ZnS-SGNR where x.y shows number of milliequivalents of sulfonic acid /100 g of sulphonated styrene grafted natural rubber.

3.3. Characterisation

3.3.1. Estimation of sulphur content

The concentration of ionic content in the ionomer, in terms of sulphur was estimated by XRF studies. Table 3.1 shows the number of milliequivalents of sulphonate content/100g polymer.

in each of the ionomer samples calculated using the relation,

$$\text{milliequivalents of sulphur} = \text{Weight \% of sulphur} \times 1000 / 32.$$

The weight % of sulphur is directly obtained from X-ray fluorescence spectroscopic analyses.

3.3.2 Characterisation of ionic groups using FTIR spectroscopy

FTIR spectra of the control NR (a), RISGNR (b) and ZnS-RISGNR (c) are shown in figure 3.1. Figure 3.1(b) shows the FTIR spectrum of the isolated graft rubber (after removing free NR and free polystyrene).

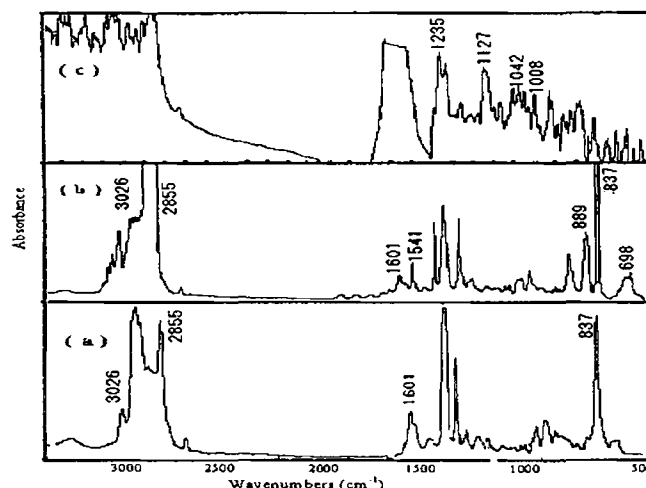


Fig. 3.1 FTIR spectra of the control NR (a), RISGNR (b) and ZnS-RISGNR (c)

FTIR spectra corresponding to Fig. 3.1(a) of NR and Fig. 3.1(b) of RISGNR show that the peaks at 3026 cm^{-1} and 2855 cm^{-1} correspond to the aromatic C-H stretching in polystyrene whereas those at 1601 cm^{-1} and 1541 cm^{-1} correspond to the C=C stretching of aromatic ring of polystyrene. Along with the characteristic absorptions of natural rubber at 837 cm^{-1} and 889 cm^{-1} , the peaks at 1452 cm^{-1} and 1375 cm^{-1} correspond to the aliphatic C-H stretching in natural rubber. A strong peak at 698 cm^{-1} stands for the monosubstituted benzene ring and which may be due to the vibration of the C-C bond connecting NR and styrene. This may be taken as evidence in favour

of a chemical reaction between rubber and styrene. The FTIR spectra^{Fig. 3.1(c)} of the ZnS - RISGNR show 1008 cm⁻¹ peak representing the in-plane bending vibrations of phenyl group substituted with a metal sulphonate group, 1127 cm⁻¹ for the sulphonate anion attached to a phenyl ring, 1042 cm⁻¹ of the symmetric stretching vibration of the zinc sulphonate group and the doublet at 1235 cm⁻¹ due to symmetric stretching vibration of the sulphonate group [10-13]. There are two kinds of reactive sites in the RISGNR, (i) the phenyl rings in the polystyrene blocks, and (ii) the residual C=C in the rubber block. Although olefinic unsaturation is inherently more reactive to acetyl sulphate than the phenyl rings, infrared spectroscopic analyses confirmed that sulphonation occurred almost exclusively [12] in the polystyrene blocks as proposed in scheme 3.1.

3.3.3. FTNMR spectroscopy

The FTNMR spectra of the control NR (a), RISGNR (b) and ZnS-RISGNR (c) are shown in figure 3. 2. The disappearance of a signal due to the rubber C=C around 2 ppm in figure 3.2 (b) with respect to figure 3.2 (a) shows that there is chemical reaction between the rubber and the styrene. In addition to the characteristic signals of NR at 1, 2 and 5 ppm, a new signal appears at 7.2 ppm. This new signal at 7.2 ppm, corresponding to the benzene ring may be due to the styrene grafted on to the NR backbone. The chemical shift of peaks in the modified polymer is due to the local conformational change, which arises due to the grafting of styrene units at the allylic carbon atom in natural rubber.

The environment of the grafted phenyl units has been further disturbed in the sulfonated graft polymer. This is clear from the chemical shift of the signals corresponding to the aromatic ring at 7.0277 ppm to 7.2781 ppm^{Fig. 3.2(c)}. The relatively large shift in the resonance signals of phenyl ring may be due to the aggregation of strong ionic groups like $-(SO_3)_2Zn$, attached to the benzene ring in ZnS-RISGNR. It can therefore be considered as a supplementary evidence for the FTIR spectroscopic observation [9].

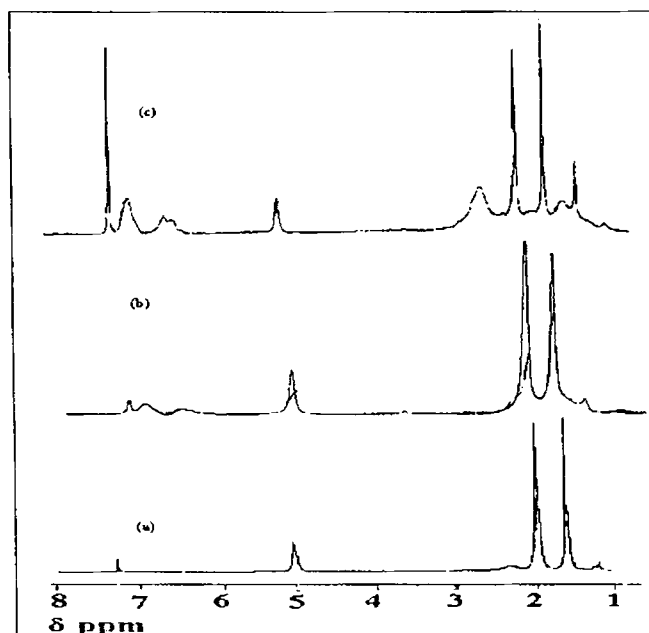


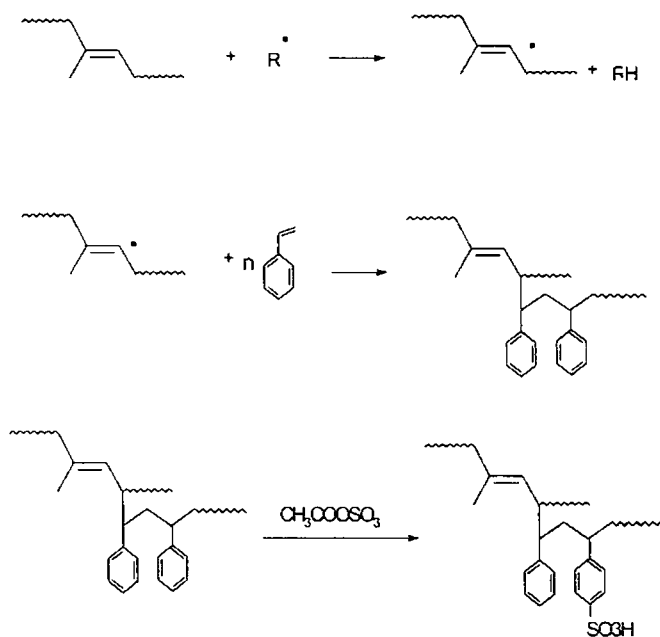
Fig. 3.2 FTNMR spectra of (a) NR, (b) RISGNR and (c) ZnS-RISGNR.

3.3.4. Thermogravimetric analysis (TGA)

Table 3.2 Results of thermogravimetric analysis

Samples	Temperature of onset of degradation (°C)	Tmax (°C)	Residual weight (%)
1	350	380	2
2	370	435	15
3	375	440	22

1- shows base polymer; 2 and 3 show ionomers containing 26.5 and 40 meq of ionic content/100 g base polymer



Scheme 3.1 Chemical reaction involved in the preparation of zincsulphonated styrene grafted natural Rubber

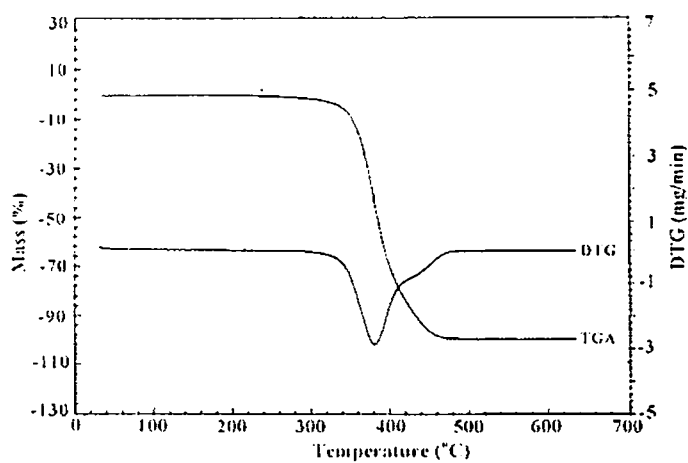


Fig. 3.3 Thermal profiles of radiation induced styrene grafted natural rubber

Figures 3.3, 3.4 and 3.5 represent both the TGA and DTG thermal profiles of base polymer, 26.5 ZnS-RISG NR and 40 ZnS-RISG NR, respectively. The T_{max} values i.e., the temperature at which the rate of degradation is maximum are shown in the table 3.2. Increase in the concentration of the ionic content in the polymer influences their melt viscosity. The change in the viscosity may be affecting their T_{max} values [12]. The increased stability of the ZnS-RISG NR when compared to RISG NR could be due to the greater stability of the aromatic sulphonate derivatives.

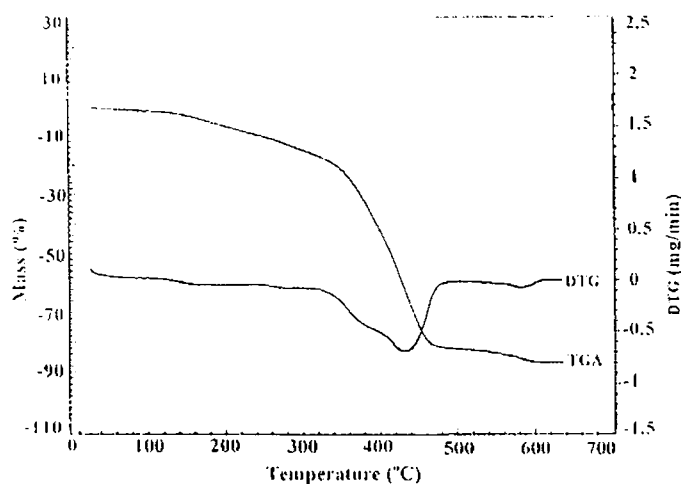


Fig. 3.4. Thermal profiles of 26.5 ZnS-SG NR

3.3.5. Differential scanning calorimetry (DSC)

Incorporation of zinc sulphonate groups in to the base polymer (T_g is $-69\text{ }^{\circ}\text{C}$) produced a new material with two thermal transitions. Figure 3.6 shows the DSC thermo grams of 26.5 ZnS-RISG NR (ionomer- 1) and 40 ZnS -SG NR (ionomer- 2). The low temperature transition (T_{g1}) for the ionomer-1, which occurs around $-64\text{ }^{\circ}\text{C}$ shows that the ionic groups have affected the transition temperature of the soft rubbery phase. At the relatively low dielectric constant of the base polymer (i.e., ~ 2 at 25°C compared to 78.8 for water) the ionic cross-linking (scheme 3.2) impose

restriction towards the segmental mobility of the styrene grafted natural rubber backbone and may increase the Tg1 for the ionomer-1.

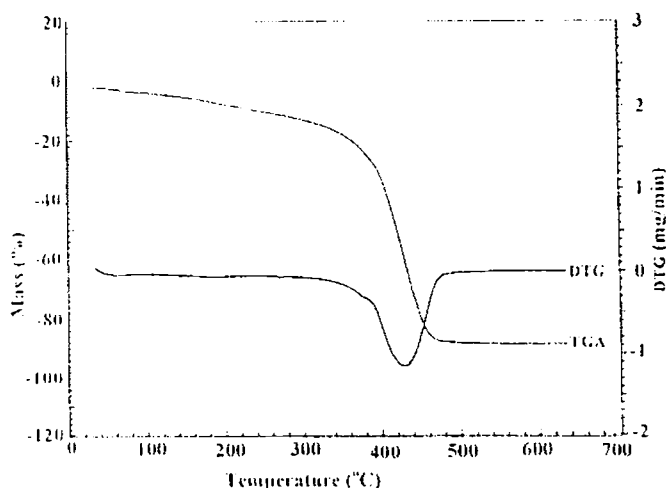


Fig. 3.5 Thermal profiles of 40 ZnS-RISGNR

Up on incorporating more ionic groups as in ionomer-2, the ionic interactions will increase little further and may be leading to the formation of stronger polar clustering as proposed in scheme 3.3. Apart from the low temperature thermal transitions, the ionomers show a second transition at higher temperature (Tg2). These transitions, which appear at 85 °C and 99 °C for the ionomer-1 and ionomer-2 respectively, are believed to be due to the influence of ionic groups attached to the polystyrene segments. The ionic cross-links, being thermo-labile, may be weakened at higher temperatures and contributes a relaxation towards i) the barrier to bond rotation around the polymer backbone, and ii) intermolecular constraints. These relaxations may produce volume shrinkage and the corresponding response appears as a drop in temperature (Tg2) in DSC thermo grams. Thus, Tg2 depends up on the barrier to free rotation around the polymer backbone, which in turn depends on the ionic interactions (or electrostatic force). It has been reported [14] that $Tg2 \propto W_{el}$, where W_{el} is the electrostatic work of removing an anion or cation from its coordination sphere.

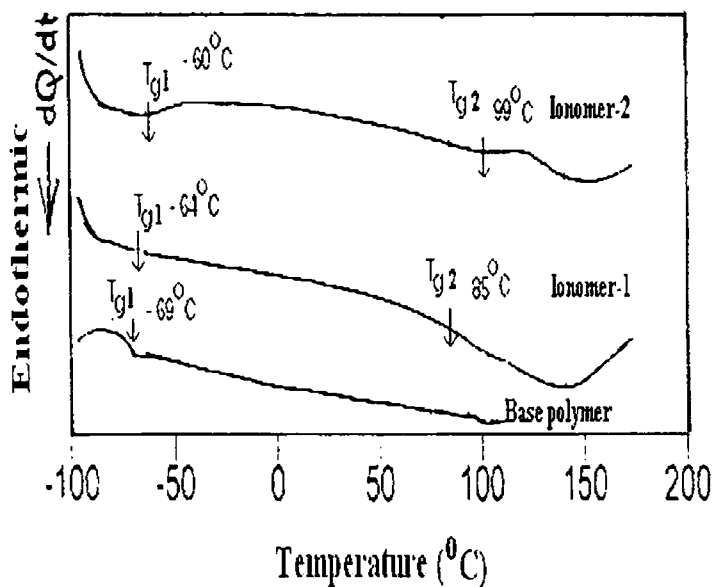


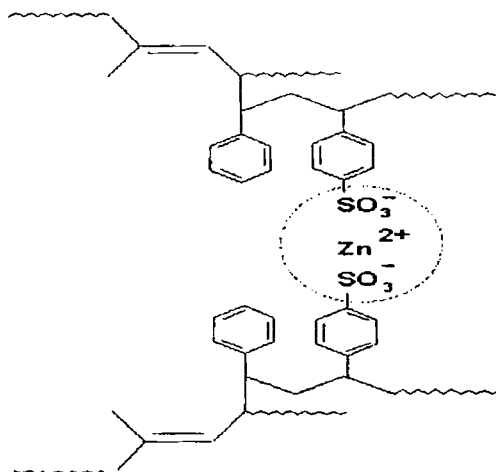
Fig. 3.6 DSC thermal profiles of ionomer- 1(26.5 ZnS-RISGNR) and ionomer- 2 (40 ZnS-RISGNR)

The ionic concentrations, which increase the ionic interactions, should influence W_{e1} or Tg_2 . The second thermal transitions at 85 °C and 99 °C for the ionomer-1 and ionomer-2 respectively with different ionic contents agree with the above theory.

Table 3.3 DMTA results of base polymer, ionomers-1 and 2

Samples	Tg_1 (°C)	$\tan \delta$ at Tg_1	Tg_2 (°C)	$\tan \delta$ at Tg_2	$\text{Log } E'$ (Pa) at Tg_1	$\text{Log } E'$ (Pa) at Tg_2
1	- 43.13	0.8313	+ 85.29	0.5490	8.0392	5.9615
2	- 20.58	0.1568	+ 87.23	0.5096	8.6274	6.4423
3	- 19.60	0.0705	+ 90.19	0.4782	8.8235	6.7307

Sample-1 shows the base polymer; 2 & 3 show ionomer samples with 26.5 and 40 meq of ionic groups respectively.



Scheme 3.2 Formation of the zinc salt of the sulphonated styrene grafted natural rubber

These observations reveal that incorporation of the zinc sulphonate groups in to the styrene grafted natural rubber produces phase-separated regions similar to an ionomer having two characteristic Tg's; one corresponding to the soft rubbery phase (Tg1) and the second may be due to the hard phase arising out of the clustering of the zinc sulphonate groups attached to the polystyrene units in the polymer (scheme 3.3). The dimension of the micro-phase clustering of polar groups in these ionomers may be falling within the size requirement to be detectable using DSC, as was reported for few ionomers [15-19]

3.3.6. Dynamic mechanical thermal analysis (DMTA)

3.3.6. (i) Loss tangent – temperature plots

Figure 3.7 shows the variation of loss tangent ($\tan\delta$) with temperature for RISGNR (base polymer), and the corresponding ionomer-1 (26.5 ZnS-RISGNR) and ionomer-2 (40 ZnS-RISGNR). The glass - rubber transition (Tg1) appearing around -43.13°C

for the base polymer has been increased in the case of ionomer-1 and ionomer-2 to -20.58°C and -19.6°C respectively.

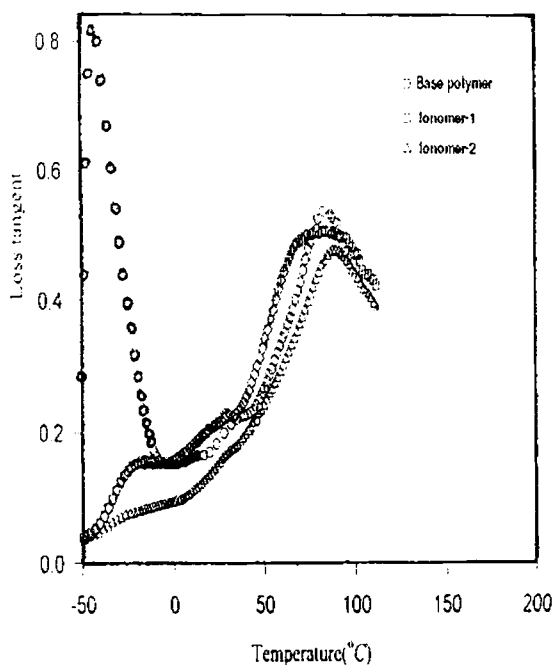
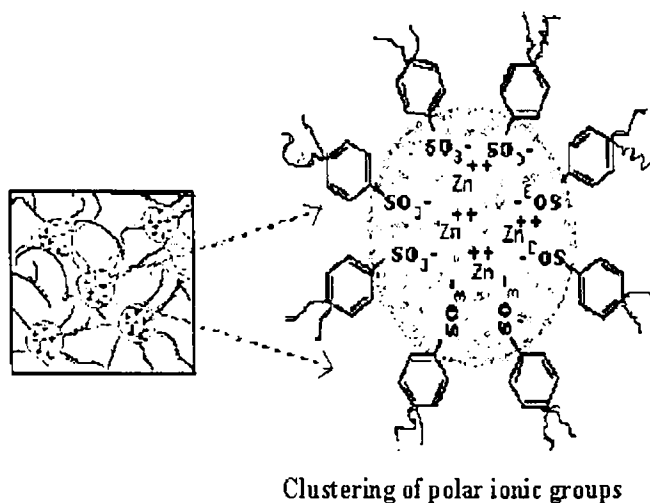


Fig. 3.7 Loss tangent- temperature curves for the RISGNR (base polymer) and their ionomers

The glass transition is accompanied by a steep descent of the modulus (Fig. 3.7) and the appearance of a pronounced loss tangent maximum. The $\tan \delta_{\max}$ (i.e., the $\tan \delta$ value at T_{g1}) was less in the case of ionomer-1 and ionomer-2 in comparison with the base polymer. Table 3.3 shows that incorporation of ionic groups cause lowering of $\tan \delta_{\max}$ of the ionomers. This may be due to the strong polar – polar interaction involving the backbone chains as represented by the scheme 3.2. The ionic groups have further influenced the mobility of the natural rubber backbone, which was affected by the grafting of styrene. The increase in the T_g 's of ionomers with

increased ion content may be due to the cross-linking and filler effects of the ionic groups. It has been observed that the ionic cross-links are as efficient as the covalent cross-links in raising T_g .



Scheme 3.3 Proposed polar clustering of ionic groups in the ionomers based on RISGNR

The loss tangent – temperature plot of the base polymer is typical of a thermoplastic elastomer. The base polymer shows two T_g 's which may be similar to the two service temperatures (or glass transitions) in thermoplastic elastomers [20]. Both the T_g 's corresponding to the soft rubbery phase (T_{g1}) and the hard polystyrene phase (T_{g2}) have been increased on ionomer modification. Incorporation of zinc sulphonate groups in to the base polymer decreased the $\tan \delta$ value at the high temperature ionic transition (T_{g2}). The $\tan \delta$ value at T_{g2} decreased as the ionic concentration increased.

These results indicate that the rubber – polar ionic cluster interactions in the case of ZnS-RISGNR ionomers are of two types: (i) polar cluster – nonpolar polymer backbone, which is similar to the interaction involving diene rubbers and reinforcing fillers, as manifested in the lowering of $\tan \delta$ at T_{g1} , (ii) polar-polar groups of the ionomer, which should have resulted in an increase in $\tan \delta$ at T_{g2} . While the rubber

– filler interaction involving the non-polar polymer backbone is of weak van der Waals' type; the same due to ionic aggregates (polar cluster) can be of much stronger type as proposed in the scheme 3.3. The incorporation of ionic groups in to the base polymer may cause a reinforcing effect as well. The decrease in the intensity of the peak at low temperature further supplements our views that the ionic groups are reinforcing. Appearance of both the low temperature as well as high temperature transitions for the zinc sulfonated ionomer samples may be considered as an evidence for the micro-phase or the “physical cross-links”.

3.3.6. (ii) Storage modulus-temperature plots

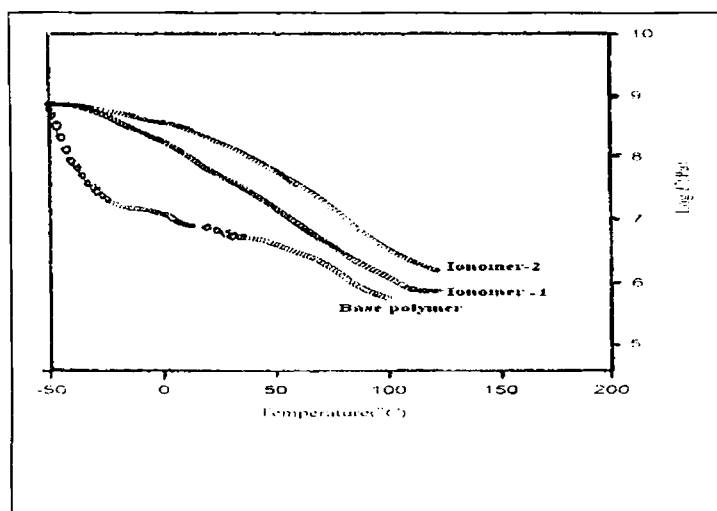


Fig. 3.8 Storage modulus-temperature curves for the RISGNR (base polymer) and their ionomers 1 and 2

Incorporation of zinc sulphate groups in to the base polymer increased the storage modulus of zincsulfonated RISGNR (Table 3.3). The appearance of an extended plateau (Fig. 3.8) may be due to the presence of sulphate groups [8]. The ionomer-1 (26.5 ZnS-RISGNR) shows higher storage modulus than the base polymer. An increase in the ionic concentration in ionomer-2 (40 ZnS-RISGNR) reveals a further enhancement in the storage modulus. The increase in the storage modulus of the

ionomers based on RISGNR may be because as the ion content changes, the relative number of ion associations in the matrix phase increases and the size of the clusters change. The effects of these two different ionic environments on the ionic modulus are different.

3.3.7 Influence of ionic groups on physical properties

The data listed in the table 3.4 document the increasing effect of zinc sulphonate groups on the physical properties of RISGNR. The tensile strength and tear resistance increased monotonically with the ion dosage up to 26.5 meq / 100 g rubber sulphonate concentration. The elongation at break of the ionomer samples showed a reciprocative change with the sulphonation level. Kraus et al have reported that the tear resistance is enhanced by the presence of those factors which tend to dissipate energy [21]. The ionic domain of ZnS-RISGNR may be acting as tear deviators or arrestors. The change in the physical properties of 40 ZnS-RISGNR ionomer sample [Tab.3.4] of higher ionic content may be attributed to the strength of the ion rich domains in the polymer matrix. The polymers at higher ionic concentrations may be transformed in to an ionically 'overcured' system with poor physical properties [22]

Table 3.4. Physical properties at 25 °C

Properties	Samples				
	1	2	3	4	5
Tensile strength (MPa)	1.2	5.4	6.9	8.7	3.8
Elongation at break (%)	248	204	189	124	82.0
Tear strength (N/mm)	12.0	28.6	53.2	84.5	62.0
Abrasion loss(cm ³ /hr)	1.92	0.93	0.82	0.73	0.98
Density (g/cm ³)	0.82	1.04	1.05	1.06	1.07
Hardness (Shore A)	42	86	89	91	93

1-shows base polymer; 2, 3, 4 and 5 show ionomers with 14.5, 21.2, 26.5 and 40 meq of ionic groups/100 g polymer

3.3.8 Reprocessability Studies

Table 3.5 shows that, the physical properties of the 26.5 ZnS-RISG NR ionomer remain constant even after three repeated cycles of mixing and molding. The morphology of ZnS-RISG NR is believed to be similar to that of conventional thermoplastic elastomers, that is, a combination of hard domains and soft segments [23-24]. The proposed larger ionic multiplet is represented in schemes 3.2 and schemes 3.3.

Table 3.5 Results of reprocessability studies of 26.5 ZnS-RISG NR ionomer

No. of Cycle	E. B. (%)	T.S (MPa)	Tear Strength(N/mm)
1	124	8.7	84.5
2	128	8.6	84
3	128	8.7	85

E.B - Elongation at break; T.S – Tensile strength

3.4 Conclusion

The present study leads to the following conclusion:

- Ionic cross-linked (zinc sulfonate) radiation induced polystyrene-g-natural rubber could be synthesized.
- FTIR spectra show that the ionic groups are attached to the pendant styrene blocks attached to the NR backbone.
- FTNMR spectra confirm the presence of ionic groups, giving support to the FTIR spectra.
- Thermal parameters inform the increased thermal degradation stability of the modified rubber. It reveals that the thermo-oxidative stability increases with increase in the ionic content of the polymer.

- DSC and DMTA studies reveal the influence of the ionic groups on the glass transition temperature of the base polymer.
- The thermoplastic elastomeric nature of the newly synthesized ionomers is evident from the retention of the stress-strain properties even after three cycles of repeated mixing and molding.

3.5. References

1. Naunton, W.J.S. *The Applied Science of Rubber*. Edward Arnold Publishers Ltd., London (1961).
2. Allen, P.W.; Ayrey, G.; Moore, C. G. *J. Polym. Sci.*, 36, 55 (1959).
3. Cockbain, E.G.; Pendle, T.D.; Turner, D.T. *J. Polym. Sci.* 39, 419 (1959).
4. Claramma, N. M.; Varghese, L.; Thomas, K.T.; Mathew, N. M. *Radiation Induced Graft Copolymerization of Styrene on to Natural Rubber*. IRMRA, 18th Rubber Conference, 165 (2000).
5. Holliday, L. Ed. in *Ionic Polymers*, Appli. Sci., London (1975).
6. Schlick, S. *Ionomers, Characterisation, Theory and Appl.* Ed; CRC Press: Boca Raton, FL (1996).
7. Tant, M.R.; Mauritz, K.A.; Wilkes, G.L. Eds., *Ionomers: Synthesis, Structure, Properties and Applications*. Chapman & Hall, New York (1997).
8. Eisenberg, A.; Joon-Seop Kim, *Introduction to Ionomers*. Wiley Interscience Publication, New York (1998)
9. US Patent 4, 184, 988 (1980), invs: Makowski, H.S.; Ludberg, R.D.; Bock, J.
10. Anil K. Bhowmick; Chakravarthy, D.; Mal, D.; Konar, J. *J. Elastomers and Plastics*. 32, 152 (2000).
11. Lu, X.; Weiss, R.A. *ACS Macromolecules*. 25, 6185 (1992),
12. Weiss, R.A.; Ashish Sen, Willis, C.L.; Pottick, L.A. *Polymer*, 32, 1867 (1991).
13. Sandler, S.R.; Karo, W.; Bonsteel, J.; Pearce, E.M. *Polymer Synthesis and Characterisation*. Section II, Expt. 14, Academic Press California, USA (1998).
14. Tse, M.F. *J. Adhes. Sci. Technol.* 3, 551 (1989).
15. Eisenberg, A.; In *Physical Properties of Polymers*; Mark, J.E.; Eisenberg, A.; Graessley, W.W.; Mandelkern, L.; Samulski, E.T.; Koenig, J.L.; Wignall, G.D., Eds.; American Chemical Society: Washington, DC; Chapter 2 (1993).
16. Kanamoto, T.; Hatsuya, I.; Ohoi, M.; Tamaka, K. *Macromol. Chem.*; 176, 3497-3500 (1975).
17. Maurer, J.J. In *Thermal Analysis: Proceedings of the Seventh International Conference on Thermal Analysis*, Vol. 2; Miller, B., Ed.; Wiley: New York; 1040-1049 (1982).
18. Tong, X.; Bazuin, C.G. *Chem. Mater.* 4, 370-377 (1992).

19. Ehrmann, M.; Muller, R.; Galin, J.-C.; Bazuin, C.G. *Macromolecules* 26, 4910- 4918 (1993).
20. Holden, G., in: *Thermoplastic Elastomers: a comprehensive review*. Legge, N.R.; Holden, G.; Schroeder, H.E.; Eds. Chapter 13, page 486, Hanser, New York, Macmillan (1987)
21. Kraus, G.; Eirich, F.R. *Science and Technology of Rubber*. Academic Press, New York (1978).
22. Chen. C. Ku; Raimond Liepins, "*Electrical Properties of Polymers: Chemical Principles*. Hanser Publishers: Munich, Chapter 3 (1987).
23. Yarusso, D.J.; Cooper, S.L. *Macromolecules.*, 16, 1871 (1983).
24. Eisenberg, A.; Hird, B.; Moore, R.B. *Macromolecules.* 23, 4098 (1990).

Chapter4

Alternative synthesis of ionomers

-
1. Part 1 of this chapter has been published in *J. Elast. Plast.* 34, 1 (2002)
 2. Part 2 of this chapter has been accepted in *Intern. J. Polym. Mater.*
-

Part 1	4.1	<i>Zinc sulphonated natural rubber ionomer (ZnS-NR)</i>
	4.1.1	<i>Preparation</i>
	4.1.2	<i>Spectroscopic characterizations</i>
	4.1.3	<i>Thermal investigations</i>
	4.1.4	<i>Comparison of styrene graft and zinc salt natural rubber</i>
	4.1.5	<i>Physical properties</i>
	4.1.6	<i>Reprocessability studies</i>
	4.1.7	<i>Conclusion</i>
Part 2	4.2	<i>Thermoplastic ionomers based on CISGNR</i>
	4.2.1	<i>Synthesis</i>
	4.2.2	<i>Results and discussion</i>
	4.2.3	<i>Thermo gravimetric analysis</i>
	4.2.4	<i>Physical properties</i>
	4.2.5	<i>Reprocessability studies</i>
	4.2.6	<i>Conclusion</i>
Part 3	4.3	<i>Comparison of natural rubber ionomers</i>
	4.4	<i>References</i>

Part.1

4.1 Zinc sulphonated natural rubber ionomer (ZnS-NR)

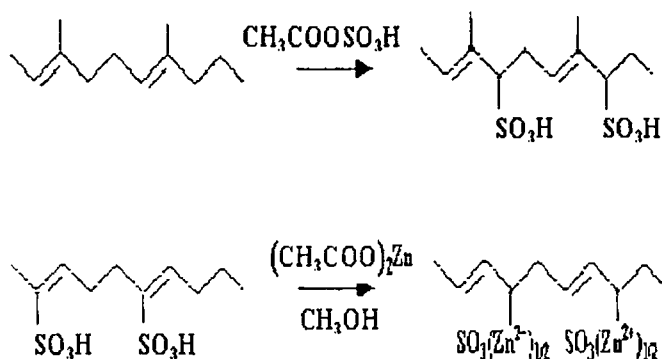
4.1.1 Preparation

4.1.1.a). Acetyl sulphate reagent

The sulphonating reagent acetyl sulphate was prepared by slowly adding sulphuric acid to a solution of acetic anhydride in DCE at 0°C. The freshly prepared acetyl sulphate diluted using DCE was warmed to 10°C and used.

4.1.1.b). Ionomers

To a 5 % natural rubber solution in dichloroethane, acetyl sulphate was added drop wise, under stirring in a cold bath. The reaction was terminated after 30 minutes by adding isopropanol.



Scheme 4.1 Sulphonation reaction of NR with acetyl sulphate followed by neutralization

The sulphonated NR was converted to the zinc salt by adding solution of zinc acetate in methanol to the agitated solution. After all the neutralizing agent was added, the solution was stirred for 30 minutes and the neutralized rubber was steam stripped,

and vacuum dried at 50 °C for 72 hrs. The sulphonic acid content was determined using XRFS and the amount of zinc by ICPAES. The resultant ionomer is designated as x.y. ZnS-NR, where x.y shows number of milliequivalents of zinc sulphonate groups/100 g NR. The chemistry of the reaction of natural rubber with acetyl sulphate and the neutralization with zinc acetate is shown in scheme 4.1.

4.1.2 Spectroscopic characterisation

4.1.2. a. XRFS analysis

Figure 4.1 shows the variation of the level of sulphonation of NR with the amount of sulphuric acid in the form of acetyl sulphate added at the experimental conditions. The ionic content increases with increase in the concentration of sulphuric acid added. The reagent conversion at the level of 32 % was established through the estimation of sulphur.

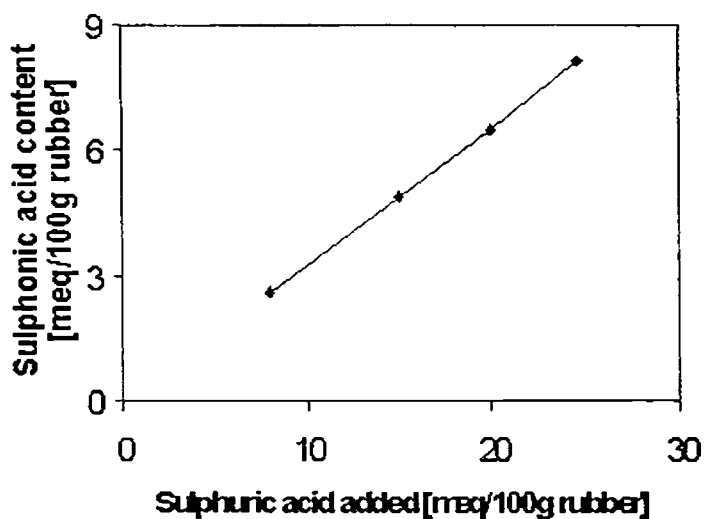


Fig. 4.1 Level of sulphonation of NR with the amount of sulphuric acid (as acetyl sulphate)

4.1.2.b. ICPAE spectroscopy

Figure 4.2 demonstrates the level of neutralization of the sulphonic acid moiety in the ZnS-NR. Irrespective of the sulphonic acid content in the sulphonated-NR, it has been found that, the level of neutralization by the zinc acetate remains the same. ICPAES measurements of the zinc present in the Zn-SNR reveal that, about 96 % neutralization of the sulphonic acid groups in the rubber occurs.

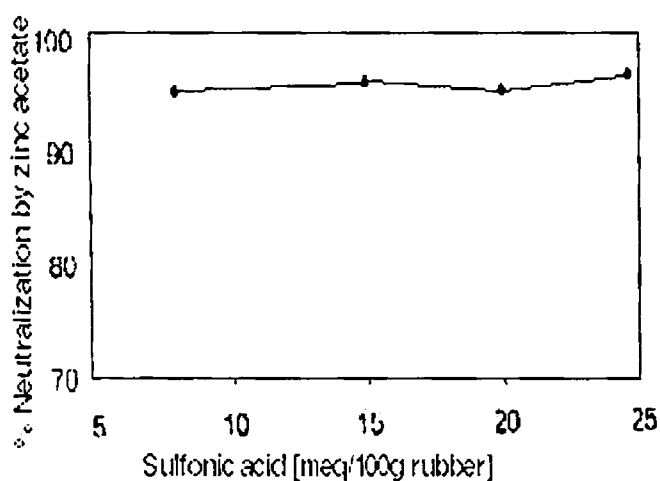


Fig. 4.2 Percentage neutralization by zinc acetate vs. sulphonic acid content

4.1.2.c. FTIR spectroscopy

The main peaks of interest in the FTIR spectra (Fig.4.3) of the control NR (b) and the modified NR (a) are 1024,1097,1149,1200,1219,1330 and 1651 cm^{-1} . The important functional groups and their assignments are given in the table 4.1. The sulphonation of NR and the formation of zinc-neutralized sulphonated NR are exemplified by the characteristic peaks [1, 2]. Maintaining a low temperature and inert atmosphere controlled the degradation of NR. This was further supported by the absence of

characteristic peaks of $>C=O$ at $1700-1900\text{ cm}^{-1}$. The unique characteristic absorption frequency of the isolated $C=C$ was higher in the ZnS-NR, and is comparable with that of $S=O$ bond [2].

Table 4.1 Important FTIR peaks of 24.6 ZnS-NR and their assignments

Functional group	Absorbance (cm^{-1})	Remarks
CH=CH	580	Cis configuration
Sulfonic acid salt	1024, 1097 & 1200	Characteristic peaks
S-O	1097	$\text{SO}_3^- (\text{Zn}^{2+})_{1/2}$
SO_3^-	1149 & 1219	Asym. stretching vibration
Sulfones	1330	Partial cross-linking
C- CH_3	1376, 1450	Sym & asym. deformation
C=C	1651	Stretching
C-H of CH_3	2850	Stretching
CH_2	2910	Asym. stretching

This may be due to the attachment of SO_3H group to the $C=C$, which tends to decrease the frequency of C-SH as shown by $2500-3050\text{ cm}^{-1}$.

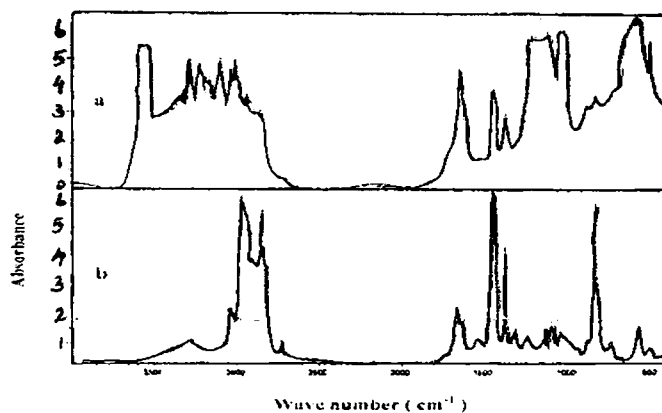


Fig. 4.3 FTIR spectra of: ZnS-NR (a), and NR (b)

IR spectrum appears only if, the vibration produces a change in the permanent electric dipole of the molecule. Hence it is reasonable to presume that, more the polarity of a bond, more intense will be the IR spectrum arising from the vibration of that bond [1]. For this reason too, the vibrations of the ionic crystal lattices often give rise to a very strong absorption as shown by the broad peak in the region 513 cm^{-1} to 664 cm^{-1} , which may be due to ionic aggregation or clusters, characteristic of ionomer. Hence figure 4.3 and table 4.1 vividly illustrate the feasibility of sulphonated NR.

4.1.2.d. FTNMR spectroscopy

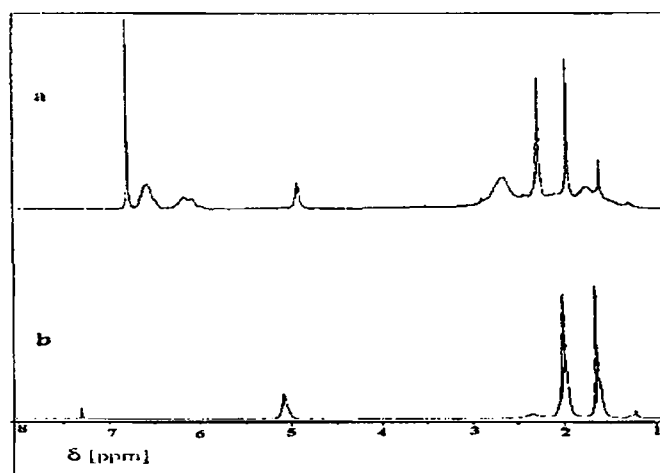
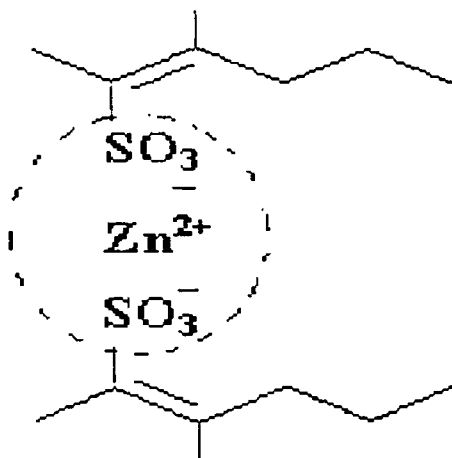


Fig. 4.4 FTNMR spectra of: ZnS-NR (a), and NR (b)

The spectra of the control NR (a) and ZnS-NR (b) in Fig. 4.4 distinguishes the differences in the C=C region at 5.10227 ppm and 5.1042 ppm respectively, which arises due to the attachment of sulphonic acid group to the alkene carbon of the hydrocarbon back bone of the NR [3]. The signals due to CH₂ groups of both samples look alike. Chemical shift of the peak in the ZnS-NR could be attributed to double bond shielding anisotropic effect arising out of local conformational changes due to introduction of sulphonic acid group into the polymer. In addition to the characteristic

peaks of NR at 1, 2 and 5 ppm respectively, few new peaks appear at 1-2 ppm and 6-7 ppm in the ZnS-NR. A new distinguishable peak at 6-7 ppm may be considered as an evidence for the strong ionic environment due to the introduction of $-(\text{SO}_3)_2\text{Zn}$ in the modified NR. It can, therefore, be considered as a supplementary evidence for the FTIR spectroscopic observation.



Scheme 4.2 The proposed structure of ZnS-NR ionomer

The results from FTIR, FTNMR, and the well documented fact that the alpha-olefins containing a 2-methyl branch undergo fast sulphonation to yield 2-alkene sulphonic acid [4], agrees with the substitution of sulphonic acid groups at the alkene carbon atom of the NR hydrocarbon backbone without perturbing the C=C structure. These observations therefore support the proposed structure of zinc sulphonated natural rubber ionomer (Scheme 4.2).

4.1.3 Thermal investigations

4.1.3 a. Differential scanning calorimetry (DSC)

The DSC thermogram of the zinc sulphonated natural rubber is shown in figure 4.5. The zinc sulphonated natural rubber, however, shows two T_{gs}, one at -59°C and a second one at 98°C in comparison with the uncured NR.

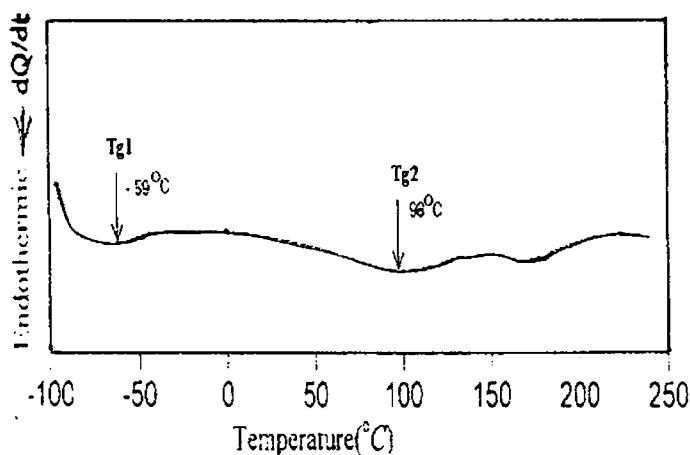


Fig. 4.5 DSC thermal profiles of zinc sulphonated natural rubber

The low temperature transition T_{g1} may be due to the soft rubbery phase. Incorporation of the ionic groups in to the NR matrix may act as physical cross-links at low temperature. These interactions between the NR backbones, probably, stiffen the chains and it results in the hindrance to the free rotation of the groups about the polymer chains. An increase in the matrix Tg of the natural rubber may be expected to be due to of the ionic modification of the natural rubber. This has been found to be true from the figure 4.5. The second transition around 98°C (T_{g2}), which appears for the zinc sulphonated natural rubber, may result from the relaxation, at elevated temperatures, of the presumably hard regions of ionic clusters (scheme 4.3).

4.1.3 b. Dynamic mechanical thermal analysis (DMTA)

The dynamic mechanical analysis [5] of the uncured NR shows only one Tg appearing at -43.87°C . Incorporation of zinc sulphonate groups in to the natural rubber gives a new material with two thermal transitions, T_{g1} and T_{g2} . The low temperature transition T_{g1} , represented in table 4.2 that appears around -20.58°C , may be due to the glass-rubber transition in the NR matrix.

Table 4.2 Comparison of the DMTA results of the styrene grafted NR and zinc sulphonated NR

Properties		SG-NR	ZnS-NR
Thermal transitions	Tg1 (°C)	- 43.13	- 20.58
	Tg2 (°C)	+85.29	+97.05
Tan δ at	Tg1	0.8313	0.1568
	25(°C)	0.1882	0.2196
	Tg2	0.5490	0.5723
Storage modulus- Log E' (Pa) at	Tg1	8.0392	8.6274
	25(°C)	6.8039	7.7058
	Tg2	5.9615	6.2745
Loss modulus- Log E'' (Pa) at	Tg1	7.95	7.82
	25(°C)	6.07	7.04
	Tg2	5.70	6.03

4.1.4. Comparison of styrene graft and Zinc salt natural rubber

Presence of the ionic groups in the NR matrix, probably serves as a physical cross-link, affects the Tg of the matrix to some extent. When the polystyrene domains in SG-NR causes very little effect on the Tg of the NR matrix, the presumed ionic domains due to the zinc sulphonate groups in the ZnS-NR produces a marginal influence. In the tan δ -temperature plots (Fig. 4.6), a higher drop in the tan δ value has been observed on incorporating the ionic groups in comparison with SG-NR. Higher stiffness of the ZnS-NR, when compared to the SG-NR, is manifested from the higher storage modulus at the experimental range of temperature as depicted in the figure 4.6. The greater restrictions imposed up on the mobility of NR backbones, by the ionic groups may be the causative increasing the glass-transition temperature.

The ionic interactions may lead to the development of ionic aggregations as proposed in scheme 4.2.

These ionic aggregations or the presumed microstructure may exist as a phase-separated region of detectable transition. Appearance of the second thermal transition (T_{g2}) at a higher temperature in ZnS-NR may be thus accounted for.

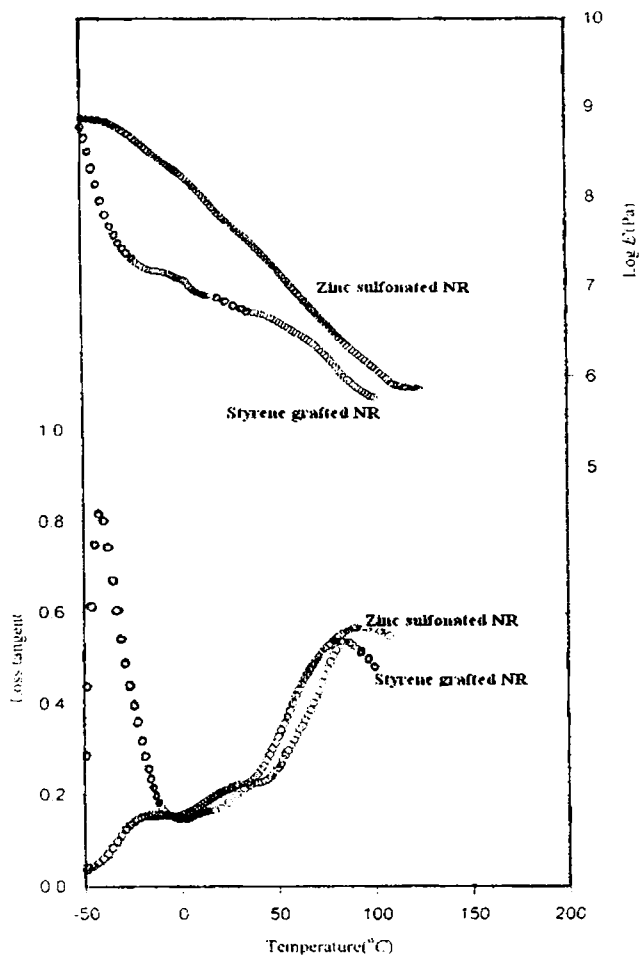


Fig. 4.6 DMTA plot of Styrene grafted-NR and Zinc sulphonated-NR

Relaxation due to the micro-phase-separated polystyrene centers, within SG-NR, may be detected as Tg2 at +85.29 °C. The Tg2 for the ionically modified NR (+97.05 °C) has been observed at a temperature of 12 °C higher than that for the polystyrene modified NR. This may be attributed to the higher temperature required for the relaxation of the ionic assemblage, held through coulombic forces, acting as physical cross-links. The steep descent and an extended rubber plateau for the zinc salt of natural rubber (Fig. 4.6), unlike SGNR, may be characteristic of the ionic network due to the sulphonated groups. The high temperature mechanical loss observed at Tg2 for the zinc salt of the sulphonated natural rubber may be due to the motion in the ion-rich phase

4.1.5 Physical properties

The values in the table 4.3 explain the increasing effect of zinc sulphonate groups on the physical properties of NR. The drastic changes occur above the sulphonic acid concentration of 20 meq/100g NR. The 24.6 ZnS-NR shows a tensile strength of 13 MPa. The same parameter for the unvulcanised base NR is only 0.36 MPa. The physical properties of the ZnS-NR at this stage confirm well with the requirements of a good thermoplastic elastomer. The influence of the ionic contents on the tensile strength of the modified NR is illustrated in figure 4.7.

Table 4.3. Physical properties of ZnS-NR at 25 °C

Properties	Samples			
	1	2	3	4
Tensile Strength (MPa)	6.4	7.5	8.6	13.0
Elongation at Break (%)	207	181	103	74
Tear Strength (N/mm)	37	46	59	86
Hardness (Shore A)	86	89	91	93
Abrasion Loss (cm ³ /hr)	0.676	0.646	0.612	0.528

*Four samples of ZnS-NR having sulphonate concentrations in which 1=10.4, 2=15.6, 3=20.2, and 4=24.6 meq/100g rubber

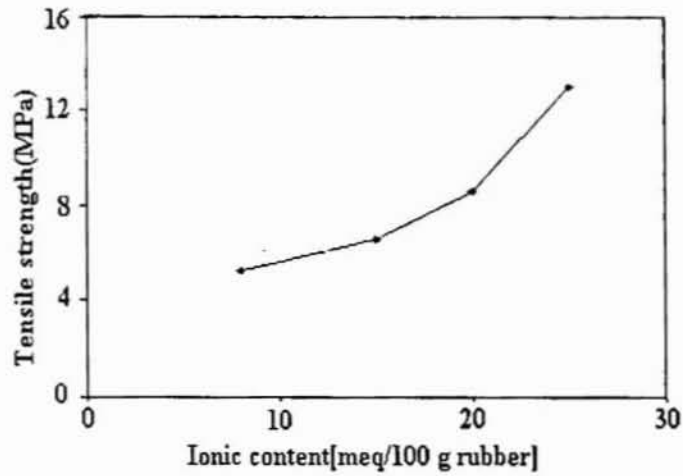
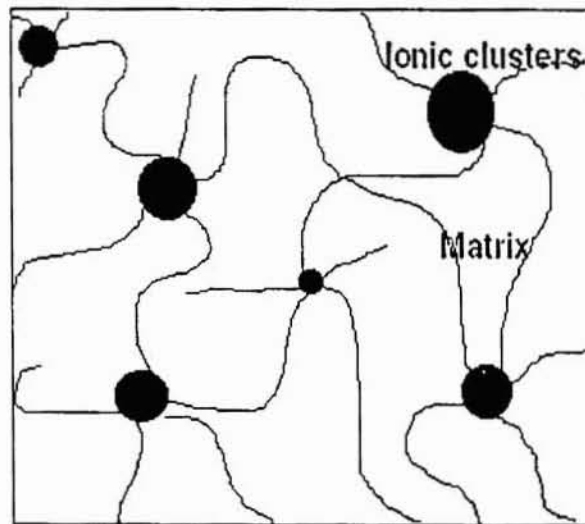


Fig.4.7. Relation between ionic concentration and tensile strength



Scheme 4.3 Proposed model for the ionic aggregation in NR matrix

The elongation at break of the ionomer samples decreased when the level of sulphonation increased, where as the tear resistance increased with sulphonation. The tear resistance of an elastomer is a measure of crack propagation [6]. The higher abrasion resistance shown by ZnS-NR sample of higher sulphonate levels [Table 4.3] could be attributed to the strength of the matrix. The hardness of ZnS-NR increased as the level of sulphonation increased. Hardness is a measure of modulus of elasticity at low strain [7]. The higher hardness may due to the higher content of ionic aggregates [8].

4.1.6 Reprocessability Studies

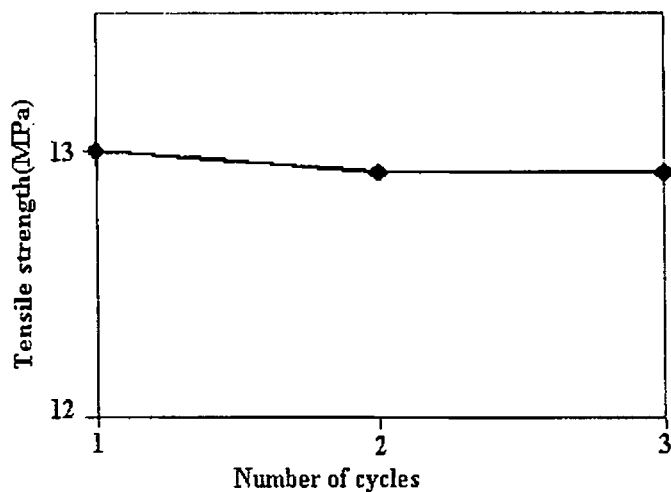


Fig. 4.8 Tensile strength of ZnS-NR at different cycles of processing.

As shown in figure 4.8, the ~~stress-strain~~ ^{tensile strength} properties of the ZnS-NR remain almost constant even after repeated cycles of mixing and molding. This shows that ZnS-NR behaves as a thermoplastic elastomer and it could be reprocessed at 120°C by mechanical recycling without deterioration in its physical properties.

4.1.7 Conclusion

The studies on the chemically modified natural rubber have allowed us to draw the following conclusion:

- Zinc neutralized sulphonated natural rubber could be prepared by reacting natural rubber with acetyl sulphate followed by neutralization of the precursor acid with zinc acetate.
- FTIR spectra show evidence for the formation of sulphonated natural rubber.
- FTNMR spectra confirm the formation of ionic groups, giving credence to the FTIR spectra.
- The modified NR has tensile strength about thirty-five times the strength of unvulcanised base NR.
- DMTA results show that incorporation of zinc sulphonate groups in to the natural rubber gives a new material with two thermal transitions, Tg1 and Tg2.
- When the polystyrene domains in SGNR causes very little effect on the Tg of the NR matrix, the presumed ionic domains due to the zinc sulphonate groups in the ZnS-NR produces a marginal influence.
- The Tg2 for the ionically modified NR (+97.05 °C) has been observed at a temperature of 12 °C higher than that for the polystyrene modified NR. This may be attributed to the higher temperature required for the relaxation of the ionic assemblage, held through coulombic forces, acting as physical cross-links.
- The steep descent and an extended rubber plateau for the zinc salt of natural rubber, unlike SG-NR, may be characteristic of the ionic network due to the sulphonated groups. The high temperature mechanical loss observed at Tg2 for the zinc salt of the natural rubber may be due to the motion in the ion-rich phase
- The ZnS-NR may be reprocessed at about 120 °C without sacrificing much of its physical properties.

Part.2

4.2. Thermoplastic ionomers based on chemically induced styrene grafted natural rubber (ZnS-CISGNR)

4.2.1. Synthesis

4.2.1 a). Chemically induced styrene grafted natural rubber (CISGNR)

Styrene was graft copolymerized with natural rubber latex using tertiary butyl hydro peroxide and tetraethylenepentamine system. The formulation for the graft copolymerization of styrene in ammonia preserved natural rubber latex is shown in table 4.4. The temperature was maintained by using the hot water bath.

Table 4.4 Formulation for the graft-copolymerization of styrene in natural rubber latex

Ingredients	Parts by mass (g)
Natural rubber (as 30 % drc latex, 0.4 % m/m ammonia)	200
Non-ionogenic stabilizer (as 20 % aqueous solution)	9
Styrene	33
Tertiary butyl hydro peroxide	0.13
Tetra ethylene pent ammine (as 10% m/m aqueous solution)	0.6
Time of grafting	24 hours
Grafting temperature/ °C	50-60

4.2.1 b). Ionomers based on CISGNR

The graft copolymer (CISGNR) was dried under vacuum at 50^o C for 72 hrs prior to use. The sulphonating agent acetyl sulphate was prepared in situ by the reaction of acetic anhydride and concentrated sulphuric acid. Excess of acetic anhydride was used to scavenge any water that might have been present. Sulphonation was carried out in dichloroethane solution at room temperature. Acetyl sulphate was added drop

wise and the reaction was terminated after 30 minutes by adding isopropanol. The polymer sulphonic acid neutralized with zinc acetate in methanol was recovered by steam stripping, and the product was vacuum dried at 50 °C for 72 hrs.

4.2.2 Results and discussion

4.2.2 a. FTIR spectroscopy

FTIR spectra of the control NR (a), CISG NR (b) and ZnS-CISG NR (c) are shown in Fig. 4.9. In the IR spectrum of CISG NR the peaks at 3026 and 2855 cm^{-1} correspond to the aromatic C-H stretching in polystyrene. Peaks at 1601 and 1541 cm^{-1} correspond to the C=C stretching of aromatic ring of polystyrene. A strong peak at 698 cm^{-1} stands for the monosubstituted benzene ring along with the characteristic absorption of natural rubber at 837 and 889 cm^{-1} .

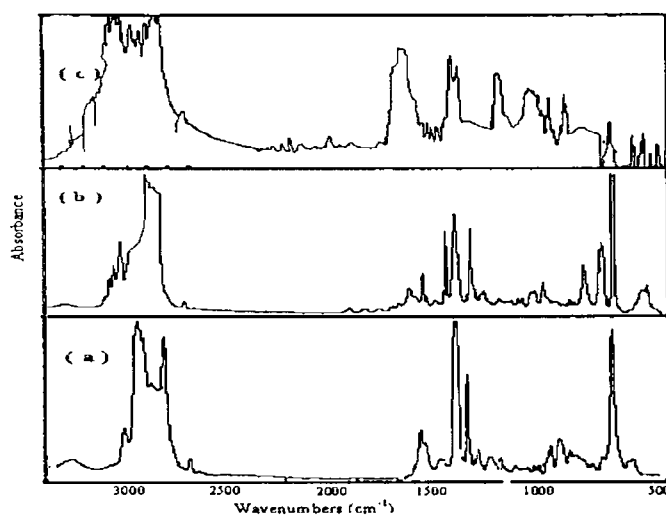


Fig. 4.9 FTIR spectra of NR (a), CISG NR (b), and ZnS-CISG NR (c)

The peaks at 1452 and 1375 cm^{-1} correspond to the aliphatic C-H stretching in natural rubber. The FTIR spectrum of the ZnS-CISG NR show 1008 cm^{-1} peak representing the in plane bending vibrations of phenyl group substituted with a metal

sulphonate group, 1127 cm^{-1} for the sulphonate anion attached to a phenyl ring, 1042 cm^{-1} for the symmetric stretching vibration of the zinc sulphonate group and the doublet at 1235 cm^{-1} due to symmetric stretching vibration of the sulphonate group [9-12]. The two kinds of reactive site in the CISG NR such as i) the phenyl rings in the polystyrene blocks and ii) the residual C=C in the rubber block is evident from the reactions represented in scheme 3.1 (chapter 3). Although olefinic unsaturation is inherently more reactive to acetyl sulphate than the phenyl rings, infrared spectroscopic analysis confirmed that sulphonation occurred almost exclusively in the polystyrene blocks.

4.2.2 b). FTNMR spectroscopy

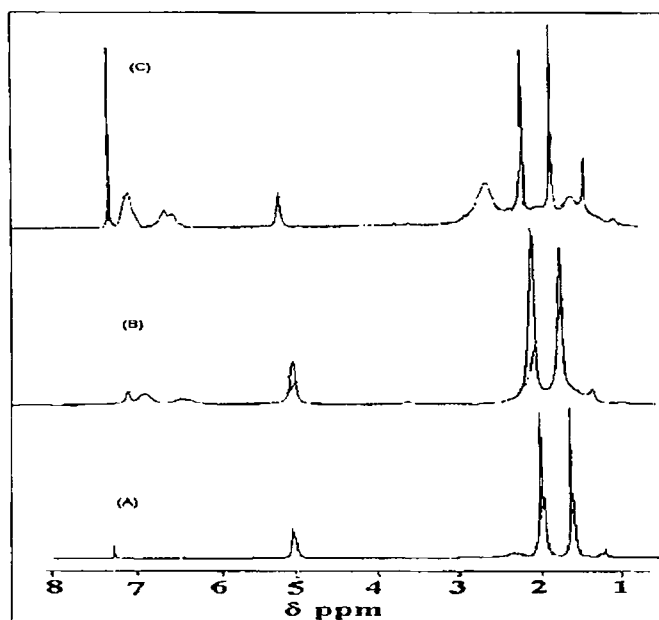


Fig. 4.10 FTNMR spectra of NR (a), CISG NR (b), and ZnS-CISG NR(c)

The n.m.r spectra of the control NR (A), CISGNR (B) and ZnS-CISGNR(C) are represented in figure 4.10. In the spectrum of CISGNR, not only the characteristic signals of NR at 1, 2 and 5 ppm are retained but a new signal at 7.2 ppm also appears. The new signal at 7.2 ppm is due to the benzene ring present in the grafted styrene units. This is evident from the positive chemical shift to the corresponding signals in CISGNR spectrum as compared to the NR. The chemical shift of peaks in the modified polymer is due to the local conformational change, which arises due to the grafting of styrene units at the allylic carbon atom in natural rubber. The environment of the grafted phenyl units has been disturbed in the sulphonated graft polymer. This is clear from the chemical shift of the signals corresponding to the aromatic ring at 7.0277 ppm to 7.2781 ppm. The relatively large shift in the resonance signals of phenyl ring confirms that a strong ionic group like $-(SO_3)_{1/2} Zn$ is attached to the benzene ring in CISGNR. It can therefore be considered as a supplementary evidence for the FTIR spectroscopic observation [9]

4.2.3 Thermogravimetric analysis (TGA)

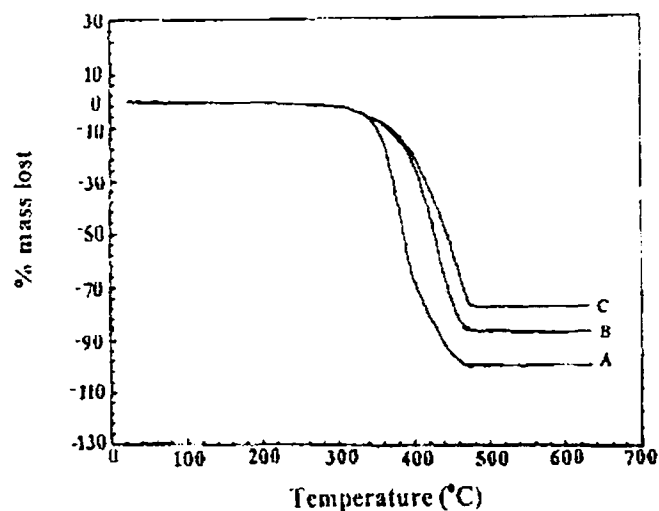


Fig. 4.11 TGA thermogram of CISGNR (A), 20.2 ZnS- CISGNR (B), and 25.5 ZnS- CISGNR(C)

and Fig. 4.12

The figure 4.11₂ shows the thermal degradation behavior of CISG NR (A), 20.2 ZnS-CISG NR (B) and 25.5 ZnS-CISG NR (C) observed from the thermogravimetric analysis (TGA). It was observed that the sample (C) is more stable, because the degradation starts at 375°C, whereas the degradation of the sample (A) starts at 350°C.

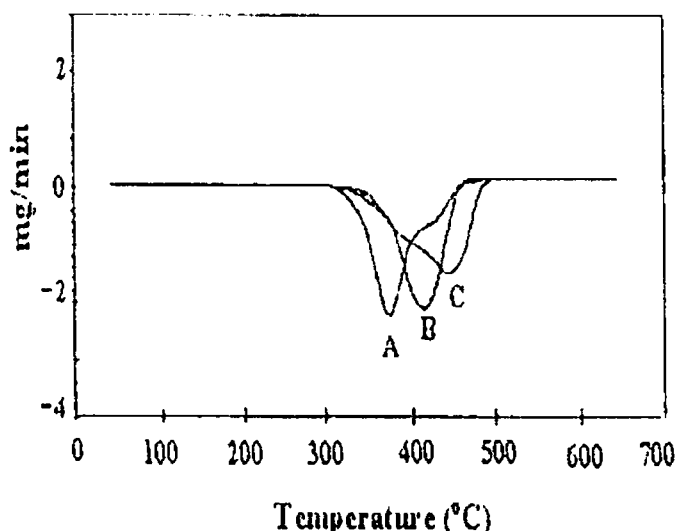


Fig. 4.12 DTG thermograms of CISG NR (A), 20.2 ZnS- CISG NR (B), and 25.5 ZnS- CISG NR (C)

This increase in stability of the ZnS-CISG NR is due to the greater stability of the aromatic sulphonate derivative [12]. The higher residual weight % shown by ZnS-CISG NR, as compared to CISG NR, could be attributed to the presence of zinc in the modified ionomeric form of the base polymer. The thermo-oxidative stability increased with increasing sulphonation level. This is evident from the T_{max} values, i.e., the temperature at which the rate of degradation is maximum, shown in figure 4.11. The differences in the TGA thermograms between the salts of different ionic content may

be due in part to differences in the viscosity of polymers, which affects the diffusion rate of the volatile degradation products of the sample.

4.2.4 Physical properties

The data listed in the table 4.5 document the increasing effect of zinc sulphonate groups on the physical properties of CISG NR. The 25.5 ZnS-CISG NR ionomer shows a tensile strength of 9 MPa. The same parameter for the unvulcanised base CISG NR is only 1.23 MPa. The physical properties of the ZnS-CISG NR at this stage confirm well with the requirements of a good thermoplastic elastomer. The elongation at break of the ionomer samples decreased and its tear resistance increased with sulphonation.

Table 4 5 Mechanical properties at 25 °C

Properties	Samples*			
	1	2	3	4
Tensile Strength (MPa)	1.2	5.7	7.6	9.0
Elongation at Break (%)	210	201	191	128
Tear Strength (N/mm)	35.0	28.4	54.2	82.5
Hardness (shore A)	42	78	82	85
Abrasion Loss (cm ³ /hr)	0.92	0.74	0.71	0.52

*Samples are 1=CISG NR; 2= 15.1 ZnS-CISG NR; 3= 20.2 ZnS-CISG NR; 4= 25.5 ZnS-CISG NR.

It is known that tear strength is enhanced by factors, which tend to dissipate energy [13]. The ionic domain of ZnS-CISG NR may be acting as tear deviators or arrestors. The higher abrasion resistance shown by ZnS-CISG NR sample of higher sulphonate levels could be attributed to the strength of the matrix; as evident from the stress-strain behavior. The hardness of ZnS-SG NR increased as the level of sulphonation

C78603

increased. Hardness is a measure of modulus of elasticity at low strain [14]. The higher hardness may due to the higher content of ionic aggregate [15].

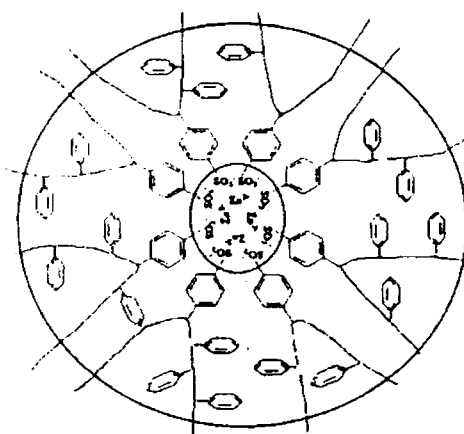
4.2.5 Reprocessability studies

Results of the reprocessability studies (table 4.6) show that, the stress strain properties of the ZnS-CISG NR remain almost constant even after repeated cycles of processing at about 120 °C

Table 4.6 Results of reprocessability studies of 25.5 ZnS-SG NR

No. of cycle	Elongation at break (%)	Tensile strength (MPa)	Tear strength (N/mm)
1	128	9.0	82.5
2	140	8.6	84.0
3	149	9.0	86.2

The morphological structure of ZnS-CISG NR is believed to be similar to that of conventional thermoplastic elastomers, that is, a combination of hard domains and soft segments.



Scheme 4.4 Proposed model for the ionic aggregates in ZnS-CISG NR ionomer

In agreement with the most important and widely applicable models for ionic aggregates [16-18], a model has been proposed for the ZnS-CISGNR ionomer (scheme 4.4).

4.2.6 Conclusion

The following conclusions were drawn from the studies on the ZnS-CISGNR ionomer:

- Zinc salt of styrene grafted natural rubber sulphonic acid could be prepared.
- The analytical techniques, XRFS and ICPAES respectively show that acetyl sulphate reagent conversion is about 32 %, and neutralization of the sulphonic acid is 96 %.
- FTIR spectra show evidence for the grafting of styrene on to the natural rubber backbone and also for the formation of sulphonated styrene grafted natural rubber.
- NMR spectra confirm the presence of ionic groups in the modified rubber, giving supplementary evidence to the FTIR spectra.
- Thermogravimetry results show that thermo-oxidative stability of the base polymer improved up on ionomer modification.
- The modified SGNR showed higher tensile strength than unvulcanized base polymer.
- Reprocessability studies reveal the thermo-reversible character of the ionically modified rubber.

Part. 3

4.3 Comparison of natural rubber ionomers

Ionomers based on natural rubber have been prepared by two techniques: 1. direct method and 2. indirect method. In the direct method ionomer has been synthesized directly from natural rubber without styrene grafting. This modified rubber ionomer is represented as ZnS-NR. In the indirect method of synthesis two steps are involved, styrene grafting and ionomeric modification. Both radiation induced and chemically induced styrene grafted natural rubber have been used for the ionomeric modification.

Three types of ionomers such as ZnS-RISGNR (chapter 3), ZnS-NR and ZnS-CISGNR (chapter 4, part 1 and part 2 respectively) have been reported. Comparison of the physical properties of these ionomers (Table 4.7) has been done.

Table 4.7 Comparison of the physical properties of the ionomers based on NR, CISGNR and RISGNR

Properties	Samples		
	ZnS-NR	ZnS-CISGNR	ZnS-RISGNR
Tensile Strength (MPa)	13.0	9.0	8.7
Elongation at break (%)	74	128	124
Tear Strength (N/mm)	86.4	82.5	84.5
Abrasion Loss (cm ³ /hr)	0.528	0.528	0.738

mechanical

Results indicate that the physical properties of the ionomers vary in the order ZnS-NR > ZnS-CISGNR > ZnS-RISGNR. However, owing to the availability of the base material, extension studies on ionomer such as effect of fillers, dielectric behavior and compatibilising property (chapters 5, 6 and 7) are carried out using ZnS-RISGNR ionomers.

4.4. References

1. Banwell, C.N., "*Fundamentals of Molecular Spectroscopy*" Third Edn. Tata McGraw-Hill Company Ltd. India, 110 (1983).
2. Xinya Lu; Weiss, R. A.; *Macromolecules*, 6185, 25 (1992).
3. Chakravarthy, D.; Mal, D., Konar, J., and Anil K. Bhowmick, *J. Elastomers & Plastics*, 152, 32 (2000).
4. Kennedy, J. P.; Story, R. F.; *Org. Appl. Poly. Sci. Proce.* 182, 46 (1982).
5. Sircar, A.K.; Galaska, M.L.; Rodrigues, S.; Chartoff, R.P. *Rubber Chem. Technol.*(3), 72, 513 (1999)
6. Kraus, G, Eirich, F.R; "*Science and technology of rubber*", Academic press New York (1978).
7. Ferrigno, T. H.; "*Hand book of Fillers and Reinforcement for plastics*", Van Nostrand Reinhold Company, New York (1978).
8. Laurer, J. H.; Winey, K. I., *Macromolecules* 9106, 31 (1998).
9. Anil K.Bhowmick; Chakravarthy, D. D. Mal and Konar, J. *J. Elastomers and plastics*, 32, 152. (2000).
10. Xinya Lu; Weiss, R. A; *Macromolecules*, 25, 6185. (1992).
11. Weiss, R. A; Ashish Sen; Willis, C. L. and Pottick, L.A. *Polymer*, 32, 1867. (1991).
12. Sandler, S. R; Karo, W; Bonsteel, J and Pearce, E. M. in "*Polymer synthesis and characterization*" Section II, Expt.14, Academic Press California, USA. (1998).
13. Kraus, G; Eirich, F. R. In "*Science and Technology of rubber*". Academic Press. New York. (1978).
14. Ferrigno, T.H; in "*Hand book of fillers and reinforcements for plastics*" Eds. Katz, H. S.and Milewski, J. V. Van Nortrand. Reinhold Company, New York. (1978).
15. Laurer, J. H; Winey, K. I. *Macromolecules*, 31, 9106. (1998).
16. Eisenberg, A; Hird, B; Moore, R. B. *Macromolecules*, 23, 4098. (1990).
17. Kutsumizu, S; Tagawa, H; Muroga, Y; Yano, S *Macromolecules*, 33, 3818. (2000).
18. Yarusso, D. J; Cooper, S. L. *Macromolecules*, 16, 1871. (1983).

Chapter 5

Effect of fillers on the properties of ionomer based on RISGNR

Part of the work presented in this chapter has been communicated to the *J. Appl. Polym. Sci*

- 5.1 *Introduction*
- 5.2 *Characterisation*
 - 5.2.1 *Differential scanning calorimetry*
 - 5.2.2 *Dynamic mechanical thermal analysis*
 - 5.2.3 *Fourier transform infrared spectroscopy*
 - 5.2.4 *Physical properties of ionomer/filler compounds*
 - 5.2.5 *Scanning electron microscopy (SEM)*
 - 5.2.6 *Reprocessability studies*
- 5.3 *Theory of filler – ionomer interaction*
- 5.4 *Conclusion*
- 5.5 *References*

5.1 Introduction

The effect of particulate and fibrous fillers on the properties of ionomers is of great interest because fillers could be used very effectively to enhance their ultimate properties [1, 2]. Such studies provide information as to how the thermal and

viscoelastic properties of the ionomer, and its biphasic microstructure, can be modified so as to obtain the best balance of physical properties and processability. The two-phase morphology of ionomers, and the resulting differences in polarity of the two phases, provide possibilities of preferential interaction by different fillers. This is evident from the results of early studies by Lundberg et al [3] on lightly sulfonated polystyrene ionomers. The influences of plasticizer on the microstructure and relaxation properties of poly (methyl methacrylate) ionomers were investigated [4]. Evaluation of the effect of carbon black (HAF) [5], silica [6], and zinc stearate [7] on the properties of EPDM based ionomers were published. The results of our studies are discussed in terms of the multiplet-cluster and EHM model of ionomer microstructure [8].

Typical advantages associated with short fibers as fillers in polymer matrices include design flexibility, high low-strain modulus, anisotropy in technical properties and stiffness, good damping, ease in processing and production economy. Fibers may also improve thermo mechanical properties of polymer matrices to suit specific areas of applications and to reduce the cost of the fabricated articles. Short fiber reinforced rubbers are usually easier to process than those with continuous cord reinforcement. Studies on the incorporation of different short fibers such as rayon, nylon and glass fibers in to natural rubber matrix, and the mechanism of reinforcement have been done extensively. The term 'short fiber' means that the fiber length should not be too long, because the fibers may get entangled with each other, causing problems of dispersion, whereas a very small length of the fiber does not offer sufficient stress transfer area to achieve significant reinforcement. Short fiber reinforcement in thermoplastic elastomers (TPE^s) has become another area of potential significance. To assess the effect of fillers on the polar and non-polar phases 26.5 ZnS-RISG NR ionomer has been used.

This chapter presents:

1. Differential scanning calorimetry and dynamic mechanical thermal analysis of the effect of particulate fillers such as HAF black, silica, zinc stearate and short fiber fillers such as nylon, and glass on the thermal transitions of the 26.5 ZnS-RISG NR ionomers.
2. FTIR studies.

3. Physical properties.
4. SEM analysis, and
5. Reprocessability studies.

5.2 Characterisation

5.2.1 Differential scanning calorimetry (DSC)

Table 5.1 DSC profiles of ionomer/filler compounds containing 10 phr filler

Samples	Tg1 (°C)	Tg2 (°C)
1	-64	+85
2	-63	+83
3	-63	+100
4	-62	+68
5	-62	+68
6	-66	+52

Samples are 1=neat ionomer; 2, 3, 4, 5 and 6 represent ionomer filled with HAF black, Silica, Nylon, Glass and Zinc stearate respectively

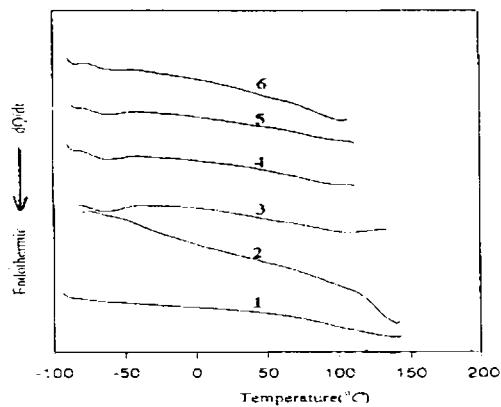


Fig. 5.1 DSC profiles of the ionomer and its 10 phr filled compounds.

Samples are 1=neat ionomer; 2, 3, 4, 5 and 6 represent ionomer filled with HAF black, Silica, Nylon, Glass and Zinc stearate respectively

The DSC results of HAF black, silica, nylon, glass, and zinc stearate filled compounds of the 26.5 ZnS-RISG NR ionomer are presented in table 5.1 The DSC profiles as shown in figure 5.1 reveal that all these fillers have influenced both the Tg1 and Tg2 of the 26.5 ZnS-RISG NR ionomer. The interaction of the active sites on the filler surface with both the matrix and the ionic domains in the ionomer may be responsible for the change in the thermal transitions (Fig. 5.1) on filler incorporation.

5.2.2 Dynamic mechanical thermal analysis (DMTA)

Results of dynamic mechanical thermal analyses for the 26.5 ZnS-RISG NR ionomer and their filled compounds have been summarized in the table 5.2.

Table 5.2 Results of dynamic mechanical thermal analyses

Materials *	Thermal transitions		Tan δ corresponds to			Log E' (Pa) corresponds to		
	Tg1	Tg 2	Tg 1	25°C	Tg 2	Tg1	25°C	Tg 2
	(°C)	(°C)			(°C)	(°C)		(°C)
1	- 21	+ 87	0.16	0.24	0.51	8.6	7.7	6.4
2	- 20	+ 99	0.11	0.16	0.60	8.9	8.5	6.6
3	- 20	+ 76	0.10	0.13	0.44	8.8	8.4	7.5
4	- 20	+ 99	0.09	0.18	0.57	8.8	8.3	6.6
5	- 20	+ 99	0.09	0.17	0.55	8.8	8.3	6.6
6	- 20	+ 99	0.09	0.24	0.72	8.4	8.4	6.1

1=neat ionomer; 2=HAF black; 3 = Silica; 4 = Nylon; 5 = Glass; 6 = Zinc stearate

Incorporation of (HAF) carbon black into the neat ionomer increases its Tg1 (-21°C) to - 20°C. Reinforcement of the matrix and the cluster phase is evident from the tan δ

values at Tg1 and Tg2 (Table 5.2 and Figs. 5.2 & 5.3). The $\tan \delta$ at 25 °C for the neat ionomer lowered on black loading, whereas the corresponding storage modulus increased. This may be due to the strong interactions involving the backbone chains [10, 11] and the clusters. The $\tan \delta$ at Tg2 was increased for all the fillers except for silica. The incorporation of silica caused a slight increase in the Tg1, which may be due to the stiffening of the backbone chain.

Incorporation of silica results in a further decrease in $\tan \delta$ presumably due to the formation of an adsorbed polymeric shell on the active filler surface. Apart from Tg1, the ZnS-RISG NR neat ionomer and its silica filled compound show a second transition (Tg2) around +87 and +76 °C respectively. The incorporation of silica caused a marginal reduction in $\tan \delta$ at the high-temperature ionic transition (Tg2), thus suggesting that the formation of the hard phase is reduced in the presence of silica. The silica seems to facilitate the dipolar relaxation of the polymer, which may be the reason for the reduction in the ionic transition for the silica filled ionomer when compared to the neat ionomer. The silanol groups in silica seem to interfere in the formation of ionic aggregates. Scheme 5.1 shows the representation of the probable mechanism of interaction between the silanol groups of the filler and the ionic aggregate.

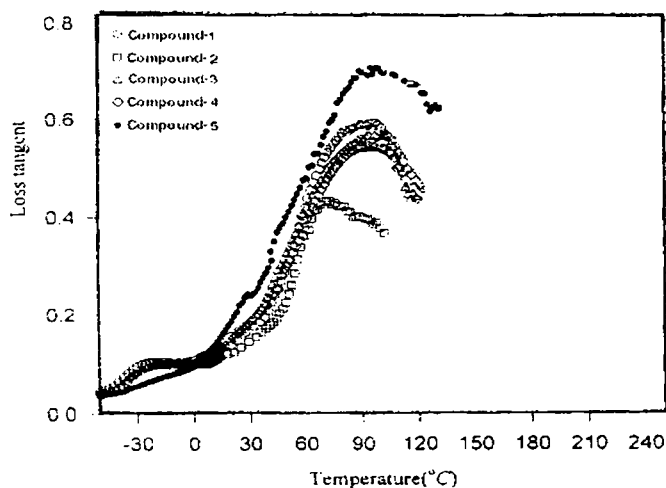


Fig. 5.2 DMTA spectra of the 10 phr filled compounds of 26.5 ZnS-RISG NR ionomer.
1=HAF black; 2 = Silica; 3 = Nylon; 4 = Glass; and 5=Zinc stearate.

The stiffening of the polymer backbone and a weakening of the ionic transition in the presence of silica may be inferred from our observations.

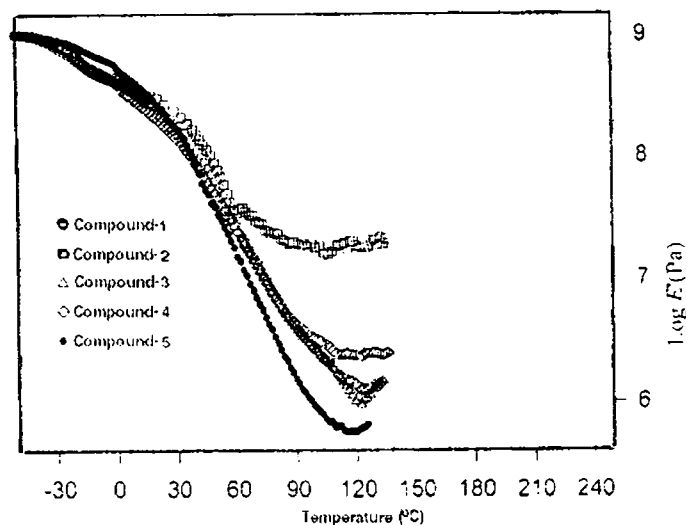
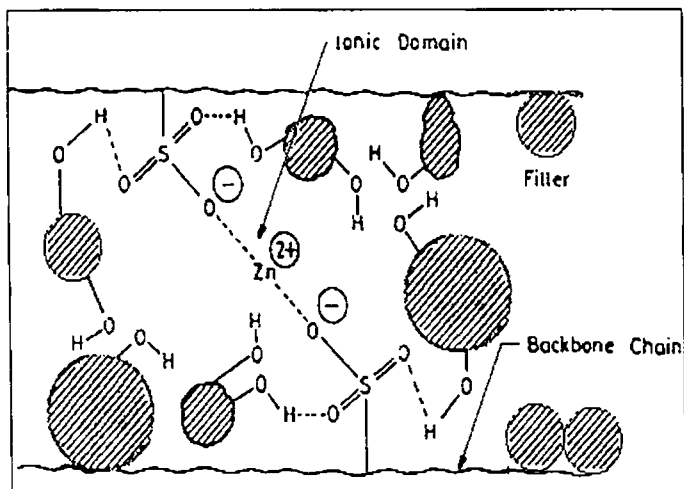


Fig. 5.3 Temperature dependence storage modulus of the 10 phr filled compounds of 26.5 ZnS-SG NR ionomer. 1 = HAF black; 2 = Silica; 3 = Nylon; 4 = Glass; and 5 = Zinc stearate

The lower storage modulus of the silica filled ionomer at Tg2, when compared to the value at Tg1, suggest that the filler weaken formation of both the multiplets and clusters present in the ionomer.

According to these results, it may be deduced that at the elevated temperatures the fillers act as facilitators for a stronger inter cluster attraction, which results in an increase in the cluster transition temperature and the corresponding $\tan \delta$. The silica, at higher temperature, may be disrupting the ionic multiplets and clusters to reduce their concentration to the minimum with a reduction in their Tg2 as shown in table 5.2. At 25 °C, except for zinc stearate, all other fillers show a reduction in the $\tan \delta$. The higher value of $\tan \delta$ at Tg2 for the zinc stearate is probably due to the plasticization of the ionic domains in the ionomers [2].



Scheme 5.1 Proposed model showing the filler-ionomer interaction

Based on these results it is assumed that the polymer – filler interactions in the case of filled ZnS-RISGNR are of two types: (i) filler–nonpolar polymer backbone, which is similar to the interaction involving diene rubbers and reinforcing fillers, as manifested in the lowering of $\tan \delta$ at T_{g1} , and (ii) ionic groups of the ionomer–polar groups present on the surface of the filler particles ($-OH$, $>C=O$, $-NH-CO-$ etc.), which is manifested in an increase in $\tan \delta$ at T_{g2} . While the rubber–filler interaction involving the non-polar polymer backbone is of weak van der Waals' type; the same due to ionic aggregates can be of much stronger type. The increase in the T_{g1} as well as T_{g2} for the filled compounds of ZnS-RISGNR shows that carbon black, silica, nylon fiber, and glass fiber act as reinforcing fillers. The decrease in the intensity of the peak at low temperature further supplements our view that the fillers are reinforcing. Appearance of both the low temperature as well as high temperature transitions for the filled zinc sulphonated ionomer samples, similar to the neat ionomer ZnS-RISGNR, may be considered as an evidence for the retention of the micro phase and the “physical cross-links” as characteristic of ionomers. The $\text{Log } E'(\text{Pa})$ –temperature plot reveals that the “network” persists even at the highest experimental temperature. From the values of the storage modulus at T_{g1} , at 25°C and at T_{g2} , it has been

observed that the silica filled ionomer is somewhat balanced with respect to the storage modulus.

The incorporation of zinc stearate in to ZnS-RISGNR ionomer increases its glass-rubber transition (T_g) from $-21\text{ }^\circ\text{C}$ to $-20\text{ }^\circ\text{C}$. The dual role exhibited by zinc stearate in ionomers based on RISGNR may be evident from the intensity of $\tan \delta$ peaks (Table 5.2) for the 10-phr-zinc stearate filled ionomer at two transitions. At T_g , zinc stearate acts as reinforcing filler (low intensity $\tan \delta$ peak) where as at the higher temperature (high intensity $\tan \delta$ peak) it plasticises the ionic domains. It was found that at $120\text{-}130\text{ }^\circ\text{C}$, zinc stearate starts to melt, weakens the strong ionic association prevailing in ionomers based on RISGNR. In the case of ionomers based on RISGNR, zinc stearate has a dual effect. The thermal profile of the zinc stearate filled RISGNR ionomer resembles the investigations of Weiss [12]. Appearance of multiple transitions for the zinc stearate compound of the RISGNR ionomer along with the detection of the anomalous melting behavior of the zinc stearate in the thermal profiles may be considered as evidence of interactions between zinc stearate and sulfonate groups in RISGNR ionomers.

5.2.3 Fourier transform infrared spectroscopy

The FTIR spectra of the neat ionomer and its compounds filled with HAF carbon, silica, nylon fiber, glass fiber, and zinc stearate are shown in the figure 5.5. The fillers have influenced the intensities of the characteristic peaks of the ZnS-RISGNR ionomers. The variation of the peak intensities of the ZnS-RISGNR with different fillers has been represented using figure 5.4. The interaction between the functional groups on the surface of the filler particles and the zinc sulfonate groups of the ionomer may be responsible for this variation. Higher the interaction between the ionic groups and the functional groups on the filler, greater will be the intensity of the peak responsible. It has been found that the ionomer reinforced with HAF carbon black gives the maximum peak intensity. This is in agreement with their physical properties.

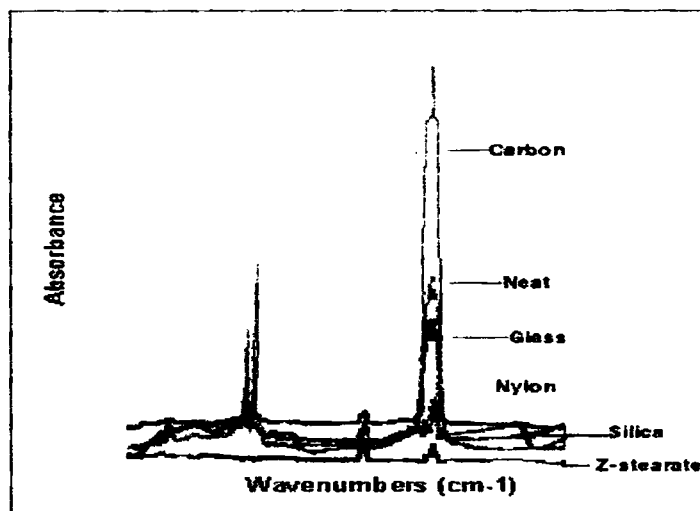


Fig.5.4 Comparison of the FTIR spectra of the neat ZnS-RISGNR with their 10 phr filled compounds

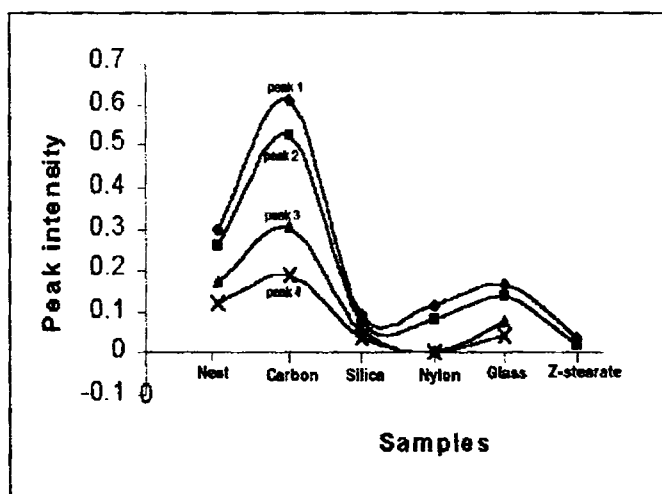


Fig.5.6 Variation of peak intensities in the IR spectrum of neat ZnS-RISGNR caused by different fillers

FTIR spectra of ionomer-zinc stearate (10 phr) compound (Fig. 5.4) and the neat ionomer reveal that the intensity of the characteristic peaks of the neat ionomer has been lowered to 10 – 15 % with the incorporation of 10 phr zinc stearate. The peaks at 2923, 2854, 2361 cm^{-1} for the neat ionomer have been showing peak intensities of 0.299, 0.255 and 0.0627 respectively. However, in the IR spectrum of RISGNR ionomer filled with 10-phr-zinc stearate as shown in figure 5.4 the peak intensities are 0.035, 0.018, and 0.039. This shift in the peak intensities upon zinc stearate filling may be due to the ion-ion interaction arising out of coulombic forces between zinc stearate and the ionic aggregates, which result in marked changes in the environment of the sulfonate groups in the zinc stearate filled ionomer.

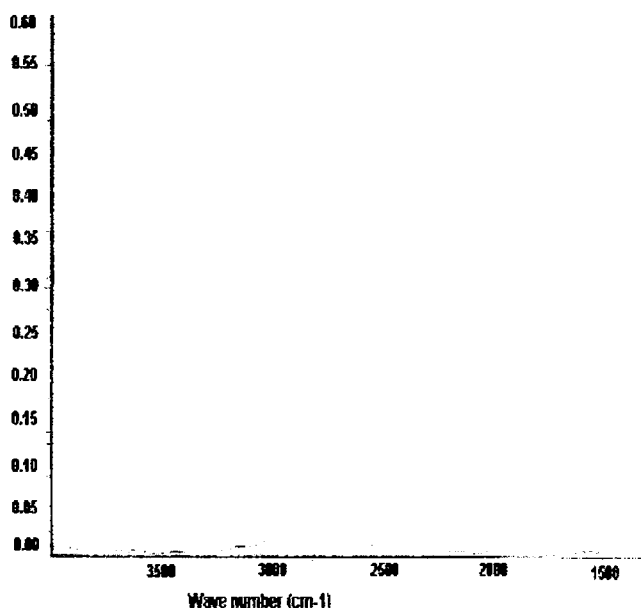


Fig.5.6 FTIR spectrum of the HAF black filled ZnS-RISGNR

5.2.4 Physical properties

5.2.4 (a) Carbon black (HAF)

Studies on the physical properties of the neat polymers and (HAF) carbon black filled ionomer compounds show that zinc salt of RISGNR shows higher tensile strength (Fig.5.7) and lower elongation at break (Fig. 5.8) in comparison with the neat base polymer.

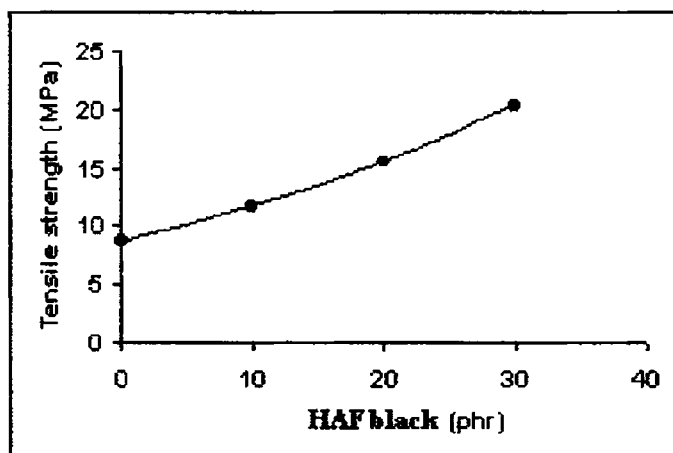


Fig. 5.7 Tensile strength of the ZnS-RISGNR ionomer / HAF black compound with the carbon content

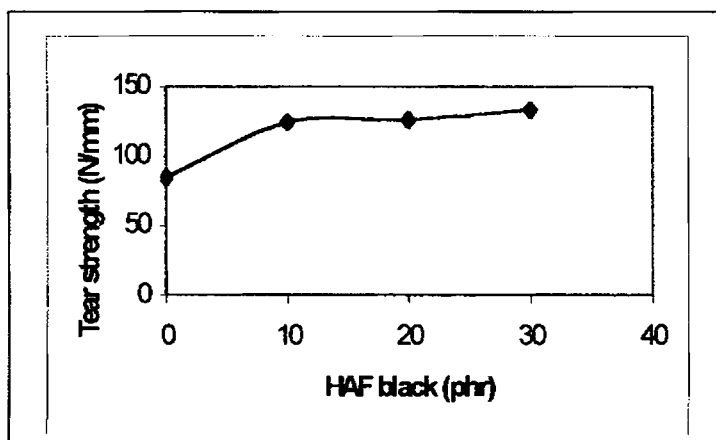


Fig. 5.8 Tear strength of the ionomer / HAF black compound with the carbon content

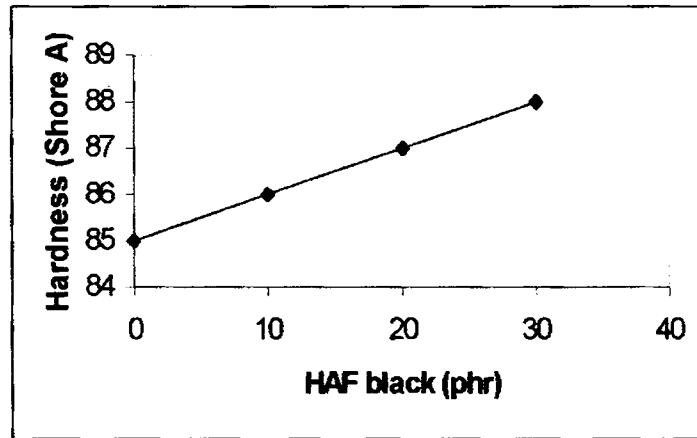


Fig.5.9 Hardness (shore A) of the ionomer / HAF black compound with the carbon content

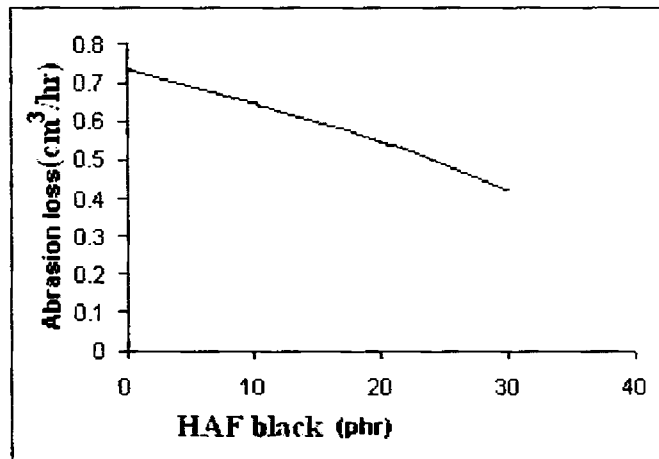


Fig. 5.10 Abrasion loss of the ionomer / HAF black compound with the carbon content

It has been observed that the hardness of the ionomer increased with increase in the carbon content (Fig. 5.9). The carbon black filled samples of the ionomer showed improved resistance towards abrasion loss (Fig. 5.10). This may be due to the

presence of ionic aggregates, which act as physical cross-links. Both the tear strength and hardness have been found to be increasing with the carbon content. Hardness is a measure of modulus of elasticity at low strain

5.2.4 (b) Silica

Table 5.3 Hardness and abrasion loss of the ionomer/silica compounds.

Compounds	Hardness (Shore A)	Abrasion loss (cm ³ /hr)
1	85	0.738
2	86	0.384
3	88	0.294
4	89	0.272

1, 2, 3 and 4 show ionomer compounds with 0, 5, 10 and 20 phr silica

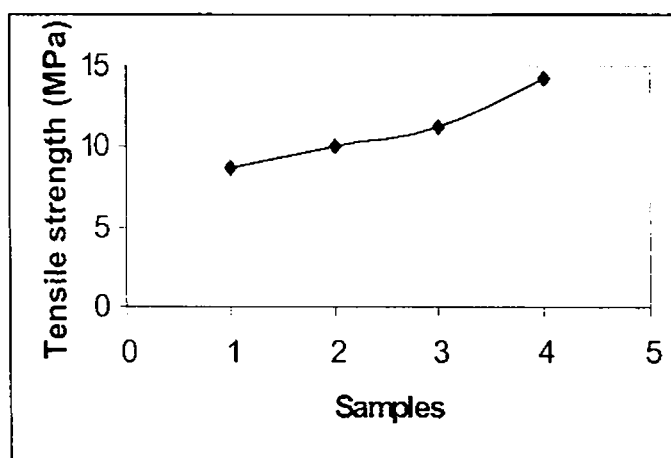


Fig. 5.11 Tensile strength of ionomer / silica compounds with silica content.

Samples: 1=neat ionomer; 2, 3, and 4 represent ionomer/silica compounds containing 5, 10 and 20 phr silica.

Measurement of the physical properties of the neat polymer and its compounds containing 5, 10, and 20-phr silica show that the hardness of the base ionomer increased and its abrasion loss decreased up on adding silica (Table 5.3). The tensile strength increased with the silica loading (Fig. 5.11). The incorporation of silica caused a decrease in the elongation at break (Fig. 5.12).

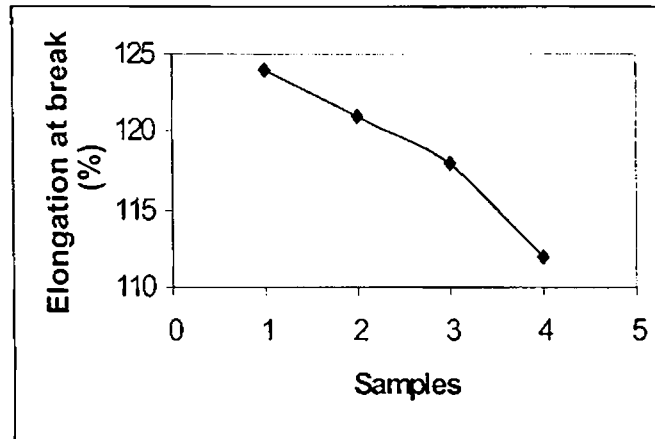


Fig. 5.12 Elongation at break of the ionomer / silica compound with silica content.

Samples: 1=neat ionomer; 2, 3, and 4 represent ionomer/silica compounds containing 5, 10 and 20 phr silica.

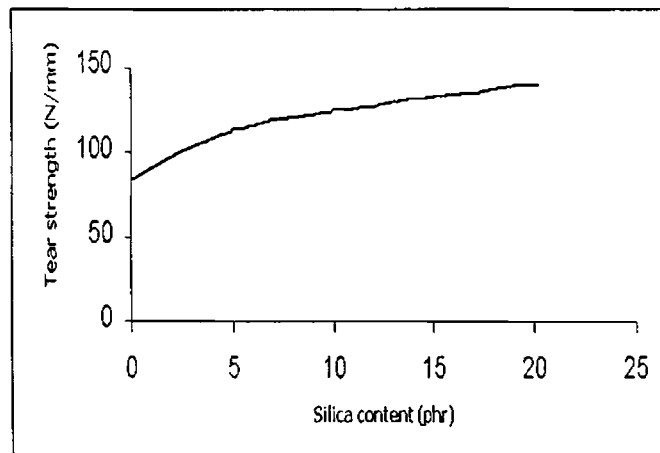


Fig. 5.13 Tear strength of the ZnS-RISGNR/silica compound with silica loading

The higher tear strength and lower abrasion loss of the silica filled ionomer may be due to the reinforcement of the matrix with the silica particles. The interaction between free – OH groups on silica with the polar centers of the ionomer may be the reason for the reinforcement.

5.2.4 (c) Short fibers (Nylon & glass)

Table 5.4 Hardness and abrasion loss of the ionomer /nylon fiber compounds

Samples	Hardness (Shore A)	Abrasion loss (cm ³ /hr)
1	85	0.738
2	86	0.591
3	87	0.546
4	88	0.436

1, 2, 3 and 4 show nylon compounds of ionomer with 0, 5, 10 and 20 phr nylon fiber

The physical properties of the short fiber (nylon and glass) filled ionomers as compared to the neat ionomer (Table 5.4 and figures 5.14 and 5.15).

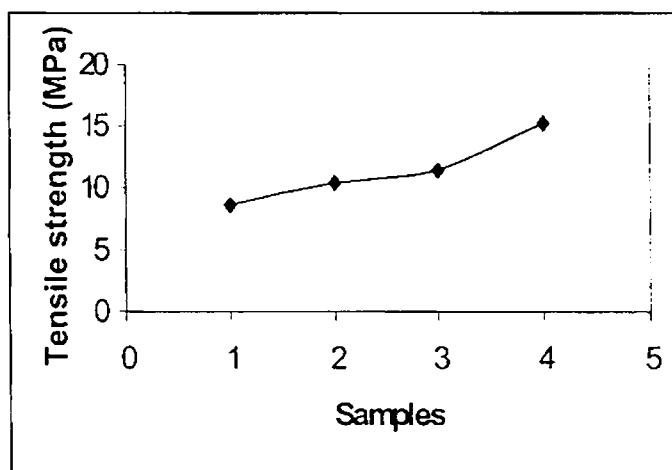


Fig. 5.14 Tensile strength of ionomer / nylon fiber compound with the fiber content.

Samples 1= neat ionomer; 2, 3 and 4 represent the compounds containing 5, 10 and 20 phr nylon fiber.

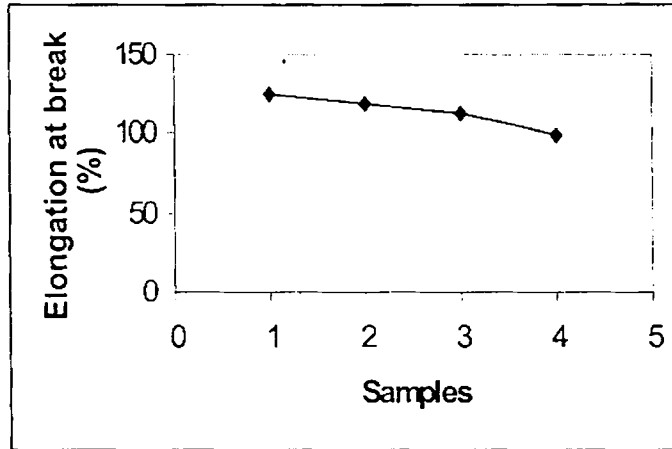


Fig. 5.15 Elongation at break of the ionomer / nylon fiber compound with the fiber content. Samples 1 = neat ionomer; 2, 3 and 4 represent their compounds containing 5, 10 and 20 phr nylon fiber.

Nylon fibers of 0.4-0.6-mm lengths were used to facilitate good dispersion. The improvement in the physical properties of the ionomer – fiber compounds may be due to the relatively good fiber – matrix adhesion. The stress transfer, in this case, may be occurring through shearing at the fiber – matrix interface. Maximum tensile and tear strength for the composite was observed at a nylon loading of 20 phr. Incorporation of nylon fibers becomes very difficult beyond 20-phr.

Table 5.5 Physical properties of the ionomer and glass composites

Samples	Hardness (Shore A)	Abrasion loss (cm ³ /hr)
1	85	0.738
2	86	0.396
3	88	0.328
4	89	0.294

Samples 1, 2, 3 and 4 show ionomer / glass fiber compounds with 0, 5, 10 and 20-phr glass fiber

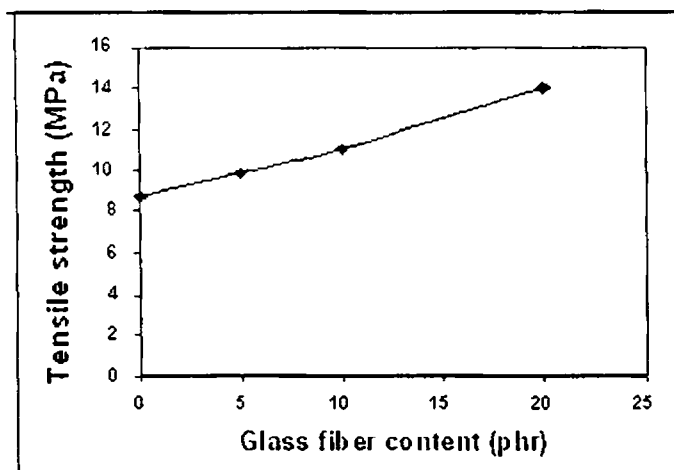


Fig. 5.16 Tensile strength of ionomer / glass fiber compounds with glass fiber content.

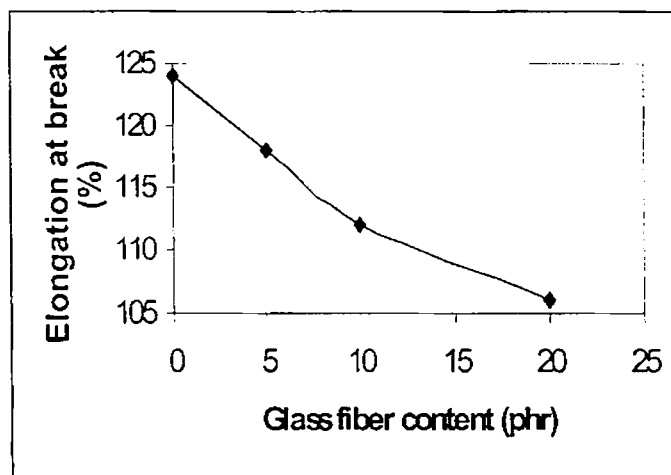


Fig. 5.17 Elongation at break of ionomer / glass fiber compounds with glass fiber content.

An improvement in the shore A hardness and abrasion loss was rendered to the ionomer at this optimum nylon fiber loading. Presence of the polar NH-CO groups on the nylon fibers interacting with polar centers in the ionomer may be the causative for

the reinforcement of the ionomer. The physical properties of the fiber – ionomer compounds have been found to be lower at low fiber content, which may be due to (1) dilution of the matrix and (2) reinforcement of the matrix by the fibers increases only as the fiber volume fraction increases. At low fiber content, the matrix is not restrained by enough fibers and highly localized strains occur in the matrix at low strain levels, causing the bond between fiber and matrix to break, leaving the matrix diluted by non – reinforcing, debonded fibers. At high fiber concentrations, the matrix is sufficiently restrained and the stress is more evenly distributed, thus the reinforcing effect outweighs the dilution effect. As the concentration of the fibers is increased to a higher level, the tensile properties gradually improve to give strength higher than that of the matrix. The concentration of fibers beyond which the properties of the compounds improve above the original matrix strength value is known as the optimum fiber concentration (OFC). This OFC is quite often found to lie between 20 and 30 phr. At very high fiber concentration (40 phr) of nylon 6 the strength again decreases, because there is insufficient matrix material to adhere the fibers together. The elongation at break for the glass fiber /

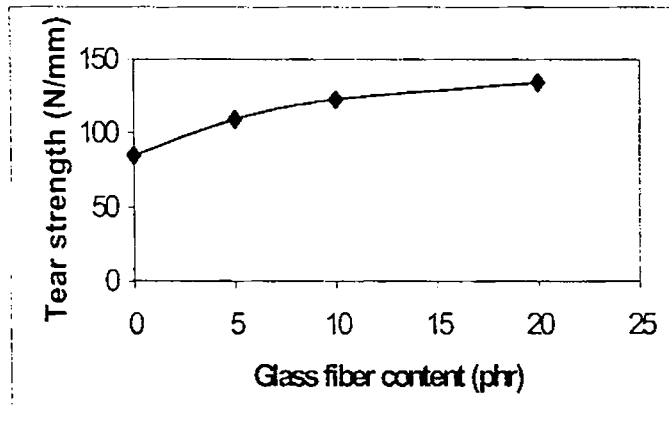


Fig. 5.18 Tear strength of ionomer / glass fiber compounds with glass fiber content

Ionomer compounds (Fig. 5.17) decreased where as the tear strength (Fig. 5.18) increased as the glass fiber content increased.

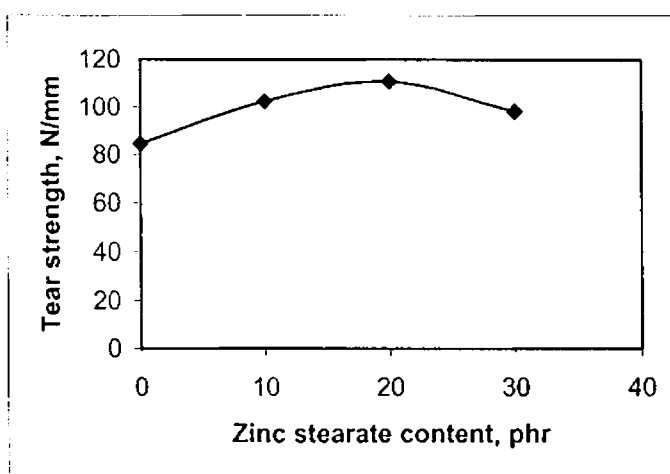
5.2.4 (d) Zinc stearate

Table 5.6 Physical properties of the ionomer / zinc stearate compounds

Samples	TS (MPa)	E.B (%)	Hardness (Shore A)	Abrasion loss (cm ³ /hr)
1	1.2	248	42	1.92
2	8.70	124	85	0.738
3	9.72	112	86	0.698
4	11.58	102	87	0.576
5	10.96	96	89	0.596

Samples 1 = neat RISG NR; 2 = neat ionomer; 3, 4 and 5 show, ionomer / zinc stearate compounds with 10, 20 and 30-phr-zinc stearate

The physical properties of RISG NR, ZnS-RISG NR and the zinc stearate filled ionomer are shown in the table 5.6. The ionomer shows higher tensile strength but lower elongation at break than RISG NR. This is due to the presence of physical cross-links arising from the ionic aggregates in the ionomer.

**Fig. 5.19** Tear strength of the ionomer/zinc stearate compound with the zinc stearate

Addition of up to 20-phr-zinc stearate increases the tensile strength but decreases the elongation at break, and at further loading, both tensile strength and elongation at

break decrease. At high loading zinc stearate may be diluting the matrix and acting as an inert filler, thus decreasing polymer – filler interaction. Improvement in the tear strength and resistance to abrasion loss of the ionomer was lowered with the addition of the zinc stearate, beyond filler loading of 20 phr. However, hardness of the ionomer increased up on the incorporation of zinc stearate.

5.2.4.e. Comparison of the physical properties

Among the fillers used for the study the properties were observed to be in the order HAF black > nylon > silica > glass > zinc stearate as shown in Table 5.7. The tensile strength was maximum for the HAF filled ionomer and minimum for the zinc stearate/ionomer system (Fig. 5.20).

Table 5.7 Physical properties of 10 phr each of HAF black, silica, nylon, glass, and zinc stearate filled compounds of the 26.5 ZnS-RISGNR ionomer

Samples	E.B. (%)	Hardness (Shore A)	Abrasion loss (cm ³ /hr)
1	124	85	0.738
2	108	86	0.646
3	118	88	0.294
4	112	87	0.546
5	112	88	0.328
6	112	86	0.698

1=neat ionomer; 2, 3, 4, 5 and 6 show ionomers filled with HAF black, Silica, Nylon, Glass and Zinc stearate respectively having 10 phr filler in each case

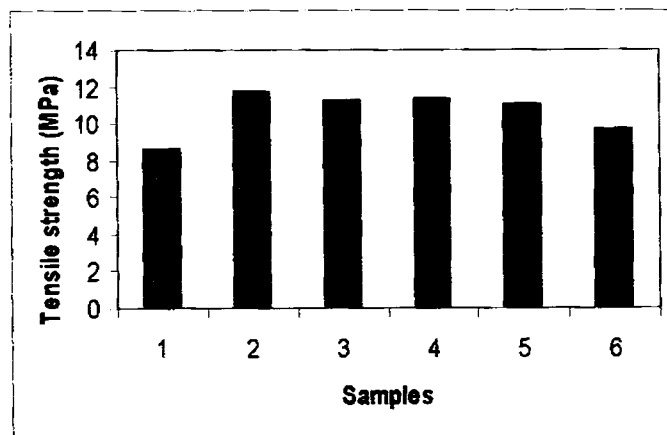


Fig. 5.20 Comparison of the tensile strength of the neat ionomer (1) with their filled compounds of HAF black (2), silica (3), nylon (4), glass (5) and zinc stearate (6)

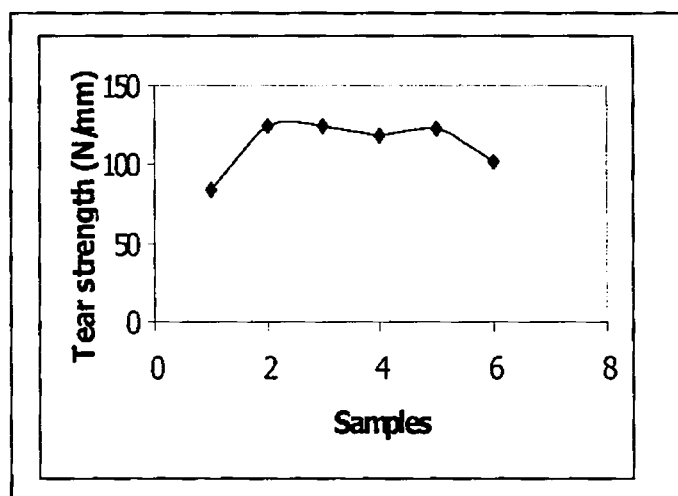


Fig.5.21 Comparison of the tear strength of the neat ionomer (1) with their filled compounds of HAF black (2), silica (3), nylon (4), glass (5) and zinc stearate (6)

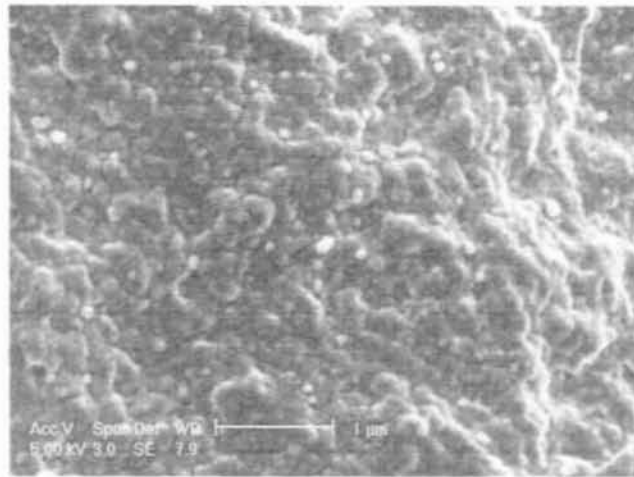


Fig. 5.22 SEM micrograph of the cryogenic fractured surface of the ionomer / silica (10 phr) compound.

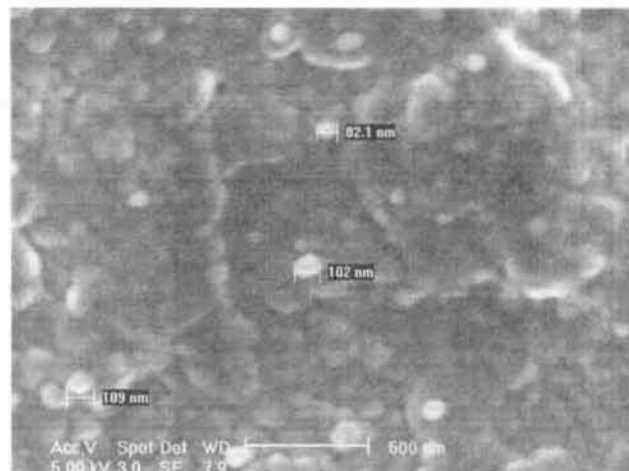


Fig. 5.23 SEM micrograph of the cryogenic fractured surface of the ionomer / silica (10 phr) compound with magnification

The elongation at break (Table 5.7), however, had its lowest value for the HAF filled system in comparison with the other filled systems of the ionomer such as silica, nylon, glass and zinc stearate.

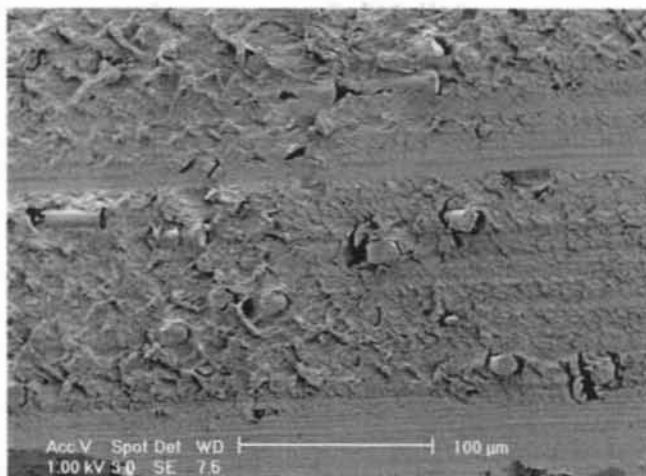


Fig. 5.24 SEM micrographs of the microtomed surface of the ionomer / glass fiber compound

Both HAF and silica filled systems have shown higher tear strength (Fig. 5.21). The shore A hardness of the silica and glass fiber reinforced compounds was higher than the other filled compounds of ionomers. Abrasion loss was minimized in the silica and glass filled systems

5.2.5. Scanning electron microscopy

In the case of silica filled ionomers, the SEM micrographs of the cryogenic fractured surface in which the fillers look very much wetted and embedded in the matrix (Fig. 5.22) These show that the fillers can be identified and the particle size and shape have been preserved (Fig. 5.23). The SEM micrographs of the microtomed surface of the glass fiber filled ionomer showed that the glass fibers are seen embedded in the

ionomer matrix (Fig. 5.24), which shows a better adhesion between the ionomer and the fibers. The fibers are seen oriented in all directions (Fig. 5.25).

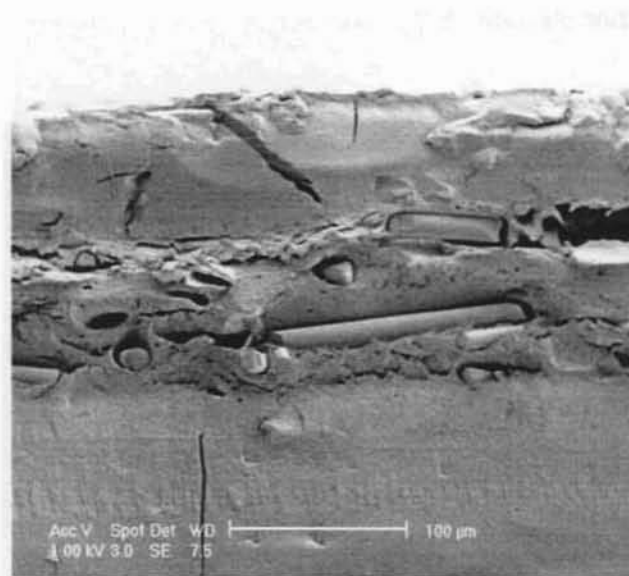


Fig. 5.25 SEM micrograph of the cryogenic fractured surface of the ionomer / glass fiber compound

The SEM micrographs of the prestretched nylon filled ionomer surface made with a knife (microtomy) at room temperature (Fig. 5.26) shows that the cut fiber ends are clearly seen and most of them are aligned in one direction. The better adhesion between the fiber and the matrix is almost clear. The enhanced physical properties of the nylon filled ionomer based on RISGNR may be due to this intact interfacial bonding, which seems to be pointing to a stronger bond at the interface. The improved physical properties of the nylon filled ionomers may be due to this strong adhesion between the nylon fibers and the ionomer matrix as shown by the SEM micrographs. The nylon fibers have been found to be in every direction. These observations are found to be in good agreement with their physical properties



Fig. 5.26 SEM micrograph of the microtomed surface of the ionomer / nylon compound.

5.2.6 Reprocessability studies

Table 5.8 Results of reprocessability studies ionomer / filler compounds

Samples	E.B. at cycles (%)			Tear strength at cycles (N/mm)		
	1	2	3	1	2	3
1	124	122	120	84.5	83.8	83.2
2	108	107	105	124.4	123.1	122.4
3	118	116	112	124.6	123.4	122.7
4	112	110	109	118.6	117.3	116.4
5	112	111	107	122.4	120.2	118.3
6	112	109	107	102.4	101.6	101.2

1- neat ionomer; 2, 3, 4, 5 and 6 show ionomers filled with 10 phr each of HAF black, Silica, Nylon, Glass and Zinc stearate respectively

It has been observed that (Fig. 27), the tensile strength of the filled ionomer compounds at all the filler loadings under study remain almost constant even after repeated cycles of mixing and molding.

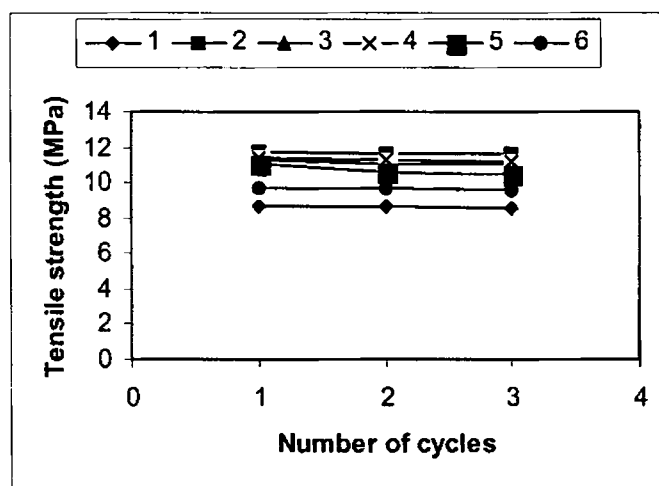


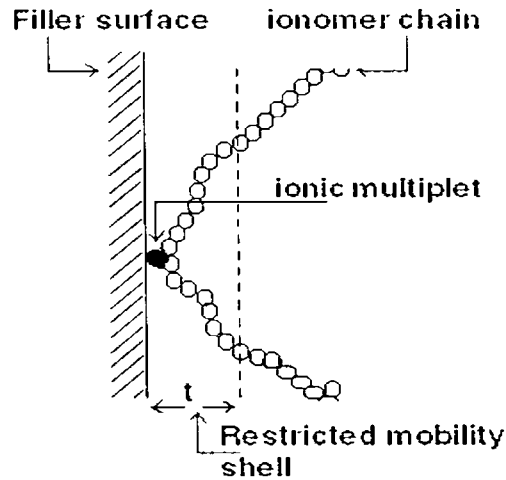
Fig. 5.27 Tensile strength of the ionomer composites at different cycles of processing. 1= neat ionomer; 2, 3, 4, 5 and 6 show ionomers filled with 10 phr each HAF black, Silica, Nylon, Glass and Zinc stearate respectively

This shows that the ionomer composites behave as thermoplastic elastomers and it could be reprocessed at 120°C by mechanical recycling without deterioration in its physical properties. The changes in elongation at breaks and tear strength remain minimum during reprocessing (Table 5.8).

5.3 Theory of filler – ionomer interaction

The interaction of the filler and the ionomer imparts an increase in stiffness and strength to the ionomer. In order to produce significant reinforcement, particle size must be less than about a micron. As specific surface area increases (i.e., as particle size decreases), strength of filled vulcanizates generally increase. It is instructive to determine how particle size influences particle-to-particle spacing in a particulate-

filled ionomer compounds. Spherical particles of diameter 'd' distributed on a three-dimensional square lattice are considered.



Scheme 5.2 Schematic representation of the ionomer-filler interaction showing the restricted mobility shell (t) around the filler. Dotted line shows the shell limit.

Although this is a simple model, which neglects structure, it nonetheless, illustrates the essential importance of particle size. The nearest neighbor particle spacing 's' for a volume fraction 'v' of filler is given by:

$$S = d [0.806/v^{1/3} - 1]$$

Particle spacing is the same order of magnitude as particle diameter. If it is assumed that there is a shell of thickness 't' around particles in which chain mobility is hindered as a result of interaction with the particles, then the volume fraction 'v₁' of the rubber phase within 't' is given by:

$$v_1 = v [(1 + 2t/d)^3 - 1] / 1 - v$$

$$2t < s$$

All of the network chains will have relaxational motions restricted by at least one filler particle as shown in the proposed model in scheme 5.2. Restricted chains have increased resistance to molecular separation, which is a precursor to crack initiation and growth. Large particles provide stiffening, and act as stress-raising inclusions,

which promote fracture in essentially unmodified bulk rubber. However, as filler particles are made sufficiently small, it becomes inappropriate to view the composite simply as rigid inclusions embedded in a matrix, which behaves like bulk gum rubber. Matrix mobility at large strain is reduced because of close proximity to filler surfaces, and this is expected to hinder crack initiation and growth.

In the case of the fracture in uniaxial tension of a hypothetical perfectly brittle elastomeric network, in which irreversible chain ruptures across the fracture plane are the only mechanism of energy dissipation. Because of the complex topology, network chains will bear different forces when the material is continuously deformed. In addition, an inadvertent discontinuity (flaw) may further magnify chain forces locally. Regardless, some region will experience the highest forces and a network strand there will reach a critical force and break. This is the start of the molecular fracture, which is a precursor to crack formation (i.e., macro-fracture). The load this chain was bearing quickly will be transferred to surrounding chains, which will become overloaded and break. Once a single molecular fracture is initiated, surrounding chains rupture quickly. A cascading process leads to facile crack initiation and immediate catastrophic propagation of a single crack across the specimen. Strength is very low, and fracture energy is equal to the energy lost by recoiling chains, which broke to create the fracture surface. Such behavior may be approximately shown by ionic cross-linked polymers.

In the case of the fracture behavior of vulcanisates containing rigid filler, since inclusions amplify matrix stress; one might expect strength to be decreased. Indeed, a gum vulcanisate containing a single rigid macro – inclusion has reduced strength, the reduction being greater for larger inclusions. However, in a micro-composite containing a significant volume fraction, say 25 %, of rigid filler particles, though crack initiation is facilitated in essentially bulk like matrix, the inclusions do provide some interference to propagation, as the crack path must deviate around filler particles. The effects trade – off, and the strength of the micro composite rubber is not much different than that of the unfilled matrix. This is the 'break- even point' for rubber reinforcement. Crack deflection and energy dissipation are minimal, and there is still a single crack tip, which grows through the largely unhindered matrix. Furthermore, catastrophic crack growth follows rather quickly after crack initiation. In the case of

highly reinforced rubber a crack may split when it meets very fine particles, presumably because strength anisotropy reaches a critical value. A crack does not simply propagate around the barrier and continue more or less perpendicular to the deformation direction. Aligned and restricted matrix chains surrounding particles inhibit continued lateral crack growth. Instead, two new cracks form, which grow longitudinally in opposite directions towards closely spaced adjacent particles. Particle spacing is critical to crack splitting.

5.4 Conclusion

- Both DMTA and DSC support the retention of the ionomer properties for the carbon black filled compound.
- DMTA plot shows that both the Tg1 and Tg2 are retained even in the silica filled ionomers. The value of the thermal transitions suggests that silica reinforces the backbone chain and weakens the ionic associations. The room temperature storage modulus for the silica filled ionomer is the highest among the selected fillers.
- The short fibers of nylon as well as glass have been found to be interacting with both the matrix-phase and the cluster-phase.
- Zinc stearate acts as an ionic domain plasticizer, presumably by the incorporation of some ionic head groups of the zinc stearate into the sulfonate multiplets, which lowers the Tg. Appearance of multiple transitions for the zinc stearate compound of the ionomer along with the detection of the anomalous melting behavior of the zinc stearate in the DSC profiles may be considered as evidence of interactions between zinc stearate and sulfonate groups in RISGNR ionomers.
- Physical properties of the filled systems show improvement over the neat ionomer. Both particulate fillers such as HAF black, silica, zinc stearate and short fibers such as nylon, and glass reinforce with the ionomers based on styrene grafted natural rubber.
- FTIR results give support to these observations

5.4 References

- 1 Meiecke, E.A.; Taftaf, M.I. *Rubber Chem. Technol.* 61, 534 (1988)
- 2 Medalia, A.I. *Rubber Chem. Technol.* 60, 45 (1987)
- 3 Ludberg, R.D.; Makowski, H.S.; Westerman, L. *Adv. Chem. Ser.* 187, 67 (1980)
- 4 Ma, X.; Sauer, J.A.; Hara, M. *Polymer* 38, 4425 (1997)
- 5 Kurian, T.K.; De, P.P.; Khastgir, D.; Tripathy, D.K.; De, S.K.; Peiffer, D.G. *Polymer*, 36, 3875 (1995)
- 6 Kurian, T.K.; Khastgir, D.; De, P.P.; Tripathy, D.K.; De, S.K.; Peiffer, D.G. *Polymer*, 37, 5597 (1996)
- 7 Kurian, T.K.; Bhattacharya, A.K.; De, P.P.; Tripathy, D.K.; De, S.K.; Peiffer, D.G. *Plast. & Rubber Proc. & Applications* 25, 2075(1995)
- 8 Eisenberg, A.; Hird, B.; Moore, R.B. *Macromolecules* 23, 4098 (1990)
- 9 Thommachan Xavier; Samuel, J.; Kurian, T. *Macromol. Mater. Eng.* 286, 507 (2001).
- 10 Gauthier, C.; Chauchard, J.; Chabert, B.; Trotignon, J.P.; Battegay, G.; Lamblin, V. *Plast. & Rubber Proc. & Applications* 20, 77(1993)
- 11 O'connor, J.E. *Rubber Chem. Technol.*, 50, 945 (1977).
- 12 Weiss, R.A. *J. Appl. Polym. Sci.*, 28, 3321(1983)

Chapter 6

Electrical behavior of ionomers at microwave frequencies

Part of the work presented in this chapter has been communicated to: *J. Polym. Sci.*
Part B. Polym. Phys. Edn,

- 6.1 *Introduction*
- 6.2 *Microwave measurement*
- 6.3 *Dielectric properties of ionomers*
 - 6.3.1 *Microwave investigations*
 - 6.3.2 *Microwave conduction in ionomers*
 - 6.3.3 *Microwave heating coefficient*
- 6.4 *Dielectric properties of filled ionomers*
- 6.5 *Conclusion*
- 6.6 *References*

6.1 Introduction

Microwaves, even though constitute only a small portion of the electromagnetic spectrum, but their uses have paramount importance in the material characterisation for industrial scientific and medical applications (ISM). Characterisation of the material is essential for the proper selection and implementation of a substance for ISM applications. The dielectric parameters over the microwave frequencies are needed to assess their suitability for use in dielectric wave guides, lenses, dielectric resonators and microwave integrated circuit (MIC) substrates; and on lossy material

for estimating their heating response in microwave heating applications. The dielectric data, besides being useful on lossy ceramics for their use as microwave absorbers; lossy pastes for the design of new food packages, for heating in microwave ovens and on biological materials for diathermy serve as a tool for investigating the intermolecular and intramolecular mechanisms of compounds. It has also been useful to estimate the amount of moisture in wood, sand and agricultural products. As the dielectric properties aid the calculation of internal electric fields resulting from the exposure to the nonionising electromagnetic (EM) fields, it has excellent medical applications. The radio and microwave frequencies are effectively used in the treatment of hyperthermia of tumors and other disorders. For ISM applications, which covers from few kHz to several GHz, the range of relative permittivity (ϵ_r) for the materials of interest is manifold. The real part ϵ' of relative complex permittivity (ϵ_r) can vary from a value of about two to few thousand while the imaginary part ϵ'' of relative complex permittivity from a small fraction to a large value of about hundreds for some materials.

There is considerable interest in the microwave probing of the electrical behavior of many polymers and their compounds due to their potentially wide range of microwave applications [1–4]. Nagakabo et al [5] have showed that composite dielectric materials could be used to make a solid organism phantom in a useful microwave frequency band. All these studies direct us to the wide possibility of the use of polymers as components in microwave applications. Development of new dielectric polymers showing response at any particular frequency of the microwave region becomes a topic of much attention, of late. A special class of polymers called ionomers, in this respect, may become an important group of materials [6]. Incorporation of low level of ionic groups in to the elastomers transforms it in to a reprocessable material possessing thermal stability [7]. Existence of ionic groups as simple or larger multiplets in the elastomer matrix may act as the thermo labile cross-links. Under a suitable microwave frequency these ionic centers may be polarizable and hence dielectric. Hence it seemed worthwhile to investigate the dielectric properties of the ionomers at the microwave region. In spite of the relatively extensive effort on the radio and microwave investigations on the dielectric properties of many conductive polymers, very little effort has been devoted to the dielectric

characterization of ionomers [8-11]. The literature describing the dielectric behaviors of ionomers, besides being fewer, are mainly dealt with the measurement at the radio frequency [12,13]. Microwave studies on the electrical behavior of the ionomers, however, have been made extensively with swollen ionomer membranes [14]. Except the studies of Dabek in which the author compares the complex dielectric permittivity of the dry and the swollen ionomer membranes measured at the S-band frequencies of the microwave region, no other extensive studies on the dielectric behavior such as complex dielectric permittivity, dielectric loss factor, a.c. conductivity, and microwave heating coefficient of the dry ionomers at room temperature in the S-band frequencies of the microwave region have been reported yet. Unlike the impedance method with the capacitance modification employed in the microwave dielectric measurement by Dabek, a novel microwave measurement technique called cavity perturbation technique has been used in our experiment. The present study envisages a new and convenient microwave method called cavity perturbation technique, where the samples can be used in the pellet, powdered, solution, bulk, or in any desired form. Cavity perturbation technique [15] is a highly sophisticated method for the evaluation of the dielectric characterisation of the materials. The experimental set-up consists of a transmission type S-band rectangular cavity resonator, HP 8714 ET network analyzer and an interfacing computer and has been described in detail in the section 2.7 of chapter 2. The cavity resonator is excited in the TE_{10p} mode. The sample was molded in an electrically heated hydraulic press for 5 minutes at 120°C , under a pressure of 10 Mpa. The molded samples were dried in a vacuum oven at room temperature for 72 hrs. Samples prepared in the form of thin strips of dimension $6 \times 2 \times 35$ mm are introduced into the cavity resonator through the non-radiating slot. Samples were again dried in an oven at 120°C for 24 hrs and the measurements were repeated for the consistency of the results. As microwave devices for industrial scientific and medical (ISM) applications [16] have been found to use S-band or preferably 2.45 GHz frequencies, only the dielectric investigations of the ionomers at the S-band frequencies of the microwave region has greater industrial importance.

This chapter deals with the microwave probing of the dielectric properties such as complex dielectric permittivity, dielectric loss factor, a.c. conductivity, and microwave heating coefficient of the ionomers based on radiation induced styrene

grafted natural rubber [17] at room temperature under the S-band (2-3 GHz) frequencies of the microwave region using the cavity perturbation technique.

6.2 Microwave measurement.

According to the theory of cavity perturbation, the complex frequency shift [18] is related as:

$$-\frac{d\Omega}{\Omega} \approx \frac{(\bar{\epsilon}_r - 1) \int V_s \mathbf{E} \cdot \mathbf{E}_0 dV}{2 \int V_c |\mathbf{E}_0|^2 dV} \quad (1)$$

But

$$\frac{d\Omega}{\Omega} \approx \frac{d\omega}{\omega} + \frac{i}{2} \left[\frac{1}{Q_s} - \frac{1}{Q_0} \right] \quad (2)$$

$d\Omega$ is the complex frequency shift. E_0 and E are the electric fields in the unperturbed and perturbed states respectively. Equating (1) and (2) and separating real and imaginary parts we get

$$\epsilon_r' - 1 = \frac{f_0 - f_s}{2f_s} \left(\frac{V_c}{V_s} \right) \quad (3)$$

$$\epsilon_r'' = \frac{V_c}{4V_s} \left(\frac{Q_0 - Q_s}{Q_0 Q_s} \right) \quad (4)$$

Here, $\bar{\epsilon}_r = \epsilon_r' - i \epsilon_r''$, $\bar{\epsilon}_r$ is the relative complex permittivity of the sample, ϵ_r' is the real part of the relative complex permittivity, which is usually known as dielectric constant and ϵ_r'' , the imaginary part of the relative complex permittivity, which is associated with the dielectric loss of the material. . While f_0 and Q_0 represent the

resonant frequencies and quality factors of the vacuum, f_s and Q_s represent that of the sample. V_s and V_c are the volumes of the sample and the cavity resonator respectively. Using the experimental data for ϵ_r' , ϵ_r'' and the equation relating complex conductivity (σ) and relative complex permittivity ($\bar{\epsilon}_r$), we can write,

$$\sigma = i\omega \epsilon_r = i\omega(\epsilon_r' - i\epsilon_r'')$$

If σ is expressed in terms of its real and imaginary components

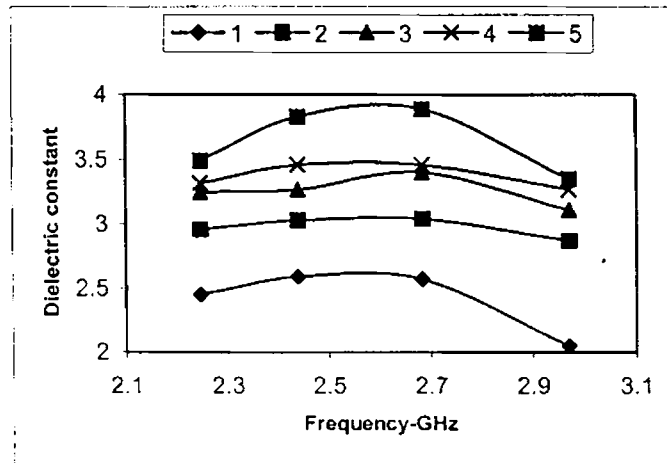


Fig. 6.1 Frequency dependence of the dielectric constant of various ionomers.

1, 2, 3, 4 and 5 represent the ionomers with 0, 14.5, 21.2, 26.5 and 40 meq of ionic content / 100 g polymer

$$\sigma = \sigma' + i\sigma''$$

where σ' , the real part of complex conductivity

$$\sigma' = \omega \epsilon_r'' = 2 \pi f \epsilon_0 \epsilon_r''$$

and imaginary part

$$\sigma'' = \omega \epsilon_r' = 2 \pi f \epsilon_0 \epsilon_r'$$

6.3 Dielectric properties of ionomers

6.3.1 Microwave Investigations.

6.3.1a. Dielectric constant

The dielectric properties of the base polymer and their ionomers probed at 2- 3 GHz frequencies of the microwave region have been investigated. These results reveal that the dielectric constant (ϵ') of the ionomers increase, reach a maximum, and then decrease with the frequency of the microwave radiation (Fig. 6.1). The ionic content in the ionomer however shows direct relationship with ϵ' up to the threshold ionic concentration of 26.5 meq. Figure 6.2 demonstrates the dependence of frequency ($\omega/2\pi$) on the dielectric loss-frequency product ($\epsilon''f$) of the ionomer. The dielectric loss factor or the imaginary part of the relative complex permittivity (ϵ'') of the ionomers with 0, 14.5, 21.2, 26.5 and 40 meq of ionic content have been investigated.

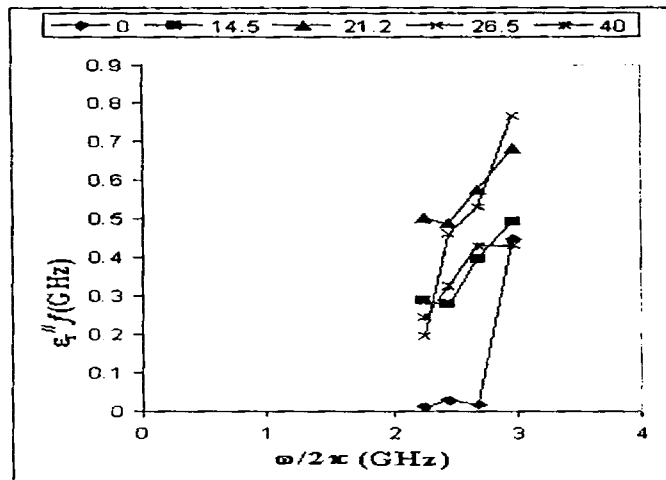


Fig. 6.2 Dependence of frequency on the dielectric loss-frequency product of the RISGNR containing 0, 14.5, 21.2, 26.5 and 40 meq of ionic groups

6.3.1.b. Complex conductivity-real part

The relative complex conductivity or the a.c. conductivity (real part- σ') of the ionomer has been observed to be affected by both frequency (Fig 6.3) and ionic content in the ionomer (Fig 6.4). Logarithmic plot of σ' against angular frequency (ω) of the microwave region (Fig 6.5) may be considered as supplementary evidence for the above observations.

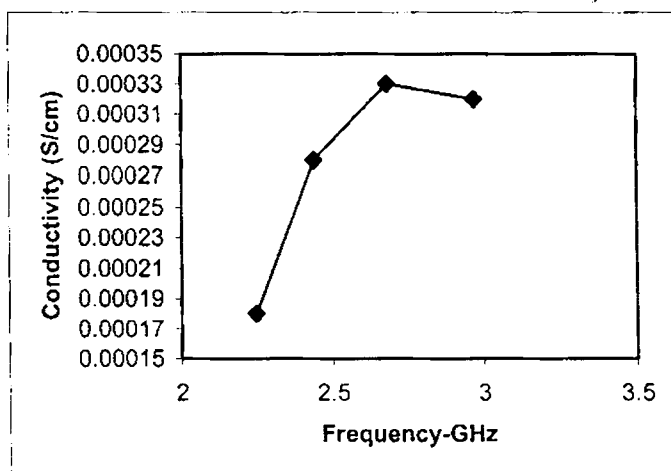


Fig. 6.3 Dependence of frequency on conductivity (real part) of 26.5 ZnS-SG NR ionomer

6.3.1.c. Complex conductivity-imaginary part

Microwave investigations of the imaginary part of the relative complex conductivity σ'' of the ionomer has been influenced by the frequency ω ($= 2\pi f$). This has been shown in the $\log \sigma'' - \log \omega$ plot of the ionomer (Fig 6.6). The $\tan\delta = \epsilon_r'' / \epsilon_r'$ is commonly employed as a direct measure of the dielectric loss, which in turn provides a measure of the conductivity [19].

6.3.1.d. Loss tangent

The loss tangents for these ionomers increase with ionic concentration (Fig. 6.8 & 6.9) and show a loss tangent threshold at 26.5 meq of ionic concentration.

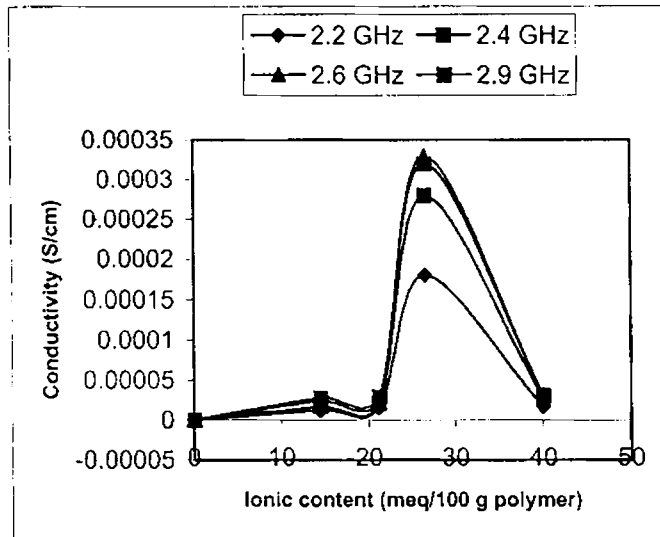


Fig. 6.4. Conductivity of the ionomer as a function of ion content in the ionomer at the S-band frequencies of the microwave region

Although σ' is customarily considered as a.c. conductivity [20] and is not well defined for disordered materials such as conducting polymers [21], σ' is often used to describe the frequency dependence of conductivity. The figure 6.4 shows that the ionic content has a dramatic influence on the a.c. conductivity of the ionomer at 2 – 3 GHz frequencies of the microwave region. The maximum percolation behavior, for the zinc salt of sulfonated SGNR at the optimum conditions of 2.6 GHz frequency and 26.5 meq ionic content, may be manifested from an a.c. component (real part of complex conductivity - σ') of 3.3×10^{-4} S/ cm in the ionomer. The same parameter for the nonionic SGNR was 1.8×10^{-12} S/ cm. The ionic conductivity of the SGNR ionomer is comparable with the conductivity of other polymers [22-25]. The natural rubber ionomer may be useful as an alternative material in Industrial scientific and medical devices that require specifications such as microwave active, thermoplastic, and ionic cross-linked elastomer of good physical properties.

6.3.2 Microwave conduction in ionomers based on RISGNR

The conductivity of the ionomer under the microwave field may be attributed to the polarization (scheme 6.1) caused by the alternating accumulation of ionic associations (Schemes 3.2 & 3.3 in chapter 3). Due to the orientation polarization of the dipoles, the possibility of dielectric relaxation (so also dielectric loss) cannot be ruled out at higher frequencies. This might result in the decrease of ϵ'' with frequency. This dipole polarization may be related to the "frictional" losses caused by the rotational displacement of molecular dipoles under the influence of the alternating microwave field.

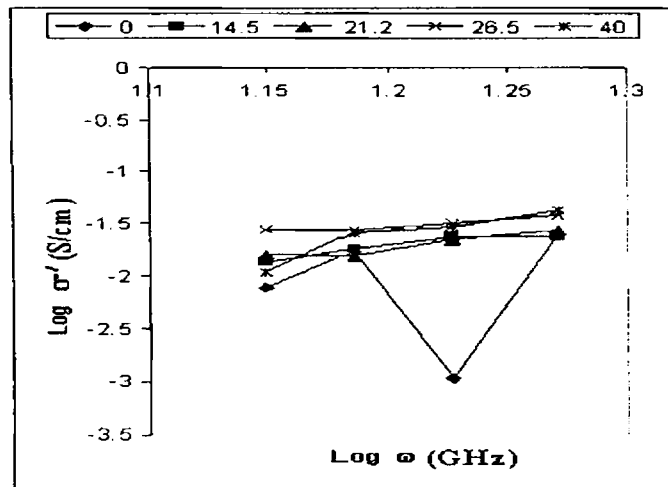
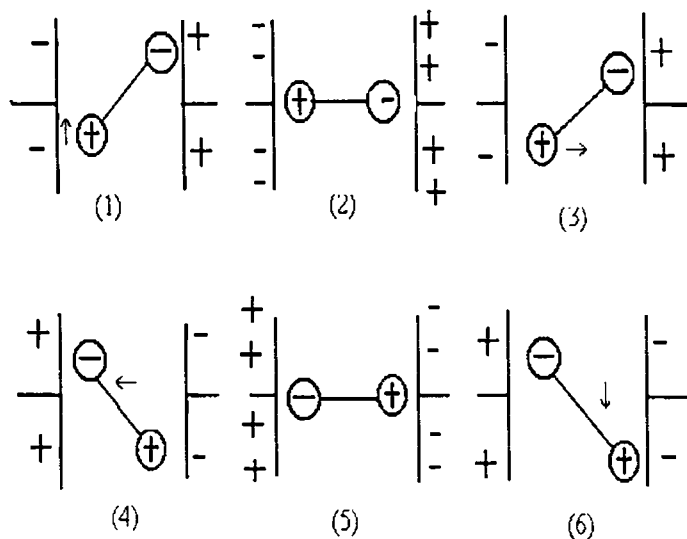


Fig. 6.5 Influence of frequency on the log (complex conductivity-real) of RISGNR containing 0, 14.5, 21.2, 26.5 and 40 meq ionic concentration

The improvement in the dielectric constant with ionic content (Fig. 6.7) may be due to the increase in the polar centers such as unassociated ionic moieties, multiplets, ionic clusters and zinc metal ions in the polymer matrix. The microwave responses of these charge centers may be contributing towards the dielectric constant. At higher frequency, the rotatory motion of the molecules may not be sufficiently rapid for the attainment of equilibrium with the field. The polarization then acquires a component



Scheme 6.1 Proposed model showing the dipole orientation in an alternating microwave field. (1), (2), (3), (4), (5), and (6) schematically represent the progressive change in the charge of polarized matrix between conducting elements modeled as a capacitor network and the resultant position of a dipole during one cycle of an a.c. field.

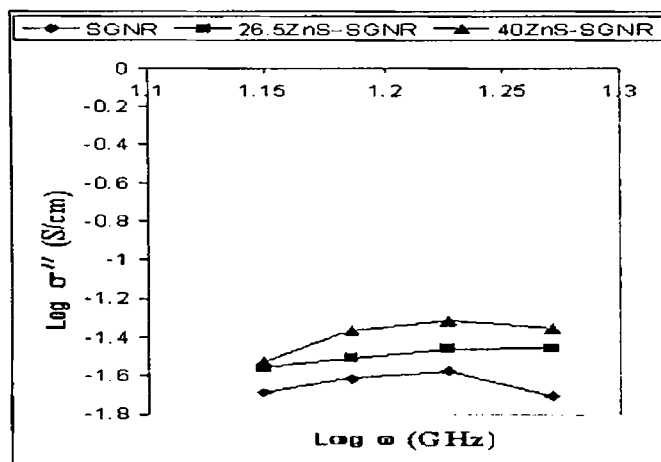


Fig. 6.6 Influence of frequency on the complex conductivity (Imaginary) of the ionomers.

out of phase with the field, and the displacement current acquires a conductance component in phase with the field, resulting in thermal dissipation of energy. When

this occurs, dielectric losses will be generated. At higher ionic content, the molecular interactions would lose the flexibility of the polymer chains.

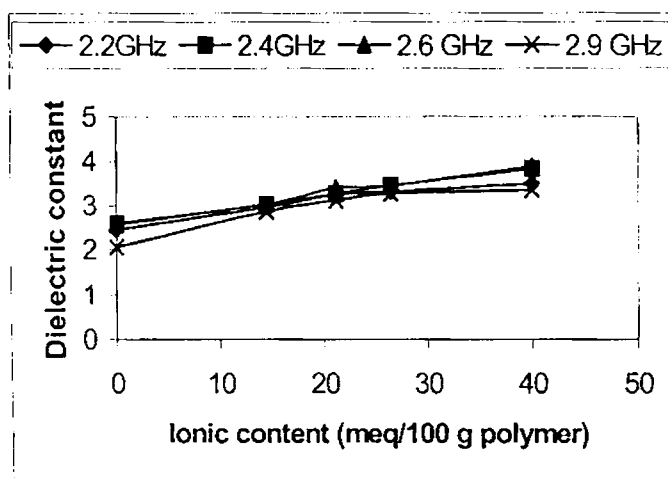


Fig. 6.7 Influence of ionic concentration on the dielectric constant.

The dipole attached to a flexible chain can reorient more easily than one attached to a stiff chain. Phase inversion and percolation threshold also would be occurring at higher ionic concentration [6]. At very high frequencies, the viscosity of the polymer hinders dipole movement and they cannot orient in the rapidly reversing field. Consequently, the dipoles do not influence the a.c. characteristics at very high frequencies. The many fold initial increase in the conductivity of the base polymer upon incorporating zinc sulfonate groups may be attributed to the formation of the ionic nano clustering, which act as centers of conductance [19]. Because the hydrocarbon backbone cannot transport the charge carriers, the formation of the ionomers multiplets represented in scheme 3.2 (chapter 3) may be expected to be the main factor for the initial increase in the complex conductivity with the increase of the ion contents.

At higher ionic content, the mobility of the charge carrier decreases. The reason may be related to the fact that the ion - dipole interaction within the clustering increases the microscopic viscosity of the phase separated polar ionic cluster region. The microscopic viscosity of the ion rich phase governs the conduction and

consequently, low microscopic viscosity is required for obtaining the high conductivity. In the case of the RISGNR based ionomers, the microscopic viscosity of the ion rich phase will be more significantly increased than the natural rubber matrix, due to the interaction between the metal ions and sulfonated groups within the cluster of the ionomer. In our ZnS - RISGNR ionomers, the zinc cations may be interacting with the sulfonic acid moieties during neutralization forming the higher multiplets.

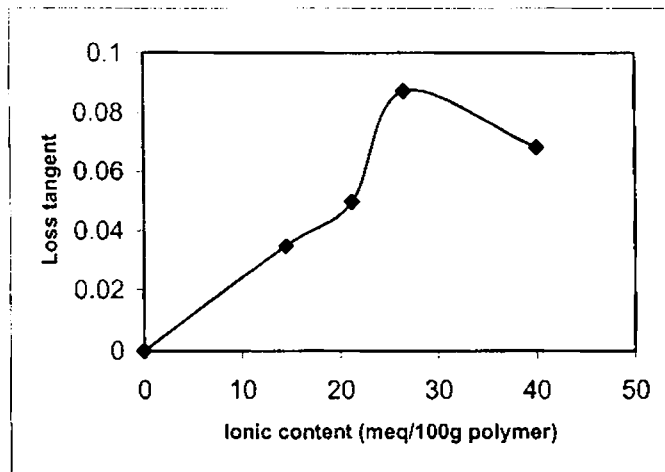


Fig. 6.8. Relationship between the loss tangents of the ionomers as a function of ionic content at 2.4 GHz frequencies.

The increase in the interactions within the ionomer may increase the thickness of the restricted mobility region or the ion rich phase. This may be consequently increasing the microscopic viscosity [25] of the ion rich phase. The decrease in the polarization ability due to the increase of the microscopic viscosity is expected to be the reason for the decrease of the conductivity at higher concentration of ionic groups. Ionic associations that influence the physical properties [26-28] of the

ionomer may be believed to affect their dielectric properties at the S-band frequencies of the microwave region.

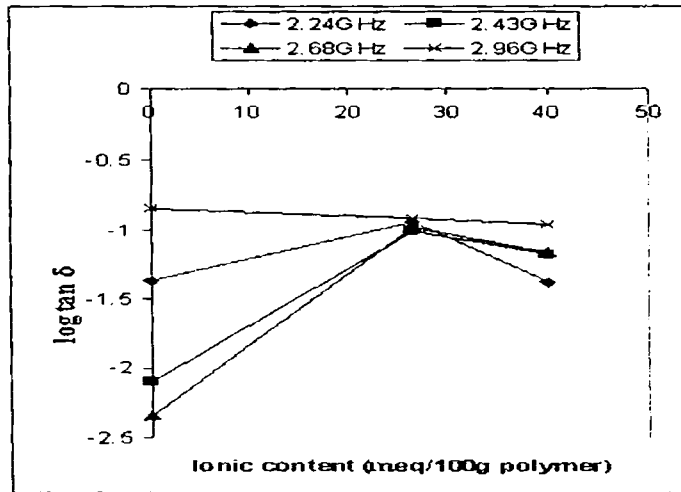


Fig. 6.9 Influence of ionic content on the $\tan \delta$ of the 26.5 ZnS-SG NR ionomer at different frequencies

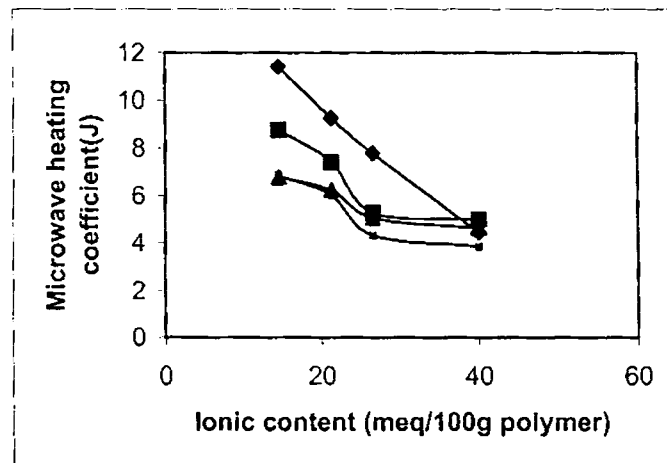


Fig. 6.10 Dependence of ionic concentration in the ionomer on the microwave-heating coefficient at different frequencies

The increase in the $\tan\delta$ up on increasing ionic concentration may be attributed to the plasticising [29] effect of the low molecular weight fractions, which may be formed during the synthesis of the ionomers. The plasticization is believed to be facilitating the polarization of the dipoles at the microwave frequencies.

Table 6.1 Dielectric behaviors of the filled ionomeric materials at the S-band frequencies

Frequency (GHz)	Materials	Dielectric constant	Conductivity (S/cm)
2.439	1	3.46	2.8×10^{-4}
	2	4.33	3.2×10^{-3}
	3	3.59	6.0×10^{-5}
	4	7.69	6.8×10^{-3}
	5	3.88	2.1×10^{-4}
	6	5.87	5.2×10^{-3}
2.683	1	3.46	3.3×10^{-4}
	2	4.19	2.2×10^{-3}
	3	3.44	7.0×10^{-5}
	4	7.29	8.8×10^{-3}
	5	3.64	1.9×10^{-4}
	6	5.67	4.9×10^{-3}
2.970	1	3.27	3.2×10^{-4}
	2	4.14	5.2×10^{-3}
	3	3.84	6.2×10^{-5}
	4	7.09	9.2×10^{-3}
	5	3.74	1.4×10^{-4}
	6	6.37	4.3×10^{-3}

Material-1, represents neat ionomer, 2, 3, 4, 5 and 6 show ionomer filled with 10-phr of HAF black, silica, nylon, glass and zinc stearate respectively

Figure 6.8 shows the variation of the loss tangent as a function of the ionic content in the ionomer at 2.4 GHz. At higher ionic concentrations, though there is plasticization,

the higher micro phase viscosity arising out of the strong inter-dipole attraction may offset the increase in the $\tan \delta$. The ionomers, at higher ionic concentration, may be transformed in to an ionically "cured" system. The loss tangent studies of the ionomers at microwave frequencies may be considered as one of the examples of analogy between the mechanical and electrical properties of the ionomers [29].

6.3.3 Microwave heating coefficient (J)

Practically all applications of polymers in electrical and electronic engineering require materials with a low $\tan \delta$. However, one application that takes advantage of a high value of tangent loss is high frequency dielectric heating. In this application, the efficiency of heating is usually compared [29] by means of a comparison coefficient J, which is defined as

$$J = 1 / \epsilon_r \tan \delta$$

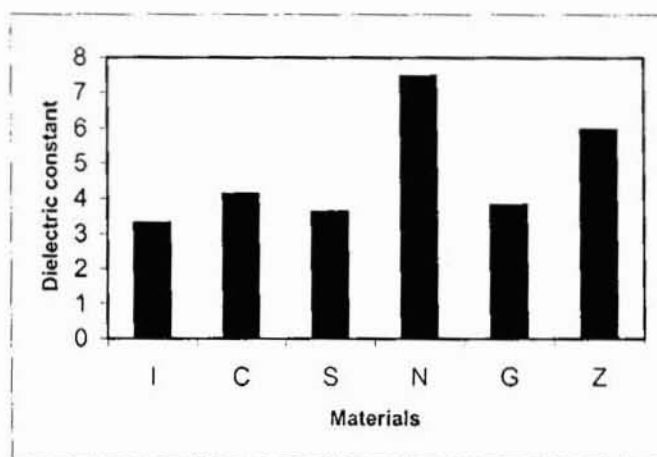


Fig. 6.11 Effect of 10 phr fillers on the dielectric constant of the ionomer at 2.247 GHz
 Filled materials are neat ionomer (I). Compounds of carbon (C), silica (S), nylon (N), glass (G) and zinc stearate (Z)

Figure 6.10 shows the variation of J with ionic content at four different microwave frequencies. Smaller the J value better will be the polymer for dielectric heating purposes.

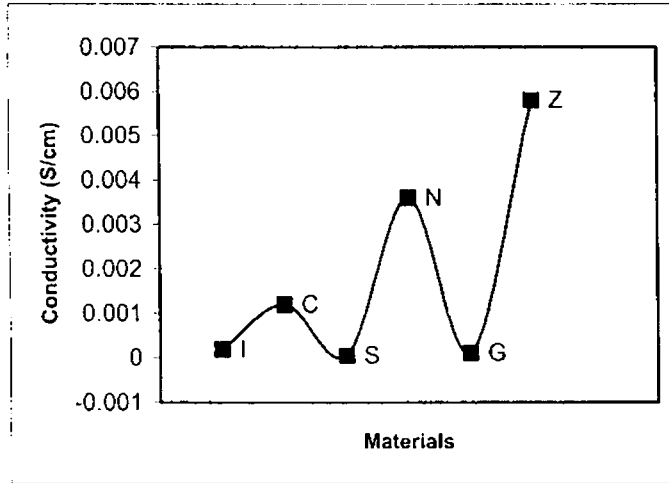


Fig. 6.12 Effect of 10 phr fillers on the a.c. conductivity of the ionomer at 2.247 GHz

Filled materials are neat ionomer (I). Compounds of carbon (C), silica (S), nylon (N), glass (G) and zinc stearate (Z)

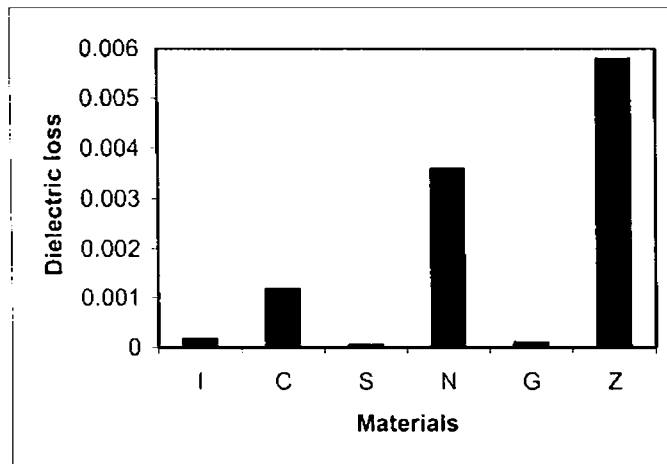


Fig. 6.13 Effect of 10 phr fillers on the dielectric loss of the ionomer at 2.247 GHz

Filled materials are neat ionomer (I). Compounds of carbon (C), silica (S), nylon (N), glass (G) and zinc stearate (Z)

There has been considerable improvement in the microwave-heating coefficient of the polymers up on the ionomeric modifications. Of course, the heat generated in the polymeric material comes from the loss tangent, but that loss may not come entirely from the relaxation loss. Rather, conductivity of the polymeric material may also contribute to the $\tan \delta$. This situation may be compared with ohmic heating of metals: where the charge carriers are electrons; however the polar centers are the causative in dielectric polymeric materials.

6.4 Dielectric properties of filled Ionomers

The fillers selected for the study are carbon black (HAF), silica, nylon fibers, glass fibers and zinc stearate. Fillers have been added to the ionomer at the level of 10-phr. Figure 6.11 shows the dielectric behavior of the ionomer with fillers at 2.2 GHz frequencies. Silica and glass show low dielectric constant and conductivities at the S-band frequencies of the microwave region. The dielectric constant (ϵ'), dielectric loss factor (ϵ'') and a.c. conductivity (σ') of the nylon filled ionomer shows the highest values at 2.2 GHz frequencies of the microwave region. Zinc stearate and carbon black fillers also give improved electrical characteristics in comparison with the neat ionomer. This has been found to be the trend from 2-3 GHz frequencies as is shown by the table 6.1 and figure 6.12 and figures 6.13. Ionomer with silica shows lowest conductivity in this frequency range. As the conductivity of nylon, zinc stearate and carbon black is found to be higher than other fillers, these filled ionomers may be used as components in microwave devices.

6.5 Conclusion

The ionic associations in the ionomer, which are held through coulombic forces, may act as the centers of polarization at the S-band frequencies of the microwave region. The measurement of the dielectric properties of the ionic SGNR at 2 – 4 GHz frequencies at room temperature showed that the complex permittivity and the

relative complex conductivity increased with increase in the ionic concentration. The ionomer had its highest microwave conductivity at 2.6 GHz. At this frequency, the maximum conductivity was obtained at a concentration threshold of 26.5 meq. In the present study it has been found that the incorporation of 26.5 meq zinc sulfonate groups in to the base polymer increases its σ' from 1.8×10^{-12} S/cm to 3.3×10^{-4} S/cm.

Microwave probing of ionomers filled with fillers such as carbon black (HAF), silica, nylon, glass and zinc stearate reveal that ϵ' and σ' of the ionomer has been affected. Silica and glass filled ionomers show lower dielectric properties compared to other fillers. Among the microwave active fillers such as carbon black, zinc stearate and nylon fibers, the nylon filled ionomer shows the highest electrical properties at the microwave region. The microwave response of these ionomers and their filled compounds may pave the way for the large-scale consumption of natural rubber in microwave devices.

6.6 References

1. Khan, S. M.; Negi, S.; Khan, I. M. *Polymer News*, 22, 414 (1997).
2. Bur, A. J. *Polymer*, 26, 963 (1985).
3. Joo, J; Epstein, A. J. *Plastics Portable Electronics*. Retec Proceedings, Las Vegas, 140 (1995).
4. Ku, H. S.; Mac Robert, M.; Siores, E.; Ball, J. A. R. *Plast. Rubb. Composites* 29,285 (2000).
5. Patent- EP 970988 A1 20000112 Inves: Nagakubo, H.; Koshika, I.; Tomono, K.; Higuchi, Y.; Oshima, T.
6. Eisenberg, A.; Kim, J.-S. *Introduction to Ionomers*. Wiley Interscience Publication, New York, (1998).
7. MacKnight, W.J.; Lundberg, R.D. *Rubber Chem. Technol.*, 57, 652 (1984).
8. Read, B.E.; Carter, E.A.; Connor, T.M.; MacKnight, W.J. *Brit. Polym. J.*, 1, 123 (1969).
9. Phillips, P.H.; MacKnight, W.J. *J. Polym Sci A-2*, 8, 727 (1970).
10. Hodge, I.M.; Eisenberg, A. *J. Non-Crys. Solids*, 27, 441 (1978).
11. Mohamed, A.B.H.; Miane, J.L.; Zangar, H. *Conference in Dielectric Materials*, Tunisian Society of Physics, Mahdia, Tunisia, (2000).
12. Hodge, I.M.; Eisenberg, A. *Macromolecules*, 11, 283 (1978).
13. Lee, K.H.; Park, J.K.; Kim, W.J. *J. Polym. Sci. Part B: Polym Phys*, 37, 247 (1999).

14. Dabek, R. *Polym. Eng. Sci.*, 36, 1065 (1996).
15. Mathew, K.T. Raveendranath, U. In: "Sensors Update" Baltes, H.; Gopel, W.; Hesse, J. Ed. WILEY-VCH (Germany), chapter 7, 185 (2000).
16. Thuery, J. In: *Microwaves: "Industrial, Scientific, and Medical Applications"*. Grant, E.H. Ed., ARTEC HOUSE, INC, Norwood, (1992).
17. Thommachan, X.; Samuel, J.; Kurian, T. *Macromol. Mater. Eng.*, 286, 507 (2001).
18. Raveendranath, U.; Mathew, K.T. *J. Mol. Liq.*, 68, 145 (1996).
19. Ezquerro, T.A.; Kremer, F.; Wegner, G. "AC Electrical Properties of Insulator Conductor Composites" In "Dielectric properties of Heterogeneous Materials" (Progress in Electromagnetic Research 6) Priou, A. Ed., Elsevier, New York, (1992).
20. Ngai, K.L.; Rendell, R.W. "Dielectric and Conductivity Relaxations in Conducting Polymers" In: *Hand Book of Conducting Polymers*, Skotheim, T.A. (Ed.), Marcel Decker, New York, (1986).
21. Ikeda, Y.; Wada, Y.; Matoba, Y.; Murakami, S.; Kohjiya, S. *Rubber Chem. Technol.* 73, 720 (2000).
22. Kyoung-Hee Lee; Jung-Ki Park; Whi- Joong Kim. *J. Polym. Sci. Part B. Poly Phys. Edn*, 37, 247 (1999).
23. Polizos, G.; Georgoussis, G.; Kyritsis, A.; Shilov, V. V.; Shevchenko, V. V.; Gomza, Y. P.; Nesin, S. D.; Klimenko, N. S.; Wartewig, S.; Pissis, P. *Polym. Inter.* 49, 987 (2000).
24. Seymour, R.B.; Ed. "Conductive Polymers" (Polymer Science and Technology; V.15), Proceedings of a Symposium sponsored by the ACS division of Organic Coatings and Plastics Chemistry, held Aug.26-27, 1980, at the second chemical congress of the North American continent in Las Vegas, Nev: Plenum Press, New York, Vol. 15 (1981).
25. Troung, V. T.; Teman, J.G. *Polymer*, 36, 905 (1995).
26. Holliday, L. Ed. In: "Ionic Polymers", *Appl. Sci.*, London, (1975).
27. Schlick, S. Ed; "Ionomers, Characterization, Theory and Appl". CRC Press: Boca Raton, FL, (1996).
28. Tant; M. R.; Mauritz, K.A.; Wilkes, G.L. Eds. "Ionomers: Synthesis, Structure, Properties, and Applications"; Chapman & Hall, New York (1997).
29. Chen. C. Ku; Raimond Liepins, "Electrical Properties of Polymers: Chemical Principles. Hanser Publishers: Munich, Chapter 3 (1987).

Chapter 7

Compatibilization of SBR/NBR blend using RISGNR ionomer

Part of the work presented in this chapter has been communicated to the *Polymer*

- 7.1. *Introduction*
- 7.2. *Processing characteristics from rheometric data*
- 7.3. *Characterisation studies*
 - 7.3.1. *Differential scanning calorimetry*
 - 7.3.2. *Dynamic mechanical thermal analysis*
 - 7.3.3. *Physical properties*
 - 7.3.4. *Infrared spectroscopy*
 - 7.3.5. *Morphological studies*
 - 7.3.5.1. *Uncompatibilized blend of 50/50 SBR/NBR*
 - 7.3.5.2. *Compatibilized blend of 50/50 SBR/NBR*
- 7.4. *Influence of carbon black*
 - 7.4.1. *Cure characteristics*
 - 7.4.2. *Physical properties*
 - 7.4.3. *Morphological studies*
- 7.5. *Location of the compatibilizer using DMTA*
- 7.6. *Compatibilization theory*
- 7.7. *Conclusion*
- 7.8. *References*

7.1 Introduction

This chapter discusses the effect of 26.5 ZnS-RISGNR ionomer as compatibilizer in SBR/NBR blend system with reference to their cure characteristics, thermal and

dynamic mechanical behavior, infrared spectroscopy, physical properties and morphological observations. Polymer blends are considered as mixtures of macromolecular species. The necessary condition is that the amount of minor component must exceed at least five percent by weight. Most of the polymer blends are found to be immiscible and incompatible. In the case of miscible blends, the overall physicommechanical properties depend on two structural parameters: (a) proper interfacial tension which leads to a phase size small enough to allow the material to be considered as macroscopically homogenous, (b) an interphase adhesion strong enough to assimilate stresses and strains without disruption of the established morphology. This unfortunately is not the case for most polymer blends [1-3]. For a very long time attempts have been made to find compatible polymeric systems or to compatibilize various polymeric mixtures. Only a few systems are known in which two homopolymers are compatible over a very wide composition range. However, compatible blends are desirable because the properties of the mixture are intermediate between those of the homopolymers, rather than giving some type of the superposition of the homopolymer properties. Several methods of compatibilization of polymers are known. There are a few patents, which describe compatible or compatibilized blends. The compatibility of the blend components is enhanced by interactions such as ionic and H-bonds, as well as donor – acceptor interactions. Ionic groups in the polymers are capable of creating specific interactions between the component polymers in the blend. The compatibility in the case of blends of an ionomer with other polar polymers arises due to ion – ion or ion – dipole interactions. Mixing the polymers in the molten state has facilitated polymer blends preparation. This type of 'reactive blending' may lead to chemical reactions, depending up on the chemical structure of the polymer. This kind of reactive melt-processing technology has many advantages. It is complementary to polymerization, has high flexibility and versatility, and makes less negative impact on the environment.

Nitrile rubber is primarily noted for its oil and chemical resistance. Oil resistance specified for the rubber products vary to a considerable extent. It is possible to use a blend of high acrylonitrile NBR with SBR to get a degree of oil resistance equal to that given by a low acrylonitrile NBR with an overall economy in cost. Products from high acrylonitrile NBR have a tendency to shrink in contact with

hot lubricating oils and replacement of a part of it by SBR may overcome this defect. Along with oil resistance property, oil seals and gaskets some times require compression set resistance at higher temperatures. Compression set resistance can be improved by blending with SBR. SBR can also improve its processing properties. For a rubber product with the specifications of good chemical, oil and compression set resistance at high temperature, the NBR/SBR blend may be a good alternative. These blends are, however, found to be immiscible [4]. Various approaches have been taken to enhance the miscibility of immiscible polymer blends [5]. The SBR/NBR blends can possibly be made miscible by using compatibilizers that can have interactions with SBR and NBR. Compatibilization of SBR/NBR blends using dichlorocarbene modified SBR has been reported [6]. An attractive alternative route for compatibilization is the use of ionomers [7, 8]. The use of ionomers containing ionic sulfonate groups, as compatibilizers, in polymer blends has been the subject of many patents [9]. DSC studies on few blends have demonstrated that zinc sulfonated ionomers act as good compatibilizers [10]. Coran et al [11] have reported the dynamic mechanical properties of various blends. The storage modulus and loss tangent of blends were correlated with the structure parameters [12]. DMTA is often more sensitive than DSC in detecting the presence of different phases in polymer blends [13]. Some segments of the styrene grafted natural rubber ionomers are chemically identical to SBR, and it is possible for the polar zinc sulfonate groups of the ionomer to have interaction with the acrylonitrile unit of NBR.

7.2. Processing characteristics from rheometric data

Master batches of SBR, NBR (without accelerator and sulfur) were prepared separately and then blended at different compositions of 70/30, 50/50 and 30/70 as per the formulation shown in the table 7.1. The 26.5 ZnS-RISG NR ionomer, used as the compatibilizer, was added to the preblended SBR/NBR at various concentrations of 1-10 phr. The required quantity of curatives were then added and mixed properly with the preblended mixes. The commonly used, sulphenamide (CBS) as primary

accelerator and TMTD as secondary accelerator have been used in blends, as they are known to produce satisfactory levels of cure in both SBR and NBR.

Table 7.1 Formulation of SBR/NBR blends

Ingredients	Mix-1(Phr)	Mix-2(Phr)	Mix-3(Phr)
SBR	70	50	30
NBR	30	50	70
26.5 ZnS-RISGNR	0,1,3,5,10	0,1,3,5,10	0,1,3,5,10
Stearic acid	1.2	1	0.8
Zinc oxide	5	5	5
CBS	0.7	0.8	0.3
TMTD	0.3	0.5	0.7
Sulphur	1.69	1.5	1.01
TDQ	1	1	1

An idea about the cross-linking within a phase and the cross-linking between the two phases can be obtained from the cure characteristics and mechanical properties of rubbers. There will be insufficient cross-linking between the phases if the two rubbers do not mix properly, which will be reflected in poor mechanical properties. In the entire blend composition there is considerable enhancement in torque (Fig. 7.1) on the addition of 26.5 ZnS-RISGNR of 1,3,5,10 phr. The torque increases progressively with ionic content up to 5 phr and then decreases in all blend compositions. The presence of 26.5 ZnS-RISGNR enhances the effect of inter diffused chains leading to optimum vulcanization. The influence of the ionomer compatibilizer on the scorch time of the 50/50 SBR/NBR blend is shown by the figure 7.2. This may be due to the effective cross-linking up on increasing molecular level homogeneity. The optimum cure time of the blend (Fig. 7.3 & Fig. 7.4) increases up to 5 phr of 26.5 ZnS-RISGNR and then decreases. This may be due to the large interfacial area formed by the uniformly distributed blend matrix.

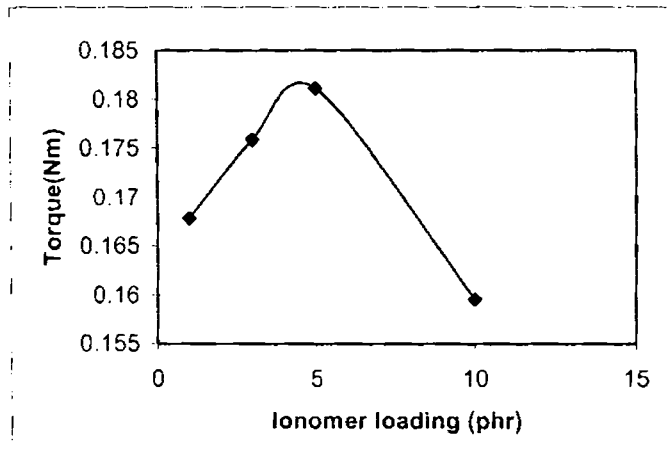


Fig. 7.1 Influence of ionomer concentration on the torque of 50/50 SBR/NBR blend compatibilized with 1, 3, 5, and 10 phr ionomers.

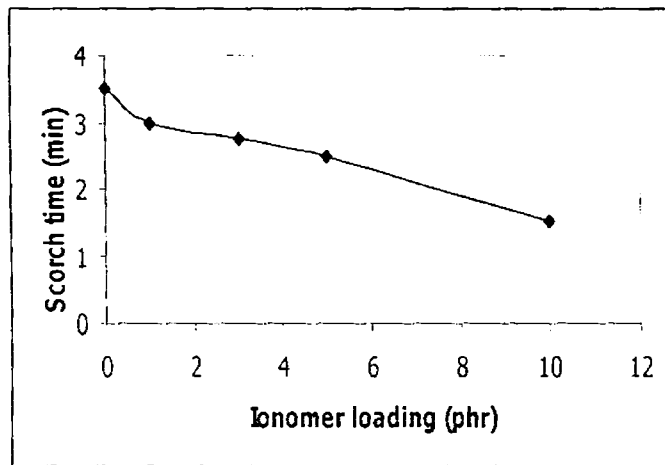


Fig. 7.2 Variation of the scorch time of 50/50 SBR/NBR blends on compatibilization with 1, 3, 5, and 10 phr ionomers.

The maximum value of optimum cure time was found in this case, as more time is needed for the formation of greater number of interface cross-links. But as the ionic

content increases further the homogenizing efficiency decreases which results in the coalescence of dispersed domains. This reduces the interfacial area and there by causes a decrease in optimum cure time. This data predicts the behavior of 26.5 ZnS-RISGNR as a compatibilizer in SBR/NBR blend, which is further, confirmed by FTIR spectroscopy, physical property measurement, dynamic mechanical thermal analysis, differential scanning calorimetry and scanning electron microscopy

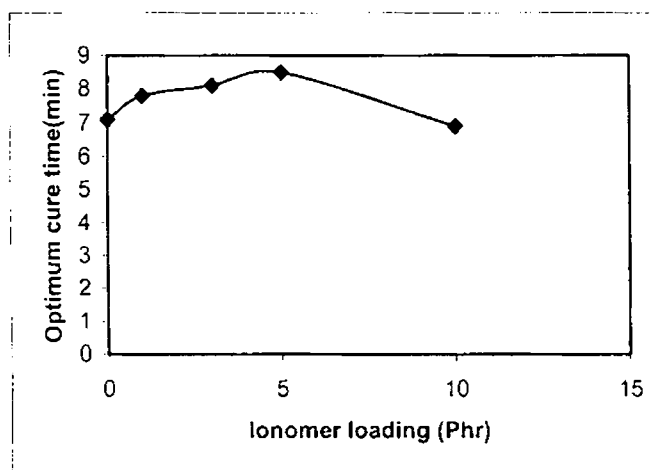


Fig. 7.3 Relation between the concentration of the compatibilizer and optimum cure time of 50/50 SBR/NBR blends.

7.3. Characterisation

7.3.1. Differential scanning calorimetry

The DSC traces of pure 50/50 SBR/NBR blend in the presence and absence of compatibilizers is shown in figure 7.5. The characteristic T_gs of SBR and NBR, for the uncompatibilized 50/50 SBR/NBR blend, appearing at -34°C and $+4^{\circ}\text{C}$ (Table 7.2) have been almost unaffected. The addition of ionomers in to SBR/NBR blend system may be enhancing the interaction between the sulfonate groups of ionomer and the –

CN groups of the NBR. The interfacial tension may be thus reduced due to their interfacial activity [7-14].

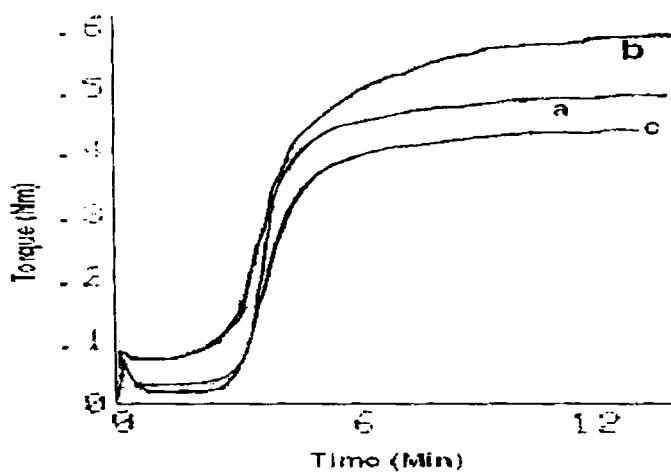


Fig. 7.4 Cure curves of the neat SBR/NBR blend (a) and their 5-phr (b) and 10-phr (c) compatibilized compounds

Table 7. 2 DSC results of blends

Samples	T _g °C	Temperature range of transition (°C)
Blend-1	- 34 and+ 4	- 50 to +10
Blend-2	- 34 and+ 4	- 50 to +10
Blend-3	- 34 and+ 4	- 50 to +10
Blend-4	- 34 and+ 4	- 50 to +10
Blend-5	- 34 and+ 4	- 50 to +10

Blend-1 (0 compatibilizer); *Blend-2* (5 phr compatibilizer); *Blend-3* (10 phr compatibilizer); *Blend-4* (40 phr HAF black and 0 compatibilizer); *Blend-5* (40 phr HAF black and 5 phr compatibilizer)

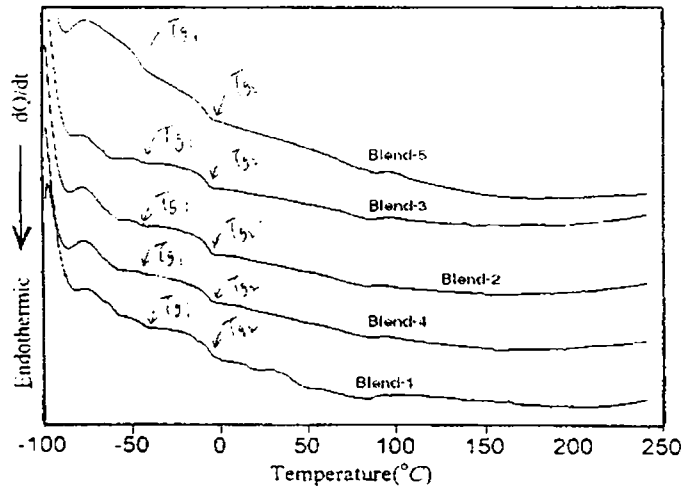


Fig. 7.5 DSC thermal profiles of SBR/NBR blend and their compounds:

Blend-1 (0 compatibilizer); Blend-2 (5 phr compatibilizer); Blend-3 (10 phr compatibilizer); Blend-4 (40 phr HAFblack and 0 compatibilizer); Blend-5 (40 phr HAFblack and 5 phr compatibilizer)

These, presumably weak van der Waals interactions operating within the SBR/NBR blend system may be rich enough to produce the technological compatibility in SBR/NBR system, as manifested by the significant achievement in the synergistic physical properties. However, these relatively weak polar-polar interactions may be rather poor for developing a fairly good phase separation to be detectable at this scanning rate in DSC. The T_g s are, therefore, seen unaffected (Table 7.2) or rather undetected. Additional information regarding the compatibilization of SBR/NBR blend may be obtained from the DMTA studies.

7.3.2. Dynamic mechanical thermal analysis

The dynamical mechanical studies of polymer blends are typically accomplished using forced-vibration methods or occasionally, free-vibration (e.g., torsion pendulum) techniques. In the dynamic mechanical case, the applied stress is

$$\sigma = \sigma_0 e^{i(\omega t + \delta)}$$

and the resulting strain is given by

$$\varepsilon = \varepsilon_0 e^{i\omega t}$$

The complex modulus can be expressed by

$$E^* = \sigma(t) / \varepsilon(t) = E_0 e^{i\delta} = E_0 (\cos \delta + i \sin \delta) = E' + iE''$$

Where E' (the in-phase component) is the storage modulus and E'' (the out-of-phase component) is the loss modulus. The loss factor is given by

$$E'' / E' = \tan \delta$$

DMTA is often more sensitive in detecting T_g in blends than DSC [18].

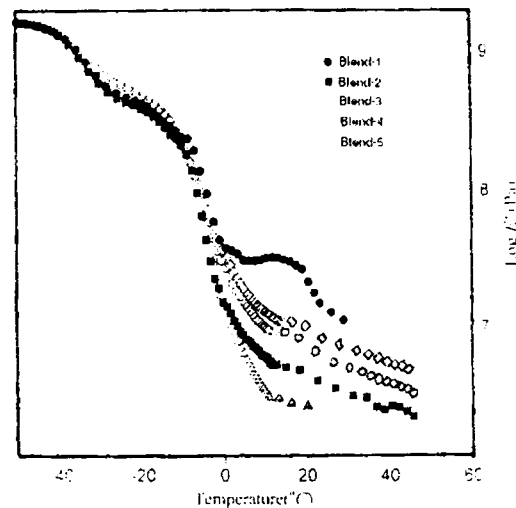


Fig. 7.6 Storage modulus-temperature plot of the SBR/NBR blend.

Blend-1 (0 compatibilizer); Blend-2 (5 phr compatibilizer); Blend-3 (10 phr compatibilizer); Blend-4 (40 phr HAFblack and 0 compatibilizer); Blend-5 (40 phr HAFblack and 5 phr compatibilizer)

It has been observed that the appearance of a single, reasonably sharp loss tangent peak at a glass transition temperature is indicative of molecular homogeneity, while the appearance of the multiple T_g 's reflects macro phase separation or partial miscibility of the blend's components [14-17]. The T_g 's of the individual components should differ by at least 20°C in order to ensure adequate resolution between possibly overlapping relaxations in immiscible or partially miscible polymer mixtures. The DMTA results of cured 50/50 SBR/NBR blend (Table 7.3) shows two T_g 's (T_{g1} and

Tg2) at $-32\text{ }^{\circ}\text{C}$ and $-2\text{ }^{\circ}\text{C}$, due to the presence of immiscible SBR and NBR phases respectively. The plot of storage modulus vs. temperature for SBR and NBR (Fig. 7.6) shows that there is a transition in storage modulus of SBR and NBR at -35 to $-14\text{ }^{\circ}\text{C}$ and -15 to $+15\text{ }^{\circ}\text{C}$, respectively. There is also another weak transition in the temperature range of -25 to $-6\text{ }^{\circ}\text{C}$.

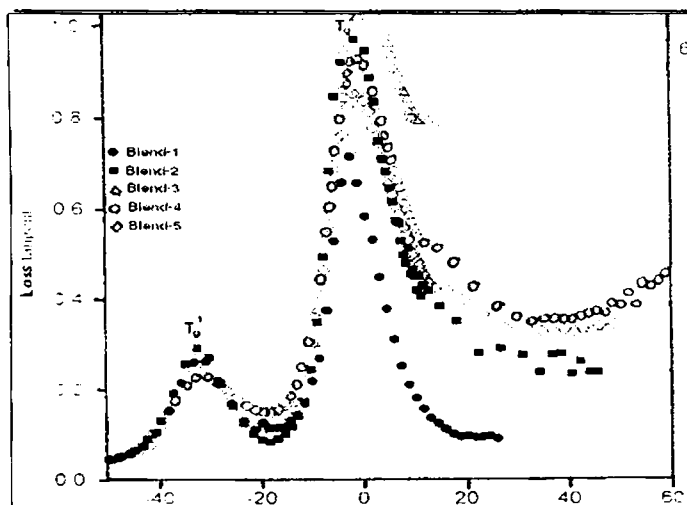


Fig. 7.7 Loss tangent-temperature plot of the SBR/NBR blend.

Blend-1 (0 phr compatibilizer); Blend-2 (5 phr compatibilizer); Blend-3 (10 phr compatibilizer); Blend-4 (40 phr HAFblack and 0 compatibilizer); Blend-5 (40 phr HAFblack and 5 phr compatibilizer)

It can be seen that SBR shows slightly higher storage modulus than NBR. It is clear that uncompatibilized and compatibilised samples show higher storage modulus compared to individual components. The appearance of the variation in the loss tangent (Fig. 7.7) corresponding to the NBR, which occur around $-2\text{ }^{\circ}\text{C}$ shows that there has been enhanced interaction between NBR and the ionomer. This might be the reason for the miscibility of SBR-NBR system and has been further supported by their improved physical properties.

7.3.3. Physical properties

Physical properties of the cured uncompatibilized SBR/NBR blend and the compatibilized SBR/NBR system measured at 25°C are summarized in table 7.4.

Table 7.3. DMTA Results of cured SBR/NBR Blends

Samples	Thermal transitions		Tan δ at			Log E' (Pa) at		
	corresponding to		T ¹ _g	T ² _g	25°C	T ¹ _g	T ² _g	25°C
	SBR (T ¹ _g)°C	NBR (T ² _g)°C						
Blend-1	-32	-2	0.27	0.73	0.09	8.8	7.8	7.1
Blend-2	-32	0	0.30	0.99	0.29	8.8	7.3	6.6
Blend-3	-32	0	0.29	1.05	0.71	8.8	6.8	6.3
Blend-4	-32	0	0.20	0.94	0.39	8.8	6.9	6.7
Blend-5	-32	0	0.25	0.88	0.36	8.8	7.0	6.9

Blend-1 (0 compatibilizer); Blend-2 (5 phr compatibilizer); Blend-3 (10 phr compatibilizer); Blend-4 (40 phr HAFblack and 0 compatibilizer); Blend-5 (40 phr HAFblack and 5 phr compatibilizer)

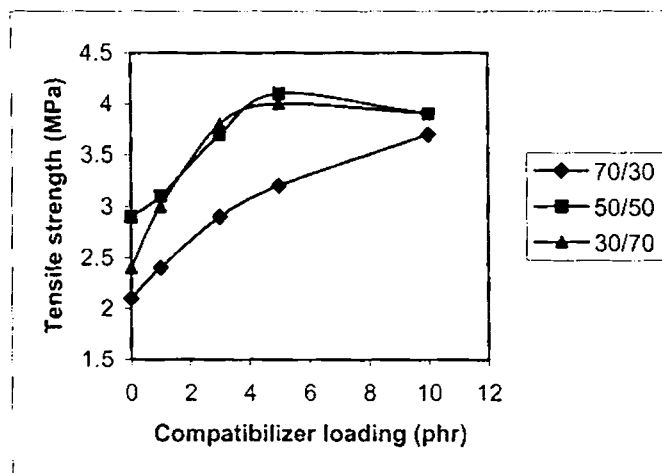


Fig. 7.8 Influence of compatibilizer on the tensile strength of three blend compositions of SBR/NBR system

Variation of tensile strength with the compatibilizer loading for different blend composition is shown in figure 7.8. It is interesting to note that the compatibilized SBR/NBR system shows synergism in tensile strength, tear strength and hardness, which may be ascribed to the formation of a technologically compatible polyblend, wherein intermolecular ionic interactions assist in compatibilization. The interfacial ionic cross-links improve the interfacial adhesion, thereby helping to transfer the stress from one phase to other phase.

Table 7.4 Physical properties of compatibilized and uncompatibilized SBR/NBR blends

SBR/ NBR	Compatibilizer (Phr)	T.S. (MPa)	E. B. (%)	Tear (N/mm)	Hardness (shore A)
70/30	0	2.1	302	14.5	41
	1	2.4	342	15.7	43
	3	2.9	432	17.8	44
	5	3.2	547	21.6	45
	10	3.7	502	20.4	46
50/50	0	2.9	317	14.9	42
	1	3.1	382	17.7	44
	3	3.7	462	21.6	45
	5	4.1	507	23.0	46
	10	3.9	487	22.8	47
30/70	0	2.4	352	17.6	43
	1	3.0	292	19.7	44
	3	3.8	417	22.5	46
	5	4.0	442	25.2	47
	10	3.9	422	24.6	49

The ionic content in the ionomer has a direct influence on the physical properties of the SBR/NBR blend. Compared to the uncompatibilized blends compatibilized sample

show an increase in the overall tensile strength. The compatibilising action is due to the interaction of acrylonitrile of NBR and zinc sulphionate moieties of ZnS-RISGNR. There is structural similarity between styrene grafted natural rubber segments of the compatibilizer and SBR. This also enhances compatibilising action of ZnS-RISGNR in the blends. If the segments of the added copolymer are chemically identical with those of in the respective phases or adhered to one of the phases then they act as efficient compatibilizers. In the 50/50 SBR/NBR blends there is higher homogeneity of mixing and more uniform mixing of the rubbers in presence of compatibilizers. The tensile strength of the blend system has been found to be increasing with increase in the concentration of the compatibilizer up to 5 phr. These compatibilizers create strong interfacial cross-links, which facilitate efficient stress transfer to the well-dispersed SBR/NBR domains. The tear strength enhances on the addition of the compatibilizing agent. It has been found that 5 phr 26.5 ZnS-RISGNR brings about higher tear strength for the 50/50 SBR/NBR compatibilized blends (Fig.7.9).

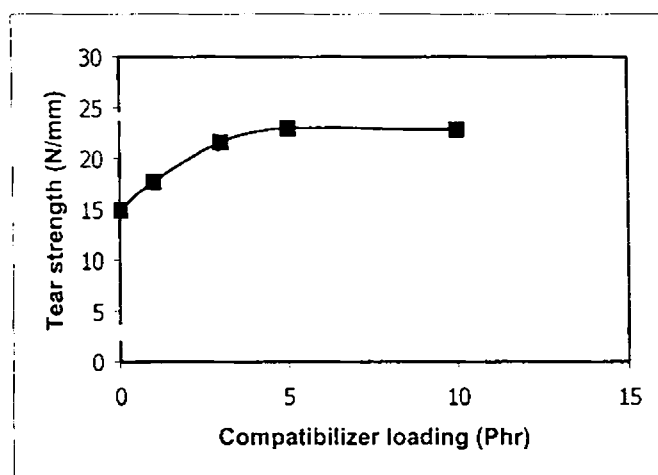


Fig. 7.9 Effect of compatibilizer on the tear strength of 50/50 SBR/NBR blend

Lower hardness of the uncompatibilized blends compared to the compatibilized blends may be due to the higher cross-linking in presence of compatibilizer. On the whole the trends of the properties are quite similar over all the blend compositions.

The mechanical properties increase with increasing the ionomer content and then level off at approximately over 5 phr of ionic content. The introduction of ionomer in to the SBR/NBR blends enhances the phase dispersion and the interfacial adhesion, which results in the improvement of the mechanical properties. At higher concentration of the ionomer i.e., at 10 phr the inter multiplet attraction in ionomer may be higher in comparison with the multiplet- NBR interaction. The ionomer at this stage may agglomerate to form particles of bigger size unsuitable for interaction with NBR. The zone size of the dispersed domains in the blend may be increased which reduces the physical properties (Table 7.4) of the blend system. The plasticising effect of the ionomer also may be responsible for the reduction in the physical properties.

7.3.4. Infrared spectroscopy

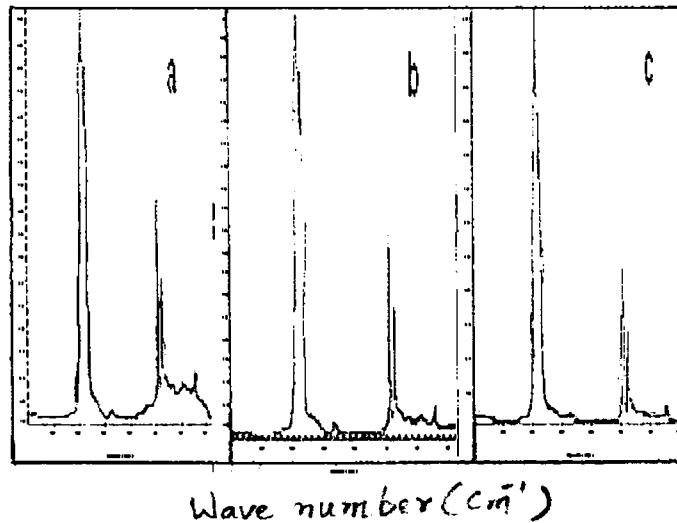


Fig. 7.10 FTIR spectra of (a) cured uncompatibilized 50/50 SBR/NBR blend, (b) blend compatibilized with 5-phr ionomer, and (c) blend compatibilized with 10-phr ionomer

FTIR spectra of cured uncompatibilized 50/50 SBR/NBR blend, and 50/50 SBR/NBR blend containing 5 phr and 10 phr of ZnS-RISGNR ionomer as compatibilizer are shown in figure 7.10. It is assumed that there would be polar-polar interactions between the zinc sulfonate groups of ZnS-RISGNR ionomer and – CN group of acrylonitrile repeat units present in NBR, which leads to miscibility in these blends. The polar-polar interaction affect IR absorption peaks of the concerned groups. FTIR spectrum of cured uncompatibilized SBR/NBR blend as shown by figure 7.10 shows aromatic substitution characteristic of SBR at 756 cm^{-1} , and the C=N stretching vibrations of the functional group of the acrylonitrile unit in NBR at about 2300 cm^{-1} . The C=C stretching vibrations appear at about 1500 cm^{-1} . The band at 1462 cm^{-1} is assigned to the –CH₂- bending vibration.

FTIR spectra of cured SBR/NBR blend compatibilized with 5 phr and 10 phr ZnS-RISGNR ionomer as shown by figure 7.10 reveal that the absorbance corresponding to the characteristic peaks in the cured compatibilized blend have been lowered. The lower shifts in the absorbance of the characteristic peaks in the FTIR spectrum of 50/50 SBR/NBR are represented in the table 7.5.

Table 7.5 Absorbance of the characteristic peaks in the FTIR spectrum of 50/50 SBR/NBR blends

Sample	$\sim 2300\text{ cm}^{-1}$	$\sim 1500\text{ cm}^{-1}$	$\sim 1350\text{ cm}^{-1}$	$\sim 750\text{ cm}^{-1}$
A	1.0	0.49	0.31	0.08
B	0.85	0.46	0.31	0.11
C	0.60	0.23	0.13	0.03

A- Cured uncompatibilized blend of 50/50 SBR/NBR; B and C show cured compatibilized blend containing 5 and 10-phr ionomer respectively

From these results, it may be believed that the origin of the specific interaction in this blend system comes from the ion – dipole interaction between the polar – CN groups of NBR and zinc sulphonate ionic groups in ZnS-RISGNR ionomer.

7.3.5 Scanning electron microscopy

7.3.5.1 Uncompatibilized blend of 50/50 SBR/NBR

The SEM photomicrographs at three different magnifications (Fig. 7.11) on the tensile fracture surface of cured 50/50 SBR/NBR uncompatibilized blend show 'crater' formation, distortions and separations on the fracture surface. These observations with respect to the uncompatibilized blend are obviously due to the inhomogeneity in the blend. The poor adhesion between the phases in the uncompatibilized blend may be the reason for their low tensile strength.

7.3.5.2. Compatibilised blend of 50/50 SBR/NBR

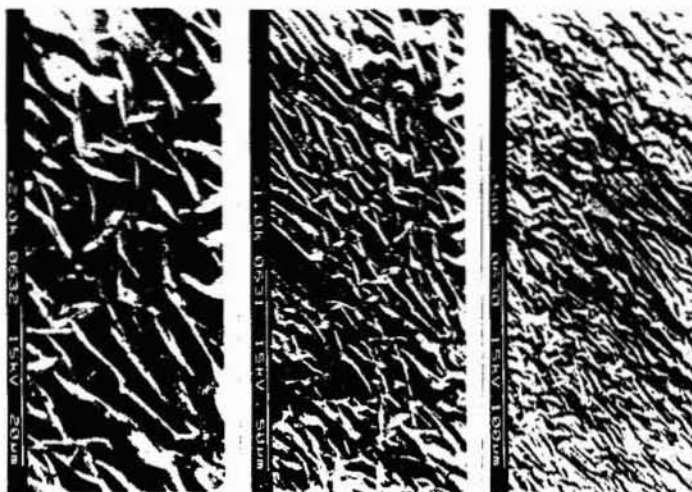


Fig. 7.11 SEM photomicrographs of the fracture surface of the cured uncompatibilized 50/50 blend of SBR/NBR with 2K (left), 1K (middle), and 0.5K (right) magnifications

The SEM photomicrographs at three different magnifications (Fig. 7.12) on the tensile fracture surface of the cured 50/50 SBR/NBR blend compatibilized with 5-phr ionomer reveal that there is uniform curing within the phases and at the interface, which results in better adhesion between the phases. The modified systems having improved mechanical properties than the corresponding unmodified blend have a better co-continuous nature of the phases permitting direct load transfer of the

components. The co-continuity of the matrix in the case of modified system is a result of improved adhesion. These SEM micrographs for the ionomer compatibilized are similar to the ionomer compatibilized systems reported earlier [6,18].

7.4. Influence of carbon black

Blending of polymers offers novel materials with tailored properties. Hence the technique has been extensively used in plastics, rubbers, composites, films, fibers, coating and adhesives. The last few years have seen a remarkable increase in the production of new type of blends such as elastomer alloys and interpenetrating networks. The most important advantage of these systems is the ease of mixing procedure. Among the broad class of polymer blends, the field of rubber-rubber blends deserves a prominent place. The main factor, which decides the ultimate properties of rubber-rubber blend, is the diffusion of one rubber in to another. The factor in turn is depending on the interaction between the component rubbers.

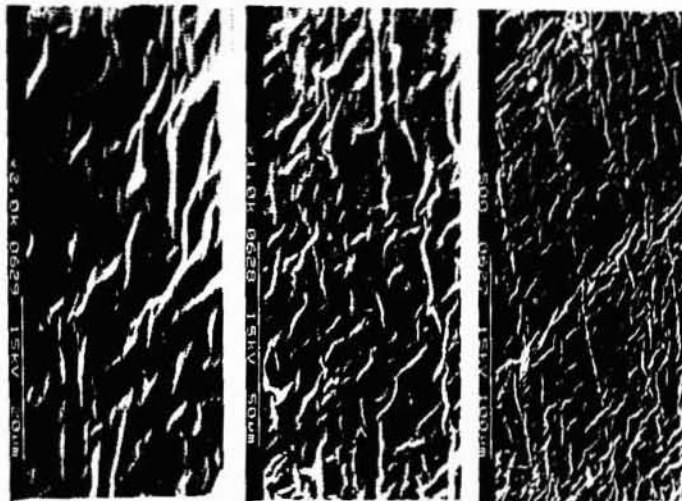


Figure 7.12 SEM photomicrographs of the fracture surface of the 5-phr ionomer compatibilized cured 50/50 blend of SBR/NBR with 2K (left), 1K (middle), and 0.5K (right) magnifications

The main use of fillers in rubber-rubber blend is to improve the processability, mechanical properties and to reduce the overall cost. Fillers are considered to improve the phase morphology of the incompatible blends. It has been found that the thermodynamic compatibility of many binary blends are further improved by many inorganic fillers. This ability of fillers comes from its tendency to reduce zone size of dispersed domains in polymer blends. This section deals with the influence of carbon black on the properties of SBR/NBR blends compatibilized by ZnS-RISGNR. Blending of the commercially important elastomers such as SBR and NBR produce materials that have excellent resistance to oils with good mechanical properties and are suitable for a wide range of applications in automobile industry. Owing to the immiscibility of these two elastomers, this particular blend system has received only limited attention in literature.

Table 7.6 Formulation of carbon black filled 50/50 SBR/NBR blend

Ingredients	Uncompatibilized (Phr)	Compatibilised (Phr)
SBR/NBR blend	100	100
26.5 ZnS-RISGNR	-	5
Stearic acid	1.5	1.5
Zinc oxide	5	5
CBS	1	1
TMTD	0.5	0.5
HAF black (N330)	10-40	10-40
Aromatic oil	1-4	1-4
Sulphur	1.5	1.5
TDQ	1	1

7.4.1. Cure characteristics

Formulation of carbon black filled 50/50 SBR/NBR blends with and without compatibilizers is given in table 7.6. The effect of addition of varying concentration of

carbon black on the cure characteristics of the uncompatibilized and 5-phr compatibilized 50/50 SBR/NBR blends are shown in the figure 7.13 and table 7.7.

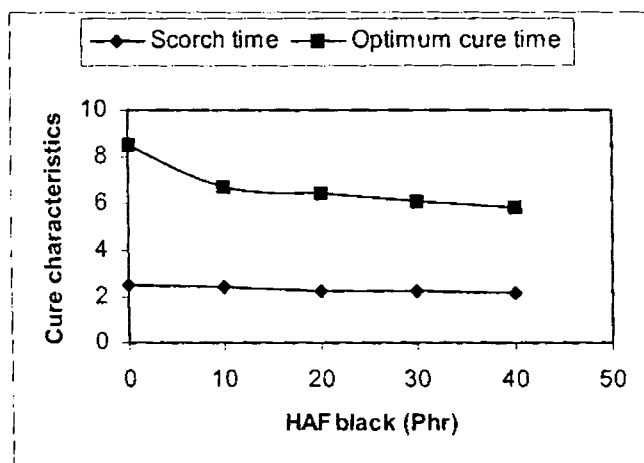


Fig. 7.13 Cure characteristics of compatibilized blend filled with HAF

The addition of small quantity of ZnS-RISG NR causes a rise in the rheometric torque of the virgin blend (Fig. 7.14 and Table 7.7) and has been further enhanced on adding carbon black as filler. It is well known that the reinforcing filler carbon black increase viscosity of rubber, specifically non-crystallizing rubbers depending on its concentration. The reinforcing effect of fillers is attributed to better polymer filler interaction. Carbon black has a tendency to migrate to SBR phase compared to NBR phase [19]. This may be due to an increased level of cross-linking. The maximum torque depends on the cross-link density and chain entanglement, which result from higher interaction of SBR and NBR through ZnS-RISG NR unit. The scorch time and the optimum cure time of the 5-phr compatibilized blend decreased with carbon black content. It is assumed that ZnS-RISG NR reduces the interfacial tension giving increased interfacial cross-linking due to more homogeneous mixing of the two rubbers. The problem due to unequal distribution of curatives is minimized resulting enhanced cross-linking of the blend. Due to this there is a decrease scorch time for blends containing ZnS-RISG NR.

Table 7.7 Rheometric data of carbon filled compatibilized and uncompatibilized 50/50 SBR/NBR blend

Material	Scorch Time (min)	Optimum cure time (min)	Max.torque (NM)	Time of Max.torque (min)
1	3.5	7.1	0.1682	3.6
2	2.5	8.5	0.1811	3.4
3	2.4	6.7	0.2689	3.2
4	2.3	6.4	0.2873	3.1
5	2.3	6.1	0.3184	3.0
6	2.2	5.8	0.3322	2.9
7	2.1	5.2	0.5663	2.9

1-Cured uncompatibilized blend; 2, 3, 4, 5, and 6 shows 5-phr compatibilized blend containing 0, 10, 20, 30 and 40 phr carbon black; 7- uncompatibilized blend containing 40 phr carbon black

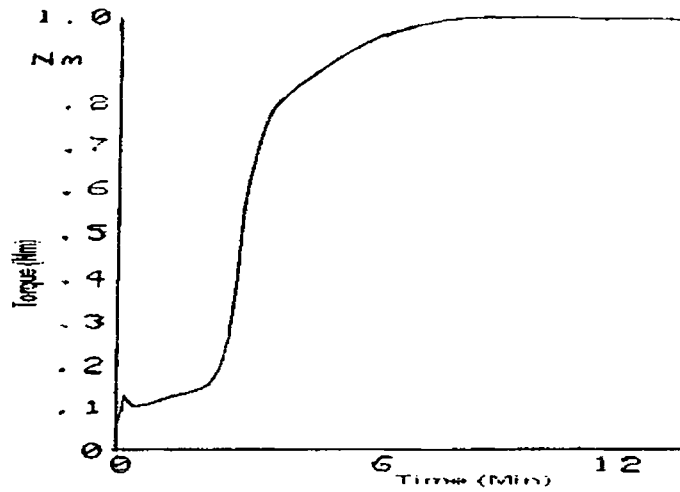


Fig. 7.14 Cure curve of 5-phr compatibilized 50/50 SBR/NBR blend filled with HAF carbon

7.4.2. Physical properties

Table 7.8 Physical properties of cured uncompatibilized 50/50 SBR/NBR blend filled with carbon black

Material	Tensile strength (MPa)	Elongation at break (%)	Tear strength (N/mm)	Hardness (Shore A)
1	2.9	317	14.9	42
2	9.45	322	29.8	51
3	13.94	314	35.8	57
4	18.20	295	38.2	62
5	20.86	272	41.6	65

1, 2, 3, 4 and 5 show cured uncompatibilized 50/50 SBR/NBR blend containing 0, 10, 20, 30 and 40 phr HAF black

Effect of carbon black on the physical properties of vulcanized SBR/NBR blends in the presence and absence of compatibilizer is shown in the tables 7.8 and 7.9 respectively. Figure 7.15 shows that the tensile strength values of compatibilized blends are higher than that of uncompatibilized blends.

Table 7.9 Physical properties of cured compatibilized 50/50 SBR/NBR blend filled with carbon black

Material	Tensile Strength (MPa)	Elongation Break (%)	Tear Strength (N/mm)	Hardness (Shore A)
1	4.10	507	23.0	46
2	12.18	364	32.3	56
3	17.02	344	36.8	60
4	20.95	321	40.6	64
5	24.69	301	44.8	70

1, 2, 3, 4 and 5 show 5-phr compatibilized cured SBR/NBR blend containing 0, 10, 20, 30 and 40 phr HAF black

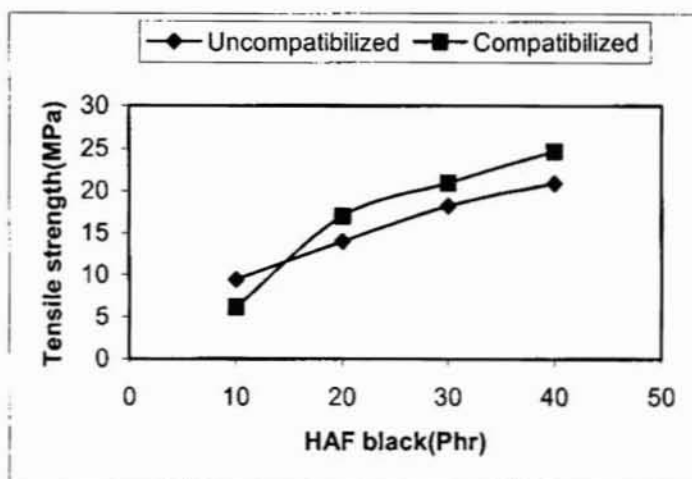


Fig. 7.15 Tensile strength of cured uncompatibilized and compatibilized 50/50 SBR/NBR blend filled with HAF carbon black

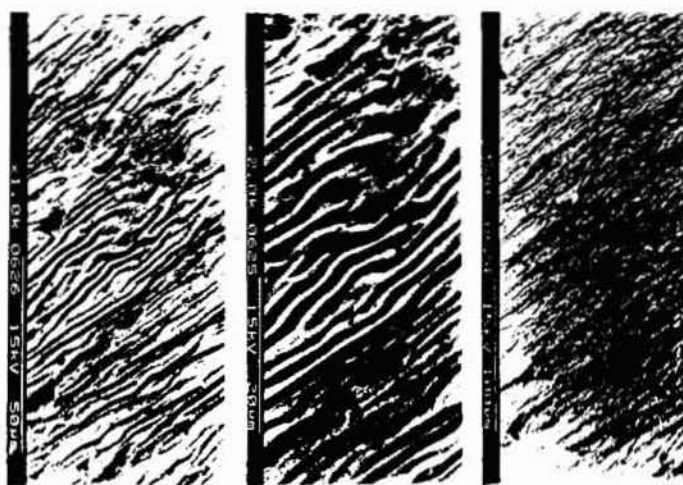


Fig. 7.16 SEM photomicrographs of the tensile fracture surface of cured 5-phr compatibilized 50/50 SBR/NBR blend filled with 40 phr carbon black (HAF) fracture surface with magnifications of 0.1K (left), 2K (middle) and 0.5K (right)

This may be due to the more interaction between compatibilizer and blend constituents. Due to the reduction of interfacial tension on these blend compositions

there is also an improved polymer filler interaction and more uniform distribution of filler in the two rubbers.

7.4.3. Morphological studies

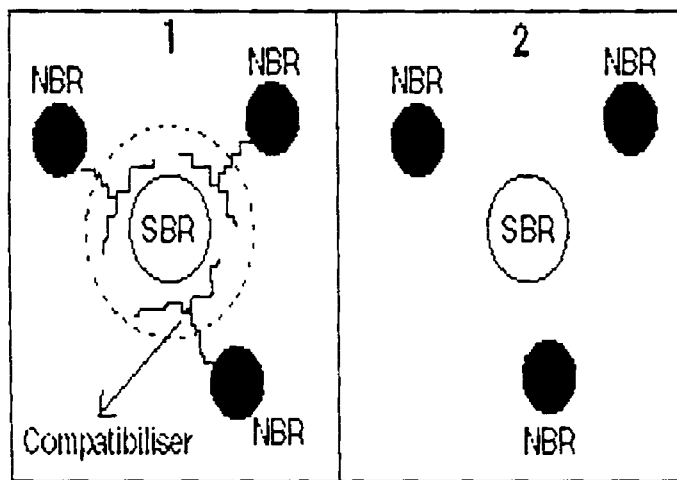
The reinforcement of the compatibilized blends with HAF carbon black has been made very clear from the SEM photomicrographs at three different magnifications of 0.5K, 1K and 2K on the tensile fracture surface of the cured 5-phr compatibilized blends with HAF carbon black (Fig. 7.16). These observations, showing uniformity of the mix, are in agreement with the tensile properties.

7.5 Location of the compatibilizer using dynamic mechanical thermal analysis

Ideally, compatibilizers locate at the interface between the components of the blend with their segments completely penetrating the respective compatible phases. Alternatively, a compatibilizer interface may be formed between the blend phases [20, 21]. In fact, some of the SGNR copolymer units of the ionomer are believed to penetrate in to the NBR phase to some degree and their polar zinc sulfonate moiety exhibits a greater affinity with the polar –CN group of NBR polymer. Determination of location of the ZnS-RISGNR ionomer in SBR/NBR blends was investigated using DMTA. $\tan \delta$ results obtained from compatibilized and uncompatibilized 50/50 SBR-NBR blends are shown in figure 7.7. The low temperature $\tan \delta$ peak for the uncompatibilized blend in the range -40 to -20 °C arises from the glass transition of the SBR matrix, and another $\tan \delta$ peak in the temperature range -15 to $+15$ °C arises from the NBR phase. While the low temperature T_g (T^1_g) corresponding to the SBR phase experiences insignificant changes, observation of the high temperature T_g (T^2_g) pertaining to NBR phase in the modified blend shows an increase in T_g (table 7.3).

These DMTA results suggest that the compatibilizer may exist primarily as a separate face (DSC shows an ionic transition for the modified blend at ~ 85 °C) presumably at the interface, and that there is stronger interpenetration of the -CN groups of the NBR with the ionic multiplet of the ionomer, which restrict the mobility of

the NBR chain in the neighborhood of the multiplet causing its thermal transition (T_g^2) T_g to rise from $-2\text{ }^\circ\text{C}$ in the uncompatibilized blend to $0\text{ }^\circ\text{C}$ in the compatibilized blend. The increase in the high temperature $\tan \delta$ and storage modulus for the NBR-rich phase in the compatibilized blend agrees with our views. The interaction of the NBR with the compatibilizer may be reducing the interfacial tension between the SBR and NBR, which may result in the partial miscibility of the components. The enhanced tensile properties of the compatibilized blend in comparison with the uncompatibilized sample as shown in table 7.4 may be considered as a supplementary evidence for the technological compatibility of the immiscible SBR/NBR blend system.



Scheme 7.1 Proposed model showing the compatibilized (1) and uncompatibilized (2) blend system

The presence of the ionomer at the interface between the SBR and NBR was investigated morphologically. Figure 7.11 shows the SEM fractographs of the uncompatibilized blends at three different magnifications. The fractured surfaces of the compatibilized blend as represented in figure 7.12 show the presence of the interpenetrating networks or bridge between the two phases. This bridge probably consists of ionomer, supporting other results, which suggests that the compatibilizer is located preferentially at the interfaces. The possible models showing the interaction of the ionomer with the blend systems are shown in the scheme 7.1.

7.6 Compatibilisation theory

The present method of compatibilization consists of the mixing of zinc-sulphonated radiation induced styrene grafted natural rubber with the SBR/ NBR polymer system, which up on mixing may be 'anchored' at the interface of SBR/ NBR polymer system. The anchoring of the ionomer on the SBR interface may be facilitated by the similarity in the 'architecture' of their structural backbones where as the anchoring of the ionomer on the NBR interface may be due to the interaction of the polar zinc sulphonated group on the ionomer with the polar – CN group on NBR. The anchoring of the ionomer at the SBR/ NBR interface increases the entropy of mixing, which therefore, reduces the surface tension or surface energy. This thermodynamic feasibility for mixing of the polymer components forces the chains of SBR and NBR to remain in close proximity. The technological compatibilization of the SBR/NBR polymer blend system has been further established through the synergistic physical properties of the blend system

The unfavorable interaction between molecular segments of the components leads to a large interfacial tension, which makes it difficult to disperse the components finely enough during mixing. This is responsible for the immiscibility of the polymer components. The poor interfacial adhesion in the solid state causes mechanical failure via these weak defects between phases. Solutions to these problems or compatibilization can be effected by the addition of appropriate graft / block copolymers or ionomers that act as interfacial agents. For effective compatibilization, the molecular weight and architecture of the block copolymer need to be carefully optimized. Formation of the copolymer species at the interface reduces the interfacial tension, leads to the stabilization which retards dispersed phase coalescence, and strengthens the interface, in the solid state, between phases. A significant achievement in the physical properties of the blend may be considered as an evidence for the significant reduction in the dimensions of the phase domains. Compatibilization shifts the balance between drop breakup and coalescence by lowering interfacial tension and introducing the stabilization; these effects produce much smaller dispersed- phase particles. Reactions at the interface are expected to lead to a reduction in the interfacial tension.

While SBR and NBR polymers are immiscible due to the very low entropy of mixing, miscibility enhancement can be achieved when an ionomer is used as a compatibilizer. The intermolecular polar – polar interactions between SBR / RISGNR ionomer with NBR lower the heat of mixing so that the thermodynamics of blending can lead to miscibility enhancement of the blend components. The use of ZnS-RISGNR ionomer is particularly attractive in this respect since the ionic groups introduce the possibility of strong ion – ion, ion pair – ion pair or ion – dipole interactions with NBR. The miscibility enhancing effect of ionic groups has been clearly demonstrated for various blends.

The incorporation of ionomer modifies the blend properties profoundly. For eg: Tg is increased, and the modulus is increased over wide temperature ranges. In contrast to non-ionic thermoplastics, in which the modulus decreases quite rapidly as a function of temperature in the vicinity of Tg, the ionomers of high ion content show only a very gradual decrease of modulus with temperature. The Tg does go up because of the ionic interactions. The viscosity increase has been found to be drastic in sulfonates, and to a smaller extent in carboxylates. The ionic interactions resulting from sulfonation raises the glass transition temperature.

7.7 Conclusion

As expected for most immiscible polymer blends, the mechanical properties of binary blends of SBR and NBR were very poor. However, addition of zinc sulphonated styrene grafted natural rubber ionomers increased the tensile properties of the blends. DSC studies of the blend samples showed multiple Tgs with insignificant changes upon compatibilization. DMTA, however, detected a Tg change for the NBR phase and it may be ascribed to the preferential polar-polar interaction of the ionomer multiplets and the -CN groups of the NBR. The dynamic mechanical results predicted the possibility of existence of an ionomer as an interphase between the components of the blends and produce a partial miscibility between SBR-NBR. The FTIR and the morphological studies gave support to this contention. It could be concluded that, the novel ionomers based on styrene grafted natural rubber may be useful as a compatibilizer for obtaining the technologically compatible blends from the immiscible SBR and NBR polymers.

7.8 References

- 1 Paul, D.R; *Polymer Blends* vol.2, Paul, D.R and Newman, S eds., Academic Press, New York p.167 (1978)
- 2 Paul, D.R; Vincen, C.E; Locke, C.E *Polym. Eng. Sci.*, 12, 157 (1972)
- 3 Schrenk, W.J; Alfrey, Jr, T *Polymer Blends* vol.2, Paul, D.R and Newman, S; eds., Academic Press, New York p. 129 (1978)
- 4 Ouhadi, T.; Fayt, R.; Jerome, R.; Teyssie, Ph. *J. Appl. Polym. Sci.*, 32, 5647(1986)
- 5 Majumdar, B.; Paul, D.R. In: *Polymer Blends Volume 1: Formulation* , Paul, D.R.; Bucknall, C.B. Eds., Wiley Interscience Pub. John Wiley & Sons, Inc., New York (1999)
- 6 Ramesan, M.T. *PhD Thesis*, M.G.University, Kottayam, Kerala, India (2000)
- 7 Roura, M. J. *Eur. Pat.* EP34704 (1981)
- 8 Inoue, K.K. *Jpn. Pat.* JPS7102948 (1982)
- 9 Weaver, E.P. *Eur. Pat.* EP86069 A2 (1983)
- 10 Lu, X.; Weiss, R.A. *Mater. Res. Soc. Symp. Proc. 29 (Proceedings of the Fall Meeting of the Materials Research Society)* (1990)
- 11 Coran, A.Y.; Patel, R. *Rubber Chem. Technol.* 54, 892 (1981)
- 12 Vongpanish, P.; Bhowmick, A.K.; Inoue, T. *Plast. & Rubber Proc. & Applications* 19, 117(1993)
- 13 Stoelting, J.; Karasz, F.E.; MacKnight, W. *J. Polym. Sci.* 10, 133 (1970)
- 14 Olabisi, O.; Robeson, L.M.; Shaw, M.T. *Polymer-Polymer Miscibility*, Academic Press, New York (1979).
- 15 Macknight, W.J.; Karasz, F. E.; Fried, J.R. "Solid State Transition Behavior of Blends", in *Polymer Blends*, Paul, D.R.; Newman, S(eds.), Academic Press, New York(1978).
- 16 Karasz, F. E. "Glass Transitions and Compatibility; Phase Behavior in Copolymer Containing Blends", in *Polymer Blends and Mixtures*, Walsh, D.J.; Higgins, J.S.; Maconnachie (eds.), Martinus Nijhoff Publishers, Boston (1985).
- 17 Utracki. L.A. *Polymer Alloys and Blends: Thermodynamics and Rheology*, Hanser Publishers, New York (1990).
- 18 <http://www.psrc.usm.edu/macrog/mpm/blends/inter.htm>
- 19 Callan, J.E; Hess, W.M; Scott, C.E. *Rubber Chem. Technol.*, 44, 814 (1971)
- 20 Fayt, R.; Jerome, R.; Teyssie, P.H. *Makromol. Chem.*, 187, 837 (1986)
- 21 Schwarz, M.C.; Barlow, J.W.; Paul, D.R. *J. Appl. Polym. Sci.*, 35, 2053(1988)

Chapter 8

Conclusion & Future outlook

The present study is an effort to synthesize, characterize and investigate the properties of new ionomers based on natural rubber. The effect of particulate and fibrous fillers on the properties of the novel ionomer, the electrical behaviour of the ionomer at microwave frequencies and the role of the ionomer as compatibiliser in SBR/NBR blend system have been studied.

Thermo-reversible ionic cross-linked radiation induced styrene grafted natural rubber (RISG NR) was synthesized. The attachment of ionic groups to the pendant styrene blocks with respect to the NR backbone was shown using spectroscopic techniques such as FTIR and FTNMR. Thermal parameters informed that the thermo-oxidative stability increased with increase in the ionic content of the polymer. DSC thermograms revealed that incorporation of the zinc sulfonate groups in to the styrene grafted natural rubber produced phase-separated regions similar to an ionomer having two characteristic Tg's, one corresponding to the polymer matrix and the second may be due to the microphase clustering of the polar zinc sulfonate. The glass transition temperature (Tg) of the RISG NR increased with increase in the ionic concentration. DMTA measurements gave two separate mechanical loss tangent ($\tan \delta$) peaks. The value of the $\tan \delta$ at Tg ($\tan \delta_{\max}$) decreased with sulfonation, and a new relaxation occurred above the matrix glass transition temperature. An extended rubber plateau with steep descent was observed in the modulus above Tg, which might be due to the ionic network in sulfonated polymer. The storage modulus ($\log E'$) of the zinc salt of RISG NR showed an increase with sulfonation in the entire range of test temperature. This showed that the physically cross-linked network persists in

the entire range of temperature. The 26.5 ZnS- RISGNR ionomer ($T_g1: -21\text{ }^\circ\text{C}$, and $T_g2: +87\text{ }^\circ\text{C}$), showed relatively better physical properties, and typical thermoplastic character. DSC results gave confirmation to the viscoelastic behavior.

Two other novel alternative methods were also used for the synthesis of ionomers based on natural rubber. Zinc neutralized sulfonated natural rubber was prepared by reacting natural rubber (without styrene grafting) with acetyl sulfate followed by neutralization of the sulfonic acid with zinc acetate. The novel zinc salt of radiation induced styrene grafted natural rubber had tensile strength about thirty-five times that of unvulcanised base NR. DMTA investigations revealed that incorporation of zinc sulfonate groups in to the natural rubber gave a new material with two thermal transitions, T_g1 and T_g2 . Comparison of styrene grafted NR with zinc sulfonated NR showed that when the polystyrene domains in SGNR caused very little effect on the T_g of the NR matrix, the presumed ionic domains due to the zinc sulfonate groups in the ZnS-NR produced a marginal influence. The T_g2 for the ionically modified NR ($+97.05\text{ }^\circ\text{C}$) was observed at a temperature of $12\text{ }^\circ\text{C}$ higher than that for the styrene grafted natural rubber. The steep descent and an extended rubber plateau for the zinc salt of natural rubber, unlike SG-NR, show the characteristics of sulphonated ionomers. Reprocessability studies showed that the newly synthesized ZnS-NR could be reprocessed without sacrificing much of its physical properties.

Novel ionomers based on chemically induced styrene grafted natural rubber was also prepared and was included in this chapter as part 2. The analytical techniques, XRF and ICPAES respectively showed the acetyl sulphate reagent conversion of about 32 %, and 96 % neutralization of the sulphonic acid. FTIR spectra gave evidence for the grafting of styrene on to the natural rubber backbone and also for the formation of sulphonated styrene grafted natural rubber. NMR spectra confirmed the presence of ionic groups in the modified rubber, thus gave supplementary evidence to the FTIR spectra. Thermogravimetry results showed the improvement in the thermo-oxidative stability of the base polymer up on ionomer modification. The modified CISGNR showed higher tensile strength than uncured base polymer. Reprocessability studies revealed the thermo-reversible character of the ionically modified CISG natural rubber.

The mechanical properties of the three newly synthesized ionomers based on NR, CISG NR and RISG NR were compared (part 3). The tensile strength of the newly synthesized ionomers decreased in the order ZnS-NR > ZnS-CISG NR > ZnS-RISG NR

Investigations on ionomers filled with particulate fillers [carbon black (HAF), silica and zinc stearate] and fibrous filler [nylon and glass] show that the incorporation of fillers improves the physical, dynamic mechanical thermal and dielectric properties of the ionomer. Both DMTA and DSC supported the retention of the ionomer properties of the carbon filled compound. The HAF black filled ionomer had the highest storage modulus at 25°C. DMTA plot showed that both the Tg1 and Tg2 are retained even in the silica filled ionomers. The value of the thermal transitions suggested that silica reinforced the backbone chain and weakened the ionic associations. The room temperature storage modulus for the silica filled ionomer was the highest among the selected fillers. The short fibers of nylon as well as glass were found to be interacting with both the matrix-phase and the cluster-phase. The value of the $\tan \delta$ corresponding to Tg1 for the ionomer decreased up on loading various fillers. The lower $\log E'$ at 25°C for the nylon and glass filled ionomers in comparison with the neat ionomer corroborated the above observations. Zinc stearate acted as an ionic domain plasticizer and lowered the Tg1 and Tg2 of the base ionomer. Physical properties of the filled systems showed improvement over the neat ionomer. Both particulate fillers such as HAF black, silica, zinc stearate and the fibrous fillers such as nylon and glass reinforced the ionomers. FTIR results gave supplementary evidence for these observations. The dispersion and the adhesion of the fillers in the ionomer matrix were evident from the morphological investigations of the filled compounds through SEM. The thermoplastic elastomeric nature of the compound was evident from the retention of the stress-strain properties even after three cycles of repeated mixing and molding.

The microwave investigation of the dielectric behavior in the novel ionomers based on radiation induced styrene grafted natural rubber using cavity perturbation technique, in the useful frequency range for industrial, scientific and medical applications (i.e. 2 – 4 GHz), showed that the complex permittivity and the relative complex conductivity increased with increase in the ionic concentration. The ionomer

showed its highest microwave conductivity at 2.6 GHz frequencies. Incorporation of 26.5 meq of zinc sulphonate groups in to the base polymer increased its σ' from 1.8×10^{-12} S/ cm to 3.3×10^{-4} S/ cm. Microwave probing of ionomer/filler compounds revealed that the dielectric parameters of the ionomer were influenced by the fillers such as HAF black, silica, nylon fiber, glass fiber and zinc stearate. Silica and glass filled ionomer showed lower dielectric properties compared to the other fillers. Among the fillers used in the present study, nylon had the highest complex conductivity at the microwave region.

The 26.5 ZnS-RISGNR ionomer was useful as a compatibilizer on the immiscible SBR/NBR blend system. As expected for most immiscible polymer blends, the mechanical properties of binary blends of SBR and NBR were poor. However, addition of ionomers gave substantial improvement in the physical properties of the blends. Optimum concentration of the compatibiliser observed was 5 phr. DSC studies of the blend samples showed multiple Tgs with insignificant changes upon modification. DMTA, however, detected a Tg change for the NBR phase. From these results it was inferred that the ionomer exist primarily as an interphase between the components of the blends and produced a partial miscibility between SBR and NBR. The FTIR and the morphological studies gave support to this contention. The novel ionomers based on styrene grafted natural rubber was useful as a compatibiliser for obtaining the technologically compatible blends from the immiscible SBR and NBR blend system.

Future Outlook

The synthesis and characterization of novel ionomers based on natural rubber opens up new vistas for a fruitful research. Investigation of hitherto untapped properties of these ionomers may pave the way for the large-scale consumption of natural rubber. Some of the areas of research where these ionomers may find suitable include:

1. Industrial exploitation

The investigations on the use of 'natural rubber ionomers' in paint manufacturing, as permselective membranes, as a catalyst in organic synthesis, and as a substitute for vulcanized rubber and thermoplastic elastomers is worth attempting.

2. Microwave devices

The microwave response of the ionomers at the C and X-band frequencies may be an area of useful study.

3. Compatibilizer

Ionomers, due to their unique properties and structure, may be useful as a compatibilising agent for any nonpolar- polar blend system such as NR/NBR, NR/CR, NR /Polystyrene, NR/PVC, NR/polystyrene etc. Ionomers of variable ionic concentrations may be attempted.

4. Ionomer composites

Both particulate and fibrous filler ionomer composites of improved properties may be developed. Fillers such as rayon, white etc may be used.

5. Solution properties

Emphasis on the solution behavior of ionomers may be one of the important outlooks.

6. Ionomer-ionomer blends

Novel ionomer-ionomer blends of specific properties may be developed.

Abbreviations

ASTM	-	American Society for Testing and Materials
DCE	-	Dichloroethane
DSC	-	Differential Scanning Calorimetry
DMTA	-	Dynamic Mechanical Thermal Analysis
FTIR	-	Fourier Transform Infra Red
FTNMR	-	Fourier Transform Nuclear Magnetic Resonance
GHz	-	Giga Hertz
HAF	-	High Abrasion Furnace Black
ICPAES	-	Inductively Coupled Plasma Atomic Emission Spectroscopy
ISM	-	Industrial, Scientific and Medical
ISNR-5	-	Indian Standard Natural Rubber – 5 Grade
NBR	-	Acrylonitrile-Co- Butadiene Rubber
NR	-	Natural Rubber
Phr	-	Parts per hundred rubber
SEM	-	Scanning Electron Microscopy
SGNR	-	Styrene Grafted Natural Rubber
TGA	-	Thermo gravimetric Analysis
TMTD	-	Tetra Methyl Thiuram Disulfide
TPE	-	Thermoplastic elastomer
UTM	-	Universal Testing Machine
XRFS	-	X-ray Fluorescence Spectroscopy
ZnS-CISGNR	-	Zinc Sulphonated Styrene Grafted Natural Rubber
ZnS-NR	-	Zinc Sulphonated Natural Rubber
ZnS-RISGNR	-	Zinc Sulphonated Radiation Induced Styrene Grafted Natural Rubber

Glossary of symbols

E'	-	Storage Modulus
E''	-	Loss Modulus
J	-	Heating Coefficient
Tan δ	-	Loss tangent or damping factor
Tg	-	Glass Transition Temperature
ϵ'	-	Dielectric Constant (Real Part)
ϵ''	-	Dielectric Constant (Imaginary Part)
σ'	-	Complex Conductivity (Real Part)
σ''	-	Complex Conductivity (Imaginary Part)
Tg1	-	Glass transition temperature of soft rubbery phase
Tg2	-	Glass transition temperature of hard phase



678603

List of Publications

1. *Synthesis and Characterisation of Novel Melt-Processable Ionomers Based on Radiation Induced Styrene Grafted Natural Rubber* Macromol. Mater. Eng. 286, 507, (2001)
2. *Ionomers* Prog. Rub. Plast. Tech. 16, 1, (2000)
3. *Thermoplastic Ionomers based on Styrene Grafted Natural Rubber* Intern. J. Polymeric Mater (Accepted.)
4. *New Ionic polymer: Synthesis and Properties of zinc sulphonated natural rubber* J. Elastomers and Plastics, vol. 34, 91 (2002).
5. *Microwave Investigations of the Dielectric and Conductivity Behavior in Novel Thermoplastic Ionomers based on Radiation Induced Styrene Grafted Natural Rubber (SGNR) using Cavity Perturbation Technique*, Polym. Sci. Part B: Phys. Edn. (Communicated)
6. *Novel Ionic Cross-Linked Natural Rubber*. Rubber Asia 53, (2001)
7. *RUBBASTICS: Heat fugitive Ionic polymers conquering the millennium*, Chemweb.com/CPS: macrochem/0103001, (2001)
8. *The Compendium of Studies of Polystyrene-g-Natural Rubber, an Alternative to Thermoplastic Elastomers*, Chemweb.com/CPS: macrochem/0107001, (2001)
9. *Novel Thermoplastic Ionomer Based on Natural Rubber* Proce. Thirteenth Kerala Sci. Cong. 558, (2001)
10. *Effect of fillers on the thermal and dynamic mechanical properties of novel ionomers based on natural rubber*. J. Appl. Polym. Sci. (Communicated)
11. *DSC and DMTA studies on the reprocessable ionic cross-linked styrene grafted natural rubber*. Polymer (Communicated)
12. *Dielectric properties of ionomers*. Materials Letters (Accepted)